“Early Stage Protein Folding of the Potassium Channel Kcv”

Chirapha Butiman

[redacted]

Submitted in fulfilment of the requirements

For the Degree of Master of Science (Research)

Institute of Molecular, Cell and Systems Biology

College of Medical, Veterinary and Life Sciences

University of Glasgow

2018

CONTENTS

LIST OF FIGURES

List of Figures

LIST OF TABLES

List of Tables

ABBREVIATIONS

~	Approximately
°C	Degrees Celsius
a-helix	Alpha Helix
aa	amino acids
Å	Angstroms
APS	Ammonium Persulfate
ATP	Adenosine 5"-triphosphate
ß-sheet	Beta Sheet
BMH	Bismaleimide
bp	Base Pair
Ca^{+}	Calcium ion
BS^{3}	Bis**(**sulfosuccinimidyl**)**suberate
$CaCl_2$	Calcium Chloride
cAMP	Adenosine 3', 5'**-**cyclic Monophosphate
Ci	Curie
CFPS	Cell free protein synthesis
CTAB	Cetyltrimethylammonium Bromide
Cys (C)	Cysteine
Da	Dalton
ddH_2O	Double Distilled Water
DNA	Deoxyribonucleic Acid
dNTP	Deoxyribonucleotide Triphosphate
DTT	Dithiothreitol
E. coli	*Escherichia coli*
EDTA	Ethylenediaminetetracetic Acid
EF	Elongation Factor

ER	Endoplasmic Reticulum
FRET	Fluorescence Resonance Energy Transfer
Ffh	Fifty-four homologue
g	Gram
GDP	Guanosine 5'-Diphosphate
GTP	Guanosine-5'-Triphosphate
HCl	Hydrochloric Acid
HEPES	2-[4-(2-Hydroxyethyl)-1-Piperazine]- Ethanesulfonic-Acid
IF	Initiation Factor
Ile (I)	Isoleucine
IP	Immunoprecipitation
IPTG	Isopropyl-ß-D-thiogalactopyranoside
k	Kilo
K^+	Potassium ion
K_2HPO_4	di-Potassium Hydrogen Phosphate
kb	Kilo Base Pair
KCl	Potassium Chloride
Kcv	Viral Potassium Channel
kD	Kilo Dalton
KH_2PO_4	Potassium Dihydrogen Orthophosphate
KOAc	Potassium Acetate
KOH	Potassium Hydroxide
Ile (I)	Isoleucine
L	Litre
kcal mol^{-1}	kilocalorie per mole
LB	Lysogeny Broth
Lys (K)	Lysine
m	Milli
mL	Milllitre
µ	Micro

M	Molar
Met (M)	Methionine
$MgCl_2$	Magnesium Chloride
MgOAc	Magnesium Acetate
$MgSO_4$	Magnesium Sulphate
mRNA	Messenger RNA
MW	Molecular Weight
MWCO	Molecular Weight Cut-off
Na^+	Sodium ion
ng	nanogram
Na_2HPO_4	Disodium Hydrogen Orthophosphate
NaCl	Sodium Chloride
NaOAc	Sodium Acetate
NH_4OAc	Ammonium Acetate
NMR	Nuclear Magnetic Resonance
OD	Optical Density
p	Pico
PCR	Polymerase Chain Reaction
PEG-MAL	Methoxypolyethylene Glycol Maleimide
PMSF	Phenylmethylsulphonyl Fluoride
psi	Pounds Per Square Inch
PTC	Peptidyl Transferase Centre
RNA	Ribonucleic Acid
RNaseA	Ribonuclease A
RNCs	Ribosome-Nascent Chains
rNTP	Ribonucleotide Triphosphate
rpm	Rotations Per Minute
r-protein	Ribosomal protein
r-RNA	Ribosomal RNA
s	Seconds
SDS-PAGE	Sodium Dodecyl Sulphate Polyacrylamide-Gel Electrophoresis
-SH	Thiol group
SecM	Secretion Monitor
SOC	Super Optimal Broth with Catabolite Repression
SR	SRP receptor

SRP	Signal recognition particle
[^{35} S]	Sulfur 35 (Radioactive Labelling)
TCA	Trichloroacetic acid
TEMED	N,N,N‟,N‟-Tetramethylethylenediamine
TF	Trigger Factor
tmRNA	Transfer-messenger RNA
TMDs	Transmembrane Domains
Tris	Tris (hydroxymethyl) aminoethane
tRNA	Transfer RNA
v/v	Volume to Volume Ratio
w/v	Weight to Volume Ratio
WT	Wild Type

ABSTRACT

Kcv is the shortest transmembrane protein across other voltage-and ligand-gated potassium channels, containing only 94 amino acids to form a functional K^+ channel with two typical transmembrane domains (2TM). Current interest in cell biology raises questions about how this most primitive of proteins can function, given its very simple structure. To better understand the distinctive structure and function of Kcv, basic structural studies are necessary, especially in regard to how folding is vital to this protein's conformation. Hence, we selected the Kcv as a small protein model to examine the early development of secondary structure during the synthesis within the ribosome throughout the tertiary structure and interaction of the nascent chain with the ribosomal protein L23 and signal recognition protein (SRP54). The research was carried out to monitor the early stages of protein folding in the 1st TM domain. The experimental strategy used the specific residues mutagenesis which involves these analysis techniques; using post-translation incorporated with the chemical modifications; PEGylation assay, cross-linking assay, and immunoprecipitation assay.

The experimental processes was as follows: truncated ribosome nascent chain (RNCs) of interest had their lengths synthesised in the prokaryotic 30S *in vitro* transcription/ translation system, the N-terminus lengths were radio-labelled with $[^{35}S]^{met}$ and eventually the post-translation products were topologically analysed using the chemical modifications; PEGylation (thiol PEG-MAL reagent), and cross-linked with two selective cross-linkers, either cysteine-cysteine cross-linker (1,6-bismaleimidoheane; BMH) or lysine-lysine cross-linker (bis-(sulfosuccinimidyl)suberate;(BS^3), and subsequently encompassing comprehensive analysis of the cross-linked products using immunoprecipitation (IP) with two desired antibodies; L23 and the signal recognition particle (SRP), respectively. The samples were resolved on SDS-PAGE gels with the autoradiography. The PEGylation image successfully presented the clear PEGylated bands from 50-70aa when employing the M15L-Cysteine (incorporating L8C with a single methionine replacement) whereas the cross-linking assay using BS^3 associated with immunoprecipitation assay presented the clearest bands from 50-70 aa when using the three single lysines (K29I/K46/47M) incorporated with the single three methionine replacement (M15/23/26L) called 'M15/23/26L-Lysine'.

This project proposes that the small 2TM protein, Kcv, begins to form as a folded structure inside the ribosome tunnel. Additionally, data from this project suggests that the

helical 1st transmembrane region of the Kcv could be first compacted in the ribosomal exit tunnel before attaching to the targeting pathway. Based on the PEGylated band from the PEGylation assay, the nascent chain is exported from the ribosome tunnel at approximately 50 aa (~30aa contributed inside the ribosome; non-PEGylated), while consequent timing of the nascent chains interaction with L23 and SRP, which have been cross-linked and precipitated with the same PEGylation profile, shows that the interaction begins to be manifested from 50aa. These results agree with previous data for the 2TM protein (F_0c) but are at odds with our labs analysis of larger 7TM protein (GPCR GPR35). Furthermore, the interaction between nascent chains, L23, and SRP54 in the ribosome exit tunnel are able to demonstrate a responsibility outline principle to the further cellular targeting pathway of Kcv, a small membrane protein which is inserted into the plasma membrane, which is the final destination.

ACKNOWLEDGMENTS

I would like to express my sincere thanks for the many people who were involved in my MRes. Project. I am grateful to my supervisor, Dr. Cheryl Woolhead, for providing insightful guidance and knowledge throughout the project and for giving her time to help correct the contents of my thesis. I am thankful for the valuable discussions were greatly appreciated when fulfilling my research.

I sincerely thank all members of the "Woolhead'' lab who kindly gave useful advice and support with regards to instruction of laboratory techniques and answering questions; including: Dr. Jon Cherry, Donald Campbell, David Steward and Dr. Hazel Bracker.

Additionally, thanks goes to my sponsor, Thai Royal Scholarship, Ministry of Science and Technology, Thailand, and also all the staff who provided the supporting documents during my studies - especially Somchai Injorhor. I want to give tremendous thanks to my work place, Excellence Centre of Silk Innovation, Mahasarakham University, Thailand, for allowing me to study at University of Glasgow, UK. I am thankful to all staff of the office of Education Affairs, London, who have been helping and supporting me whilst living in the UK.

Importantly, I give thanks to my beloved family, my parents and my Thai friends for their love and support of me being abroad. I hope I have made them proud.

Special thanks to all the people who helped me to improve my scientific writing for this dissertation and also made me laugh; Lynley Capon, Saemus Grant, Adityo Paul and Louie Charles Atkins-Turkish.

Finally, thanks to all the friends I have met whilst studying in University of Glasgow; a special mention to Lin Bin (Cookie), Jacek Kurek, Chaitong Churuangsuk, Zoa Zhigo (Steve), Ryo Iwase, Pracha Yambanyang, Patchani Srikhamsuk and Pichaporn Dokmai.

January, 2018

INTRODUCTION

Membrane and Membrane Proteins

All organisms, prokaryotic and eukaryotic, present the biological membranes/plasma membranes, called 'phospholipid bilayers,' that serve as a semi-porous barrier between the delicately balanced inner and outer surface of the cells. The plasma membranes of animals are located in the outermost layer of the cell. Unlike the animal plasma membranes, most plants and bacteria present underneath the cell wall (Borrell et al., 2016). Membranes are composed of the lipids that are amphipathic molecules, including a hydrophilic head group and hydrophobic tail group. Compositions of plasma membranes are variable depending on species and cellular types which contain carbohydrates, proteins, and lipids held together by noncovalent bonds (Watson, 2015). In composition, lipids contain four distinctive groups that are generally exhibited in the membranes, namely glycerophospholipids, sphingolipids, glycolipid, and sterol (Borrell et al., 2016). Much research evidence reveals that membranes play important roles in the cell, such as maintaining the balance of cells, selective transport to regulate substance diffusion across the cells (Karp, 2006) and equalising the ions down electrochemical gradients (Watson, 2015). Additionally, embedded protein receptors in the membranes are responsible for cell signalling or acts between cell to cell communication (Nugent, 2010).

Membrane proteins are defined as being between two regions of compartments in cytoplasm and extracellular space. Like other proteins, the membrane proteins are synthesised by the ribosome and thereby subsequently associated with water as well as the lipids to be functions within the cellular environment (Vinothkumar & Henderson, 2010). By classification, membrane proteins have been grouped into two main categories based on their functional association with the biological membranes, including (i) integral membrane proteins /transmembrane proteins or intrinsic proteins that are inserted through the bilayer, and (ii) peripheral membrane proteins or extrinsic proteins, whereby the structural parts are not directly embedded into the membrane, but interact with the surface of the membranes (Cooper & Hausman, 2009). It has been discovered in recent studies that membrane proteins can be recognised and are inserted into endoplasmic reticulum (ER) via two pathways, such as 1) using a conserved mechanism by signal recognition particle (SRP) and receptor for membrane targeting at Sec61 for translocating, and 2) a recently discovered pathway accompanied by different factors, including transmembrane domain (TMD), selective cytosolic chaperones, and assistant receptors at the ER (Hegde & Keenan, 2011).

Transmembrane domains (TMDs) are a part of membrane protein that generally exhibits as integral proteins containing a helical segment connected by cytoplasmic and extracellular loops (Fig. 1). Transmembrane domains are amphipathic containing both hydrophobic and hydrophilic regions that can orientate within the membrane. These domains are composed of the membrane-spanning segments of the polypeptide chain that anchor the hydrophobic environment interior to the lipid bilayer containing largely amino acid residues with nonpolar side chains. The peptide bonds are polar when they reach the environment without water, and most peptide bonds in the lipid bilayer enable the formation of hydrogen bonds with another one (Albert et al., 2002). According to transmembrane design, the architecture and orientation relies on a thermodynamic mechanism to prevent mismatch between protein and lipid membranes. (Killian, 2003)

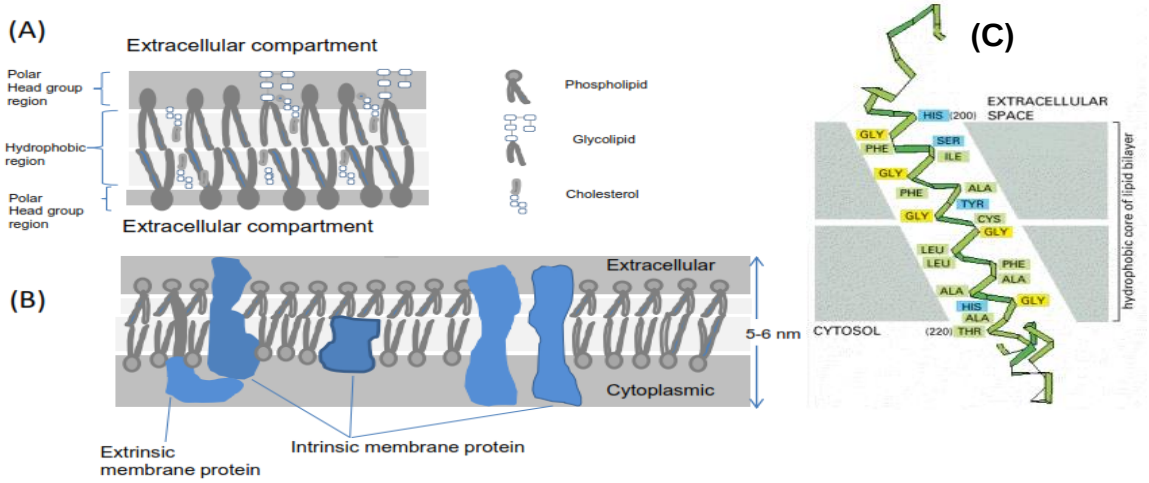

Figure 1: The structure of membranes; (A) the basic constitution of lipid bilayer and (B) the schematic representation of membrane proteins arrangement (Adapted from Wilkins et al., 2011). In comparison (C); a schematic illustration of transmembrane domain connecting extracellular space and cytosol by X-ray diffraction (data based on Deisenhofer et al., 1985).

Ion Channels

The evolution of all organisms has relied upon the membranes that are present to separate the charge and space in the cells. Ion channels are integral proteins that are generated as a pore in the cell membranes that enable the passage of molecules and ions through the lipid bilayer (White, 1999: Hille, 2001; Beckstein, 2004). To illustrate some ion roles in the cell, the studies found that ion channels use approximately 30 % of storage energy

in the cell to operate the gradient of Na^+ and K^+ ions during the transition (Ackerman & Clapham, 1997). Additionally, many studies found that the diffusion-limited rates of selective ions can be moved by about 10^7 ions per channel and per minute (Hille, 2001). Furthermore, ion channels help to mediate electrical signalling and regulate the ions flux as tiny voltage gradients across the lipid bilayers in the cells (Hille, 1992) and this electrical activity leads the cell to communicate between the cells (Hille, 2001). Therefore, hydrophobic cores from the lipid bilayer are essential to provide the energetic barrier when the ions are transported at ~50 kcal mol^{-1} (Parsegian, 1969). Ion channels are classified into two major classes by properties and mechanisms: ion permeation and gating.

(i) Each ion channel, e.g. Na^+, K^+ and Ca^+ has the selective permeability that allows ions to be specified by name. The substantial selectivity involves various factors mainly: size, valency, and hydration energy (Grant, 2009) and determines the permeability ratio from the reversal membrane potential under biological conditions at zero net current (Roux et al., 2011).

(ii) The gating system is another crucial property of ion channels to control membrane potential by closing and opening the gate and ion passage, switching between the two conditions. Hence, three gating mechanisms are classified, including voltage-dependent, ligand-dependent, and mechano-sensitive gating. The voltage-gate ion channels can adjust the electric conductance that correlate with the membrane potential. Mostly, voltage-dependent gating generally occurs in the ion channel. In contrast, the ligand-dependent gating plays an important role in the cardiac ion channel. The last gating is mechano-sensitive or stretch-activated channel about which we still have limited information. Interestingly, this ion channel can adjust an electric signal in the channel conduction (Grant, 2009). In spite of the many roles of ion channels, the most notable main task is responsibility for sending and signalling to keep the equilibrium in both closing (non-conducting) and opening (conducting) states in the cells (Minor Jr, 2009). The structures of ion channels can differ greatly in the number of the individual protein subunits or group subunits. Generally, a structure of cation channels is formed by six hydrophobic transmembrane domains including C-terminus and N-terminus. The pore which is generated within the central loop within the transmembrane domains at 5^{th} and 6^{th} (Bradding & Wuff, 2017).

However, two main typical forming ion channels have been found to be different. The sodium and calcium channels comprise only a single (α) subunit which has four repeats of six transmembrane domains (6TMDs) per channel. In comparison to voltage-gated potassium channels, voltage-dependent are generated from four separate subunits, each containing a single six–transmembrane domains (6TMDs) per channel (Ackerman, 1997) and mostly the ion channel proteins are assembled in oligomers to function (Tabassum & Feroz, 2011). Over many decades of investigation, it has been found that ion channels have very

high diversity and there are over 300 different types in virtually all physiological cell functions (Gabashvili et al., 2007). Therefore, ion channels have numerous significant roles in many cell mechanisms, including the regulation of water levels and hormone secretion, sensory systems, recognition, and behaviour (Kandel et al., 2000: Gabashvili et al., 2007).

Potassium Channels

Potassium channels (K^+) are the largest family and have the most diversity located in cell membranes (Hille, 2001), known as integral membrane proteins that exist in many cell types, except some parasites (Kuo et al., 2005). In humans, potassium ions transport K^+ across the membrane cellular functions, such as neuronal resting membranes, and have significance in the excitability of individual neurons and heart and brain tissue. Much published work indicates that if protein channels malfunction, it would result in serious human health and diseases (Minor Jr, 2001). Since the potassium channel gene was first cloned from the *Drosophila Shaker* locus (Pongs et al., 1988) more than a hundred different types of potassium channels have been identified. These have been classified and other numerous types are still being discovered (Mathie et al., 2003). Thus, many different K^+ channels are categorised from α structure and subunits in three main types including;

(i) 6TMDs are the biggest class of K^+ channels which contain two subclasses: the first is the Ca^+-activated (BKKca, IKca and SKCa) and the second is the voltage-gated K^+ with twelve sub-families (Kv1 to Kv12) (Buckingham et al., 2005). Kv is activated by changes in transmembrane voltage (Gutman et al., 2005). The channels are formed from six trans-membrane domains and a single pore-forming domain.

(ii) 4TMDs are a special class of potassium channels, also known as tandem pore domain (K2P) channels. The channels present with four transmembrane domains and two pore-forming domains (P1 and P2). Both pores include the selective filter motif, however only P1 conserves the GY(F)G but not in P2 which has a different sequence of GIG or GLG (Kim, 2005).

(iii) 2TMDs: inwardly rectifying (Kir), the function is to regulate the intracellular factors and control the K^+ ions passing into the cell from outwards (Schrempf et al., 1995). Kir is expressed in both states of excitable and non-excitable tissues. Structurally, Kir has a fundamental structure with the two transmembrane domains, a single pore loop, N-terminus and C-terminus domains (Kubo et al., 2005). Formed from tetramers, either hetero or homo were categorized into seven families (Kir1-Kir7) (Hibino et al., 2010). Kir channels are important for the functional regulation of K^+ homeostasis and membrane potential in many cell types, mainly vascular cells, heart, brain, and pancreas (Kubo et al., 2005).

All three types of potassium channels (Fig. 2) present different structures, such as semi-symmetrical or symmetrical structures that mostly require four P domains per single channel in two transmembranes (2TMDs) and six transmembranes (6TMDs). In contrast, four transmembranes (4TMDs) require only two P domains (Salkoff et al., 2005).

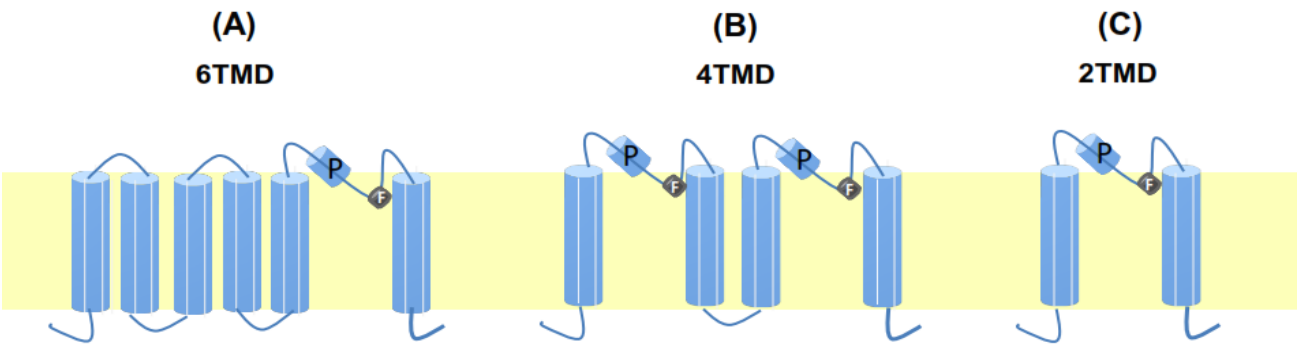

Figure 2: The transmembrane topology, pore forming and selectivity filter among three main types of potassium channels, (A) 6TMDs or voltage-gate K^+ channels contain six transmembrane domains and a single pore-forming domain, (B) 4TMDs channels/tandem pore domain (K2P) are an unusual structure of K^+ channels containing 4 transmembrane and 2 pore domains, and (C) 2TMDs channels/inwardly rectifying contain two transmembrane and a single pore forming domain (Adapted from Buckingham, 2005).

K^+ channels are highly selective, over 10,000 times more for K^+ than Na^+ ions (Doyle et al., 1998). The selectivity can also indicate the efficiency discrimination of a protein channel between ions, e.g. between K^+ and Na^+ (Hertel et al., 2010). The central pore of K^+ channels are predicted to have greatly higher selectivity possible due to ion interaction as well as the pore walls (Hille, 2001). A selectivity filter might be contained in a cylindrical pore that is present inside the diameter about 3-3.4 Å. The pore loop, with a signature sequence indicating the highly conservative K^+ channels, will determine the selective filter and binding of oxygen dipoles. In comparison, potassium binding sites are mostly from carbonyl dipoles from which the amino acid residue is derived from the signature sequence TVGYG (Heginbotham et al., 1994). It is well known that the most typical structure of K^+ channels are thought to be composed of two transmembranes that are associated to a single pore loop with a highly conservative signature sequence or consensus motif selectivity filter TxxTxG (Y/F) G, (where X is a variable amino acid, Doyle et al., 1998). Prior studies reveal that the potassium ion

channels are highly encoded from viruses especially from the hosts living in fresh water habitats (Siotto et al**.**, 2014).

Viral Potassium Channel Kcv

The Kcv potassium channel is the most primitive across most K^+ channels and is well known by the complex name of *Paramecium bursaria* Chlorella, PBCV- 1, genus Chloroviruses, family Phycodnaviridae. The symbiotic life between green algae (Chlorella strain NC64A) in paramecium *P. bursaria* containing virus to replicate Kcv (Plugge et al., 2000). Thus, the study found that the PBCV-1 was the first known to encode the functions and the structures of a K^+ channel called Kcv (Gazzarrini, 2003). Interestingly, the life of Chlorella is protected from lytic viral infection by endosymbiosis and without protection, the algae will be infected and killed rapidly (Plugge et al., 2000). As a result, the Kcv genes from the infection stage, present the remarkable structures and functions of K^+ channels both in eukaryotes and prokaryotes (Thiel et al., 2011).

Function of Kcv in the Life Cycle of the Virus

The Kcv is a package of virion that plays an important role of the virus during initial infection stage to the Cholorella-like green algae host. As shown in the (Fig.3) illustration, the Kcv is located in the membrane of the viral particles (Frohns et al., 2006; Mehmel et al., 2003). The PBCV-1 initially infects the chlorella by attaching a virus vertex and fusing it to the external cell wall. Eventually, the DNA genome and various proteins present in the host membrane (Thiel et al., 2010). Apparently, the host cell is promptly charged from the process of the K^+ conductance and depolarization. Eventually, the K^+ efflux happens according to the degradation of the cell wall and viral DNA is released (Wang et al., 2011).

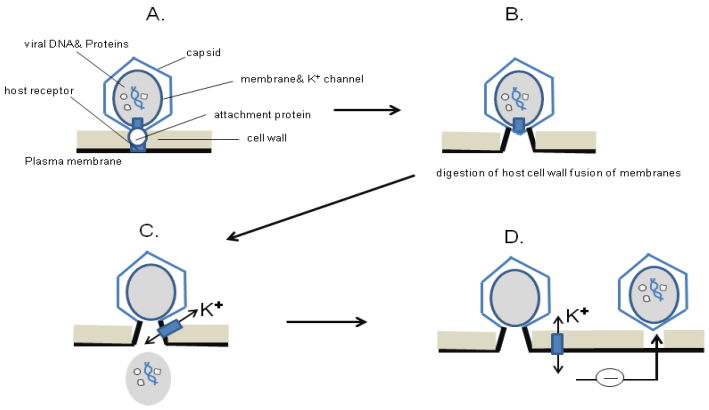

Figure 3: The PBCV-1 infection stages in unicellular green algae (Chlorella NC64A) by endosymbiosis, PBCV-1 including capsid is attaching to the plasma membrane of the host (A), Digestion of the host cell wall and consequential fusion of membranes between virus and host cell results in the Kcv release to the cell membrane (B), Elevated K^+ conductance in the host cell leads to depolarization of the charge (C), and (D) membrane depolarization may help the mechanism to avoid multiple infections (Adapted from Mehmel et al., 2003).

Members of viral Kcv for coding Potassium Channels

The first known Kcv-PBCV-1 is viral, however, there are additionally three viral Kcv types in the family Phycodnaviridae which infect different hosts. Most viral Kcvs have the symbiotic life with the unicellular green algae, except for EsV1-1 which has the filamentous brown algae as a host (Thiel et al., 2011). The details of each Kcv is shown in Table 1.

Table 1: The member of viral Kcvs which is the code for the potassium channels.

Virus types	Genome size (Kb)	Host	Amino acids
PBCV-1	331	Chlorella NC64A	94
ATCV	288	Chlorella SAG3.83	82
MT325	314	Chlorella Pb1	95
EsV-1	336	*Ectocarpus siliculosus*	124

* (Adapted the information from Thiel et al., 2011)

Kcv Expression in the Heterologous Systems

According to functional evolution, excellent evidence shows that the Kcv channel can be expressed by virus replication. In addition to that, expression of the Kcv mRNA or cDNA is able to form variant functions of the K^+ channel as described previously, in particular Ba^{2+} sensitive in heterologous expression systems using *Xenopus laevis* oocytes (frog eggs) or mammalian cells, mainly HEK293 cells and Chinese hamster ovary (CHO) cells (Plugge et al., 2000: Gazzarrini et al., 2002; Kang et al., 2004: Gazzarrini et al., 2009). In terms of heterologous expression systems, the *Xenopus* oocytes are widely employed as biological systems for characterisation and expression of channel proteins and other transporters from animals (Sigel, 1990). Further, the Kcv protein also can be expressed *in vitro*, or through the over expression in a eukaryotic system, as well as being able to be successfully purified and functionally reconstituted into an artificial lipid bilayer at a single channel level (Pagliuca et al., 2007; Shim et al., 2007).

Kcv Structure and Function

Apparently, the viral Kcv channel presents all its structures in resemblance to the typical pore module of all K^+ channels. Tetramer function is formed by the Kcv that also presents itself in other typical K^+ channels, including gating, selectivity to voltage and susceptibility to K^+ channels blocker, such as Ba^2 (Plugge et al., 2000: Gazzarrini et al., 2009) and other complex eukaryotic channels (Shim et al., 2007). In contrast to other viral K^+, Kcv is a miniature sized protein that has a similar structure to the bacterial K^+ channel (KirBac1.1) that contains the longer length of 333 amino acids (Kuo et al., 2003). To illustrate both of these two structures, the schematic is shown in (Fig. 4). The Kcv channels are modulated by two transmembrane domains, TM1 and TM2 with a pore region between two domains that are linked by a P-Helix (Tayefeh et al., 2009: Hertel et al., 2010). This typical structural formation of two transmembranes presents a filter region bearing and the sequence TxxTxGY/FGD (Fig. 5), an extracellular turret, and short twelve amino acids (12aa) at N-terminal domain, that form a short helix (Tayefeh. 2007b). The Kcv channel is predicted to terminate at either the TM2 at the C terminus of cis-membrane (Gazzarrini et al., 2002), or in this part is totally merged into the lipid bilayer (Braun et al., 2013).

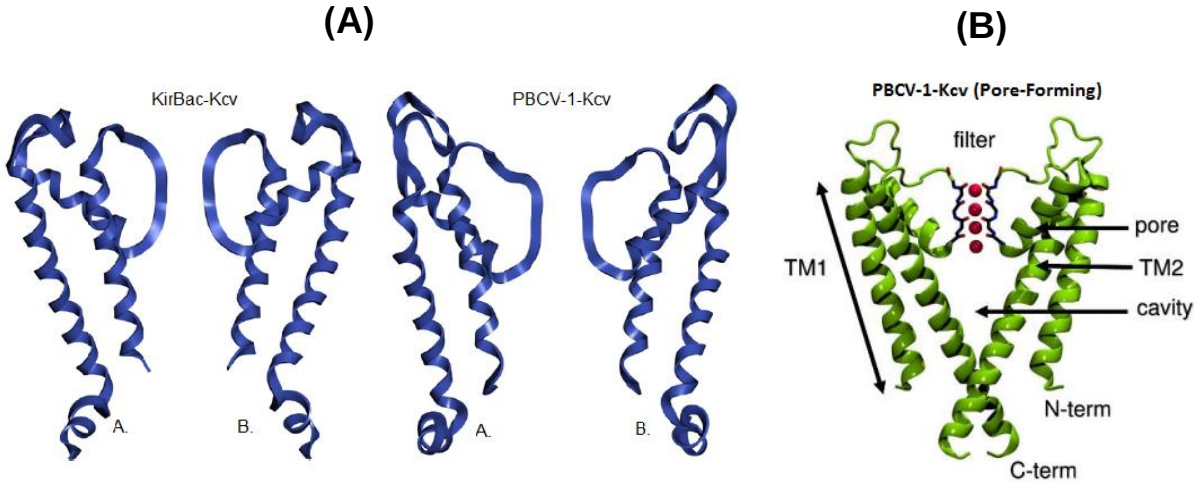

Figure 4: Tetramoric potassium channels; (A-Blue) represents the similarity between structures of KirBac-Kcv and Kcv-PBCV-1 in two opposite sides. The images were created by MOLCAD (Thiel et al., 2011); (B-Green) illustration showing details of structures and functions of Kcv (Tayefeh et al., 2009).

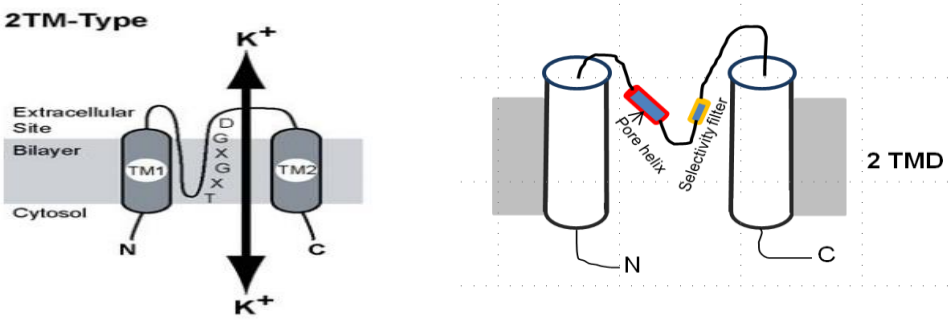

Figure 5: The typical Kcv topology with a 2 TM-type. The pathway of ion conduction is established by signature sequence "TXGXGD" representation between the two C-Terminal transmembrane domains (modified from Tayefeh, 2007a)

The Ribosome

In all living cells, proteins are produced on the ribosome at the peptidyl transferase centre (PTC). It is well known that the ribosome is an "intracellular nanofactory" responsible for translation and the production of nascent polypeptides by addition of amino acids (Green & Noller 1997). In regard to ribosomal structure, the bacterial ribosome consists of two subunits, a small 30S subunit and a large 50S subunit which in association make up the 70S ribosome (Ramakrishnan et al., 2002; Seidelt et al., 2009). Similarly, the eukaryotic structure contains two subunits; a small 40S subunit and a large 60S subunit but they are much larger and more complex than the prokaryotic structures, formed as the 80S ribosome (Ban et al.,

2000; Carter et al., 2000; Wimberly et al., 2000; Schluenzen et al., 2000; Wilson & Daudna Cate, 2012). The RNA present in two ribosomes; (i) prokaryotic ribosome, the small 30S subunit consists of 16S RNA and the large 50S subunit comprises two RNAs; 58 RNA and 23 RNA, and (ii) the eukaryotic ribosome, the small 40S subunit contains an 18S RNA and the large 60S subunit presents three RNA; 5S RNA, 5.8S and 28S RNA (as shown in Fig. 6). Despite difference in size and some components, the process of protein synthesis of prokaryotic cells and eukaryotic cells are likely to have the same main processes; initiation, elongation, and termination (Berg et al., 2002).

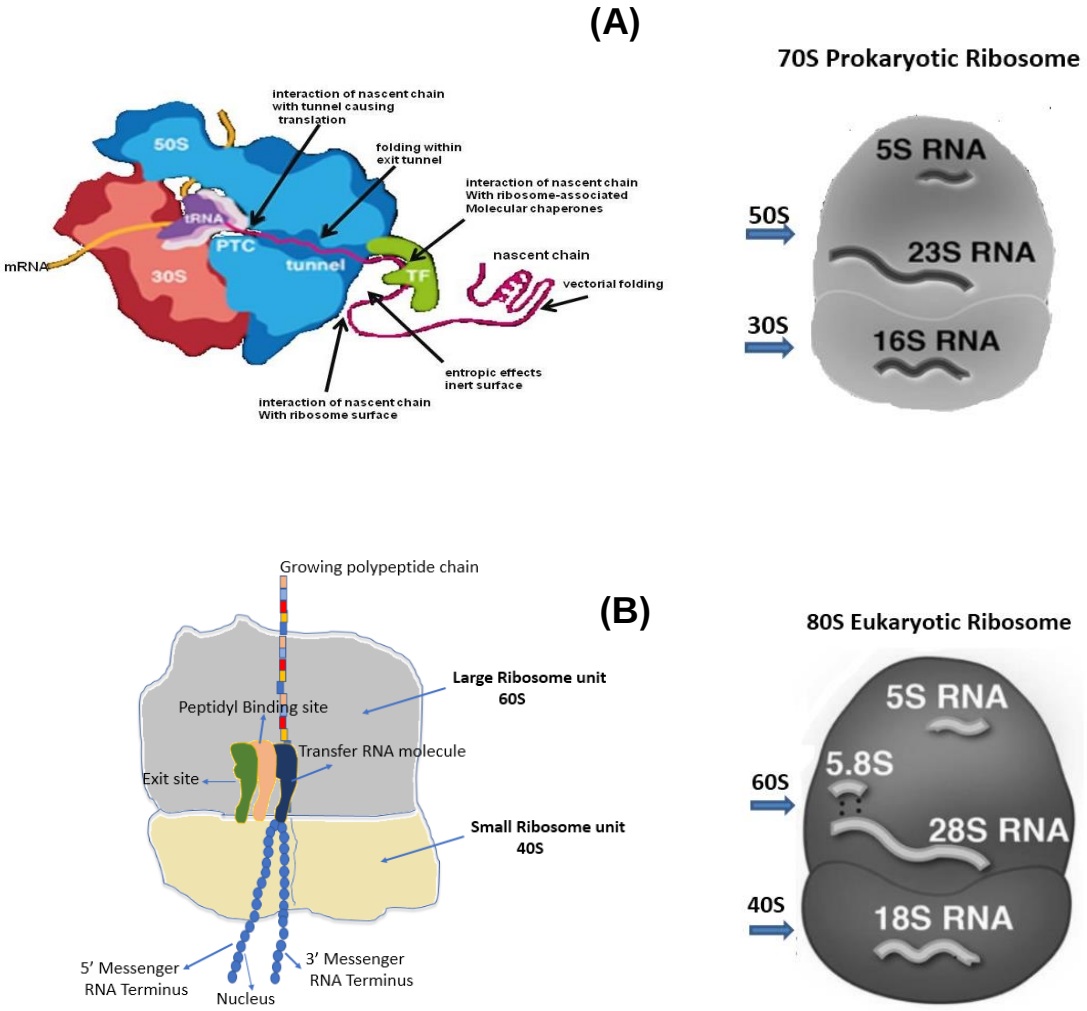

Figure 6: The schematic of the ribosome structure; (A) represents the function and structure of prokaryotic ribosome, including the small ribosomal subunit (30 S), the large ribosome subunit (50S). Comparison between the two subunits is the PTC, which includes tRNA and the elongating nascent chain (Adapted from Christodoulou Group Website, 2016), and (B) illustrates(the function and structure of eukaryotic ribosome containing the small subunit (40S) and the large subunit (60S).

Prokaryotic Protein Synthesis

The translation is the final step of the gene expression from the mRNA to the protein (Huang, 2011). In prokaryotes, the process that starts during transcription takes place inside the cell. The complex initiation is formed on the 30S small ribosome subunit that requires essential factors to achieve the process – referred to as 'three intermediary complexes'- these being the beginning phase, including (i) aminoacylated and formylated initiator tRNA (fMet-$tRNA_f^{Met}$), (ii) mRNA, and (iii) the three factors (IF-1, IF-2, and IF-3) (Laursen et al., 2005). Convincing demonstration suggests that all IFs members play essential roles for supporting translation initiation more accurately and faster (Hartz et al.,1989). At the beginning of the process, IF-3 has initial contact with the binding site at the small subunit, where it can explain the anti-association effect and dissociation of the ribosome. In addition to that, IF-3 presents a two-model protein that is thought to select the fMet-$tRNA_f^{Met}$ as well as correct the starting codon (Hussain, 2016). IF-3 allows IF-1 to bind to the ribosomal A-site and subsequently translocate to the initiator tRNA to the ribosomal P-site (Petrelli et al., 2001). Previous studies suggest that binding between IF1 and A-site of the small subunit (30S) is predicted to move the tRNA in order to associate with the ribosomal P-site by hampering the ribosomal A-site (Carter et al., 2001). The initiation factor (IF-2) is a GTPase binding site that stimulates the fMet-$tRNA_f^{Met}$ binding to the small ribosomal (30s) as a ternary complex IF-2 GTP fMet-$tRNA_f^{Met}$.GTPase which leads to binding in the ribosomal P-site (Milon et al., 2010; Lockwood et al., 1971). Hence, IF-2 is the last factor to post fMet-$tRNA_f^{Met}$ in the ribosomal P-site of the large subunit (70S) and when the dipeptide formation has initially formed, the IF-2 is also gradually dissociated from the ribosome (Gualerzi et al., 2001). Finally, IF-3 next binds to the ribosomal E-site due to the prevention mechanism of association with the large subunit (Dallas & Noller 2001) In addition to that, the initiation process of the prokaryotic translation from the mRNA to the proteins, the purine rich sequence (Shine-dalgarno) is present in the 5' region of the mRNA that is located between 5-8 base pairs (5'-ACCUCCUUA-3') upstream AUG (Shine & Dalgano, 1974). Evidence reveals that the 30S initially binds with the Shine-dalgarno sequence near to the AUG starting codon that is complementary to the 3' end of 16S RNA (Gualerzi & Pon, 1990). At this point, the translation pathway undergoes trough elongation, or termination unless it obtains protein or recycles some of the imperfect proteins (Fig. 7).

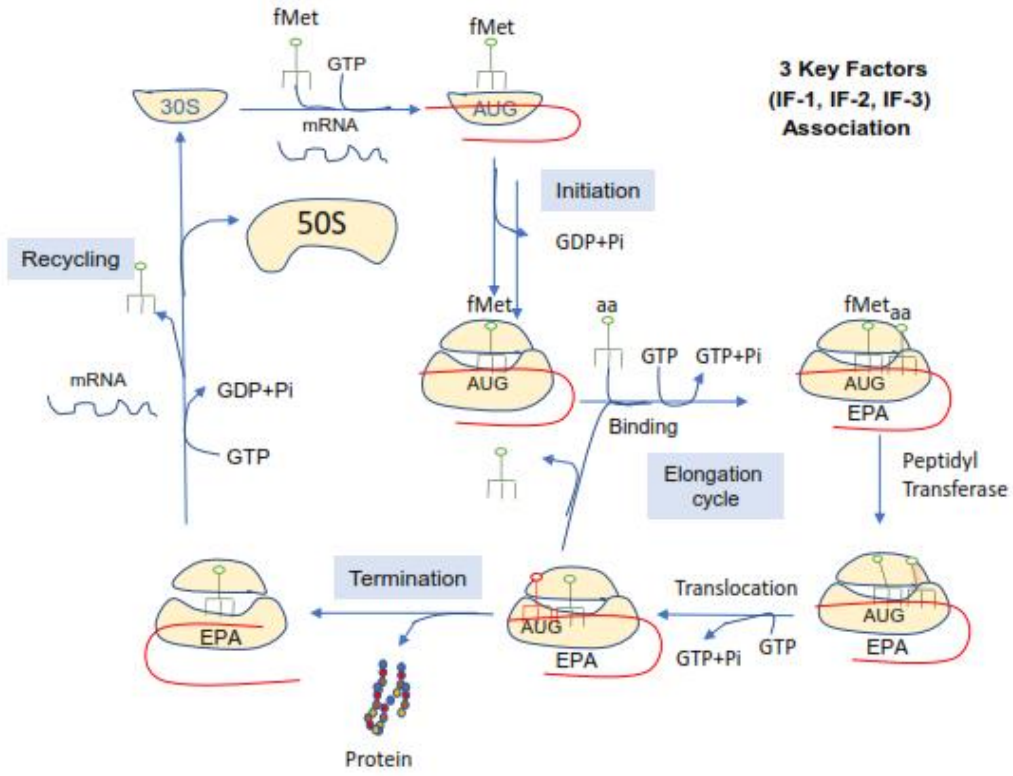

Figure 7: The overview of the protein synthesis of prokaryotic cells. The cartoons show the four steps of the protein synthesis and the ribosome function during the process. Association of intermediate complexes involved in the pathway; tRNA, mRNA, IFs, and GTP interaction (Adapted from Hershey et al., 2012).

Eukaryotic Protein Synthesis

In contrast to the prokaryotic translation pathway, eukaryotes have some beginning genetic codes and special aminoacyl-tRNAs and their synthetase. Generally, the translation takes place on the ribosome where the eukaryotic ribosomal two main subunits are present. These are larger in size than the prokaryotes and named; 40S subunit and 60S subunit (Wilson & Daudna Cate, 2012). However, the mechanism of ribosome coordinates to mRNA as well as the initiating site, are totally different. Prokaryotic mRNAs are bound to the ribosome due to base pairing while the eukaryotic mRNAs are matched by a codon scanning method (Kozak, 1999). The eukaryotic protein synthesis is relevant to the protein complex factors in which there is apparently sequential utilisation in each main step, including, initiation, elongation and termination (Merrick et al., 1997). The translation is the biogenesis for converting the mRNA to protein by association to the ribosome. First, the 40S subunit of the

ribosome is bound with mRNA to form the 40S-mRNA complex and the 60S subunit is formed as the 80S-mRNA. Although AUG is the initiating translation codon in all eukaryotes, the eukaryotic mRNAs do not contain a purine rich sequence/binding sequence on the 5' end like in prokaryotes. When the 40S subunit binds to the cap 5' mRNA, the nearest start codon AUG is searched by scanning stepwise through the 3' direction. The rapid scanning process requires energy in the form of ATP.

Earlier studies show that energy is obtained while the tRNA anticodon is inducing conformational change in the ribosomal A-site (Rastogi, 2002; Allnér & Nilson, 2011). The met-tRNA facilitates initial anticodon binding with AUG, the methionine codon which is the most common start codon in most eukaryotic proteins. The initiation of the protein synthesis always begins with a methionine. The important initiating factors of eukaryotes involve nine factors which have different subunits. Eukaryotic initiation factors have the prefix named eIF. The factors have been defined by their functions. The eIF2 induces met-RNA binding with the 40S subunit and promotes binding of anticodon to the mRNA codon. The eIF2 and eIF3 are incorporated in the initiation process to enhance the binding of met-tRNA and mRNA located nearest to the 5' end (Rastogi, 2002; Mayeur et al., 2003). The eIF4 acts as the energy protein that possesses ATPase and RNAhelicase activities (Rastogi, 2002; Svitkin et al., 2001). The eIF5 stimulates the releasing of eIF2 and eIF3, the pairing of met-tRNA with the start codon AUG. Upon this step, eIF5 forms the complex with eIF2 to trigger the GTP-binding protein. Finally, the 60S subunit is associated with the complex of tRNA, mRNA, and the 40S subunit. The elongation and termination of the synthesis, the chain termination is released from only one single factor 'eRF' that can recognise all of the three stop codons; UAA, UAG, and UGA (Rastogi, 2002; Chavatte et al., 2003).

Cell Free Protein Synthesis (CFPS) System

Cell free protein synthesis (CFPS) is termed in biological technology as the activation of protein production systems without utilisation of any living cells (Hodgman & Jewett, 2011). The cell free protein synthesis is becoming widely used as an advantageous cellular base tool that can establish highly efficient protein production over many decades. The technology has been developed inspiring the research work to have better understanding of the protein pathways; such as transcription and translation (Carlson et al., 2012). According to the timeline of the technological invention system, the basic concept of the CFPS relies on the sequence processes; first bacteria is grown, the cells are harvested, and then undergo lysis. (Swartz et al., 2012). Recently, the basic process is one of CFPS systems that were established as a standard protocol for protein production, including cell culture, cell lysis, centrifugation, run-off reaction, dialysis, and centrifugation. *E.coli* S30 extract is used as the

basis for the CFPS system that provides an ensemble of components from the crude cell lysates. This cellular lysate is composed of active enzymes and auxiliary factors that are essentially used during the protein synthesis processes; transcription, translation, and protein folding (Kwon & Jewett, 2015). According to much published work, it has been revealed that protein folding *in vitro* systems of either *E. coli* 30 extract or wheat germ extract prevent the hydrophobic region of the target protein from other unwanted factors by providing an optimised natural environment. Additionally, there are various useful supportive aspects to *in vitro* folding systems; associating co factors (ion-sulfur groups), promoting formation of disulfide bond, and disulfide bond isomerization (Kim & Swartz, 2014; Carlson et al., 2012).

Proteins Targeting Pathway of the Nascent chain

After being newly synthesised, assistant factors actively associate nascent polypeptides targeting the correct localisation, such as ribosomal proteins, signal recognition particle (SRP) and other intermediate complexes.

Ribosomal Protein

Since being discovered over 40 years ago, there has been a lot of speculation about the role of the diversity of ribosomal proteins. However, the definition is based on the proteins located within the ribosome or on the ribosomal RNA (Korobeinnikova et al., 2012). The studies show that the location of the ribosome can be related to the biogenesis steps or translation within the ribosome (Ferreira-cerca et al., 2005). The ribosome tunnel of bacteria comprises a tunnel, which is formed by 23S RNA containing the segment of ribosome proteins L4, L22, and L23. As shown in (Fig. 8) the L23-RNA complex is situated in the A-site domain of the peptidyl transferase centre (PTC) (Vester & Garret, 1984). If measured, a constriction region in the ribosome is approximately 30 Å from the PTC. At that point through the rim of the ribosome, there are the conserved ribosomal proteins, including L22, L23, L24. and L29 (Kramer et al., 2009). Ribosomal protein L23 is a primary protein from the ribosome of *Escherichia coli* (Fig. 8), that has been used for cross-linking in the study of puromycin for many decades (Vester & Garret, 1984). L23 is present at the large unit (50S) of the ribosome near the exit tunnel (Fedyukina & Cavagnero, 2011). Much published work has been carried out with ribosomal proteins and findings reveal the interaction they have to the co-translation factors (SRP) at the exit tunnel (Ferreira-cerca et al., 2005). Furthermore, it was found that L23 is important for *E. coli* growth as well as being responsible for Trigger Factor (TF) in the ribosome (Kramer et al., 2002).

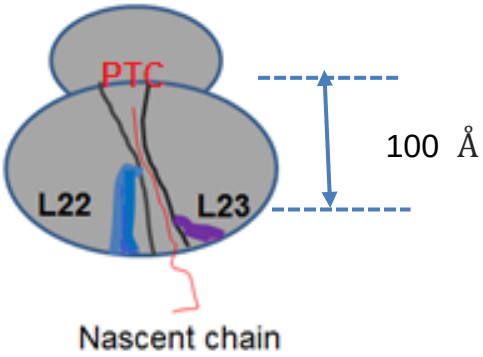

Figure 8: The contribution of ribosomal proteins at the large unit of the prokaryotic ribosome which is close to the ribosome exit tunnel.

Signal Recognition Particle (SRP)

The Signal Recognition Particle (SRP) plays a significant role to intermediate the newly synthesised membrane protein to the endoplasmic reticulum (ER) membrane during the translation process (Keenan et al., 2001). This process is known as translocation. The SRP is an abundant cytosolic ribonucleic protein/protein-RNA complex present in variant composition across cellular organisms (Lütcke, 1995; Keenan et al., 2001; Nagai et al., 2003). Throughout all species, SRP have a universal conserved function and consist of two essential components: the SRP54 protein and SRR RNA (in bacteria; Ffh and 4.5S, respectively (Walter & Blobel, 1981). As shown in (Fig. 9), the SRP54 (Ffh) comprises three domains, such as the N domain (α-helical domain), the G domain (GTP binding region that together with GTPase), and the M domain (methionine rich/α-helical domain). The M domain consists of a hydrophobic groove that serves as a signal sequence binding site and α helix turn-helix motif that binds the 4.5S RNA (Luirink et at., 1994). A homolog, SRP54/Ffh known as 54kDa/48kDa proteins, also share a similar sequence and a similar structure and function (Bernstein et al., 1993). Therefore, both homolog proteins are being used to determine extensive protein interaction and targeting that can reveal the process of cell adaption and evolution.

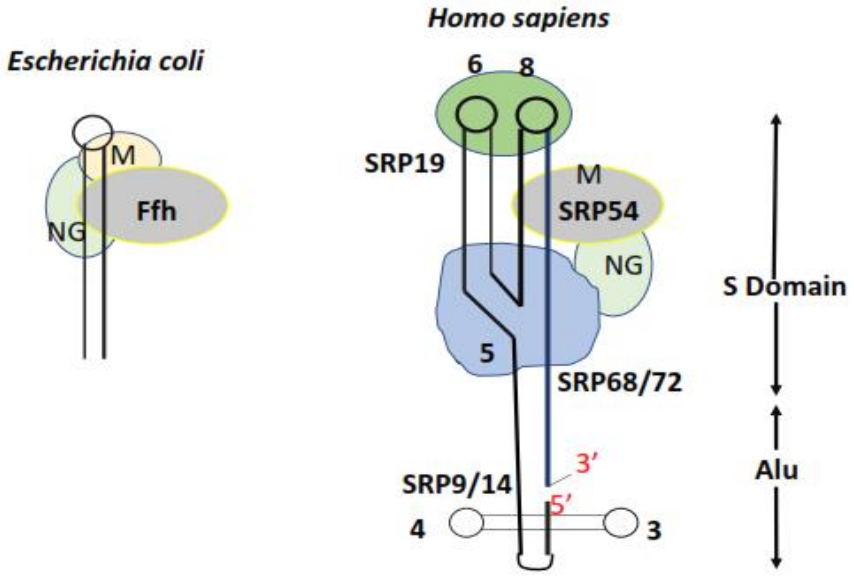

Figure 9: Structure, localisation and distinct domains of SRPs between *E.coli* (prokaryotic cell) and *H. sapiens* (eukaryotic cell) (Adapted from Nagai et al., 2003)

SRP Function as the Protein Targeting Pathway

All cells absolutely need a transport system for co- or post-translational targeting of secretory proteins to the right location (Luirink & Sinning, 2004). Following the nascent polypeptides synthesis from the ribosome, the signal recognition particle (SRP) or a ribonucleoprotein complex will target the ribosome-nascent chain complexes to the translocation site (Beckert et al., 2015). At this point in both prokaryotes and eukaryotes, the nascent chain will be delivered through the protein biogenesis pathway in the vicinity of the endoplasmic reticulum (ER) and are linked to their final destination in the extracellular space in the plasma membrane. The ER is an organelle that is located in the intracellular space where the protein folding and assembly is (Luirink & Sinning, 2004; Zhang & Kaufman, 2006). Generally, a translocation process happens when the ribosome associates with the nascent chains, then the protein is translocated into the translocon site at the ER of the cell. Furthermore, the important auxiliary process, RNC-SRP/SR complex is regulated by GTPase which is present in SRP and SR. Thus, the conformation will be changed from inducing the interaction with the ribosome (Luirink & Sinning, 2004). The folding event recognises a signal peptide by the SRP-RNA-protein complex (called cargo) that provides the conserved mechanism for targeting the hydrophobic sequence at the N-terminus site of nascent polypeptides, when the nascent chain emerges beyond the exit ribosome tunnel (Duadna & Batey, 2004). However, in addition to the above, the RNC/SRP-SP will be transported to translocon ER membrane targeting Sec61p (Eukaryotes), or SecYEG (Prokaryotes), where

variant Sec(x) refers to the complex in the ER-membrane. Upon the biogenesis pathway, when the RNC is delivered to the Sec61p or SecYEG site, the nascent polypeptides can either combine into the lipid bilayer or translocate to the secretory pathway (Akopian et al., 2013). The sample overview of the protein targeting is shown in (Fig. 10).

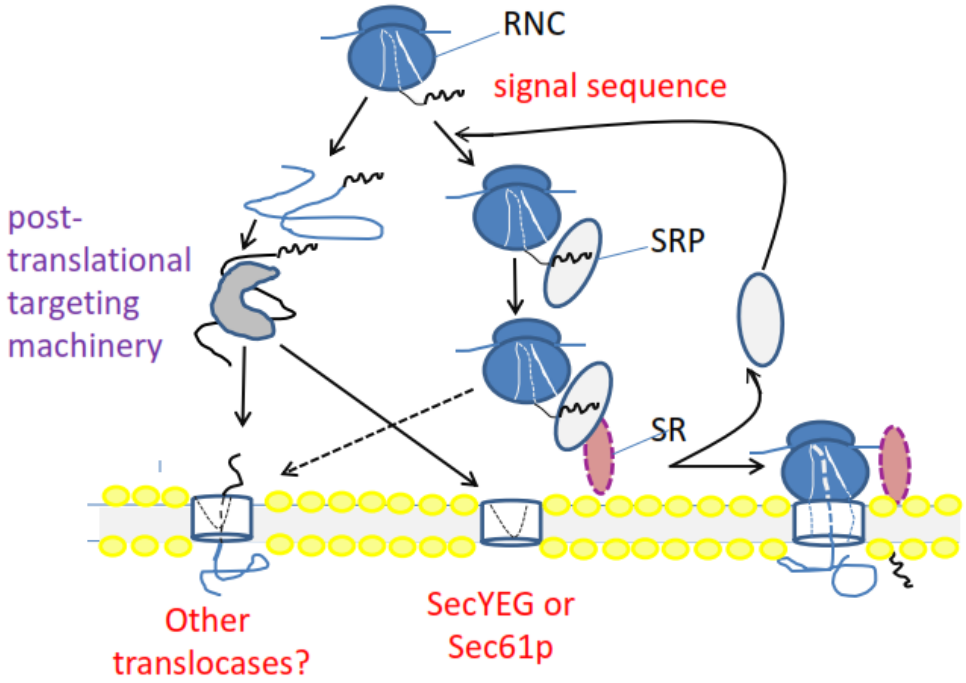

Figure 10: The schematic pathway of the SRP mediates the ribosome nascent complex to the translocon SecYEG in prokaryotes or Sec61p in Eukaryotes. The sequence pathway passes through the ER and finally targets the biological membrane (Adapted from Akopian et al., 2013).

Protein Folding

Protein folding is the bioprocess whereby the functional structural formation from the polypeptide chain (linear polymers) folds into a three-dimensional structure. The initial process is to embed the integral part onto the biological membrane thermodynamically in the most stable state. Recently, much published work has determined the folding process as well as the elucidation of the many questions about how proteins still maintain their native state. Therefore, folding is commonly studied by isolating proteins in different states of solution such as in a diluted aqueous condition, and in a state of equilibrium. This allows the study of relaxation kinetics following perturbations, including the use of chemical denaturants, temperature or pressure (Booth, 2003; Woudby et al., 2013). The protein will be folded from an unfolded form to fold by itself (Williamson, 2012). Co-translational protein folding is an area

of increasing interest. The folding of proteins occurs after the polypeptides leave the ribosome, and interact with auxiliary factors. This is very important for membrane proteins, especially the intrinsic hydrophobic properties which still require further research. Many published papers suggest that the membrane proteins establish their tertiary structure by successfully co-translationally inserting into the membrane. However, secondary structure formation is not well understood. In regard to the timing of the folding process, the protein sequence is folded very rapidly. The exact timing of secondary and tertiary folding is critical for the prevention of mis-folding proteins. Hence, protein mis-folding is thought to degrade polypeptide chains (Cabrita et al., 2010). As a result, predictions about the protein folding process of ribosomes can be made. Many researchers have studied the nascent chain formation from the peptidyl transferase centre (PTC) through the ribosome tunnel which accommodates the peptide chain depending on their formations, such as a fully extended nascent chain of approximately 25 residues and fully folded structure (α-helical) at roughly 50-60 residues (Voss et al., 2006; Seidelt et al., 2009; Bhushan et al., 2010). Fluorescence study (Mario et al., 2016) shows the possible concept of the small protein folding event inside or outside the *E.coli* ribosome in different residues, formations, and ribosome destinations (Fig. 11). This gives rise to questions about whether protein folding happens inside or outside the ribosome. However, when the nascent chains leave the ribosome they must be directly associated to the cellular mechanism. Review of literature suggests that the folding process needs associated-complexes when they present the activity in the intracellular cells, that the environment might be very crowded by the assembly proteins. Therefore, the factors during co-translation and targeting are very important for proteins (Zhou, 2013). The auxiliary protein folding will be mentioned below.

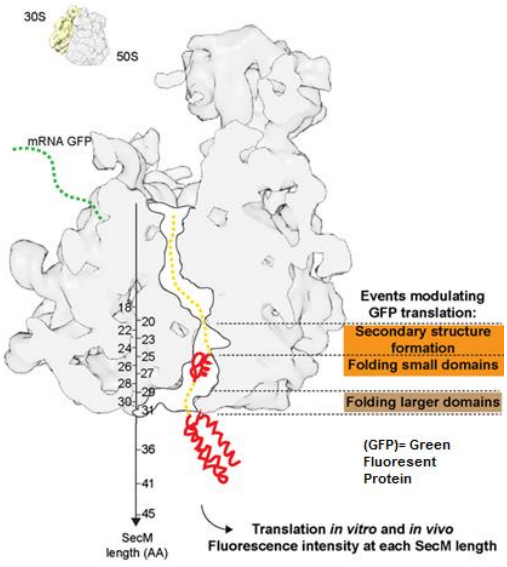

Figure 11: Conceptual folding inside or outside the *E. coli* ribosome tunnel by translation *in vitro* and *in vivo* of fluorescence intensity at each SecM length (Mario et al., 2016)

Kcv Nascent Chain Integration into the Membrane

Watson et al., (2013) show that the Kcv nascent peptides are synthesised in the ribosome as general proteins and co-translate to the endoplasmic reticulum (ER) via the Sec61 translocon. The secretory containing hydrophobic transmembrane domains are laterally inserted into the membrane (phospholipid bilayer) to form the Kcv ion channel, by initial integration of N-terminus which is translocated to N-glycosylation machinery in the ER lumen at the Sec61 complex. Consequently, transmembrane domains in the nascent chain are able to orient their conformation within the optimum conditions in ER to obtain an inherent structure. The study found that the orientation can occur in both *in vitro* and *in vivo* systems. Gebhardt et al., (2011) demonstrates that the membrane is achievably anchored and interacts with the Kcv viral channels to function as an ion channel by the two putative transmembranes model. The experiment findings show that, at the upper halves both TM1 and TM2 interactions with the external region are more rigid, while the lower parts are softer. The outer two transmembranes rigidity can be described by the aromatic acids that are connected to the membrane. The experiment shows the potential integration of transmembrane domains into the bilayer. Both inner transmembrane domains are linked together with the rigid outer transmembrane domain by a pair of aromatic acids.

Force Maintaining the Proteins Structure After Folding

In proteins, the primary structural connection between amino acids are relative to the strong covalent peptide bonds that link a disulphide bond whose covalent bonds combine with the side chain. Basically, two cysteine residues are required to form with the sulfur atom of the thiol group (-SH) for a disulfide bond which is conserved among the proteins. Many studies suggest that the disulfide bond plays a crucial role in proteins, for example, structures and functions. Furthermore, the most significant factor of proteins structural-stabilising is from the forces that are very relevant from the basic hydrophobic interaction to the electrostatic salt-bridges (Thangudu et al., 2008; Dombkowski et al., 2014).

Hydrophobic interaction

Early studies found convincing evidence that hydrophobicity is a vital factor for protein stability in the folded configuration of many native proteins (Kauzmann. 1959; Pace et al., 2011). Greater understanding of hydrophobic evidence is the contribution of a nonpolar side chain. Thus, the stability involves two main factors; hydrophobicity of the side chain and the touching surface which contacts the water during protein folding, and the other is the van der Waals interaction of the side chain after protein folding or unfolding (Yutani et al., 1987; Pace et al., 2011). In addition, previous experimental studies explained why there is

approximately 80% of hydrophobic residue buried inside the protein core (Lesser & Rose, 1990).

Van der Waals force

van der Waals energy is electrostatic interaction of fixed or induced dipoles. The interaction tends to arise most frequently among residues of polarisable chains whose residues refer to methyl or methylene groups. Basically, the van der Waals interactions are more likely to deal with the aromatic hydrophobic residues (Petsko & Ringe, 2004). Previous studies suggest that van der Waals interactions make an important contribution to the stability of the protein because non-polar groups are hidden. Interaction between non-polar residues has led to contribute to increased energy within molecules (Pace et al., 2014). The van der Waals energetic contribution are 8-16 Kj/mol which is the weakest force of the protein stabilisation (Lins & Brasseur, 1995; Petsko & Ringe, 2004). Additionally, the van der Waals energy resembles the roles played by the H-bond due to energetic association for protein stabilisation (Cross, 2013 unpublished).

Hydrogen bond (H-bond)

The hydrogen bond (H-bond) is one of the most important forces containing electrostatic properties (dipole-dipole). The interaction occurs when a hydrogen bond is shared between proton donor (N, F or O)) and proton receptor (Pauling, 1960; Cross, 2013). This intermediate interaction of H-bond plays a critical role in specification and direction to the hydrophobic and hydrophilic transient structures (Hubbard & Haider. 2010). The H-bond is of prominent significance in forming the secondary structures of α helix and β sheet that most proteins are composed of. Thus, the H-bond force can be a determiner and immobilizer of protein folding when its secondary structures are associated with and distributed to the tertiary structure (Bordo & Argos, 1994). In addition, the kinetics and energy of the H-bond make an optimum interaction in the folded structure (Hubbard & Haider, 2010).

Salt-bridges

The role of salt-bridges in protein stabilisation is still unclear, despite a lot of research over the last decades. The basic problem is from the variation of salt-bridges depending on the ionization of the participating groups that are influenced by protein environment as well as other reflections, including thermal fluctuation and their life cycle which comes from the flexibility of the protein (Karshikoff & Jelesarov, 2008). However, convincing evidence reveals that the salt-bridges interaction occurs between the opposite charged side chains that are able to form the interaction with H-bonds. Regarding the salt-bridges formation, in general proteins

side chains possess the amino acids positive charge, such as lysine and arginine that can form the salt-bridges with the anionic residues; glutamate or aspartate side chains (Dill, 1990). At present, experimental findings have confirmed that salt-bridges play an important role in protein folding as a thermodynamic stabilisation force (Meuzelaar et al., 2014).

PEGylation Assay

In the present study, the PEGylation assay is being used for protein modification, in order to investigate the Kcv secondary structures inside the ribosome. We will introduce a mass-tagging strategy of the nascent polypeptide to detect the folding event at the exit side of the ribosomal tunnel, when nascent chains emerge from the exit tunnel and then methoxy-polyethylene glycol maleimide (PEG-MAL) containing a large molecule (5kDa) can be attached to the cysteine residues. As shown in (Fig. 12), upon the PEGylation reaction, the PEG-MAL reagent allows thiol groups of “free” cysteine residues to conjugate to determine the formation of the folded intramolecules. (Doherty et al., 2005). Based on the PEGylation principle, if a cysteine resided within the ribosome tunnel then PEG-MAL is highly inaccessible compared to a cysteine outside the tunnel (Lu & Deutsch, 2005). Preliminary experiments have shown that PEGylation is working effectively with this protein, and that the first TM domain forms the secondary structure within the ribosome tunnel. The protocol of studying channel structure and function recommends that the treatment of PEG-MAL (PEGylation) will PEGylate or shift in size of molecular weight by approximately 10 kDa (Robinson et al., 2006).

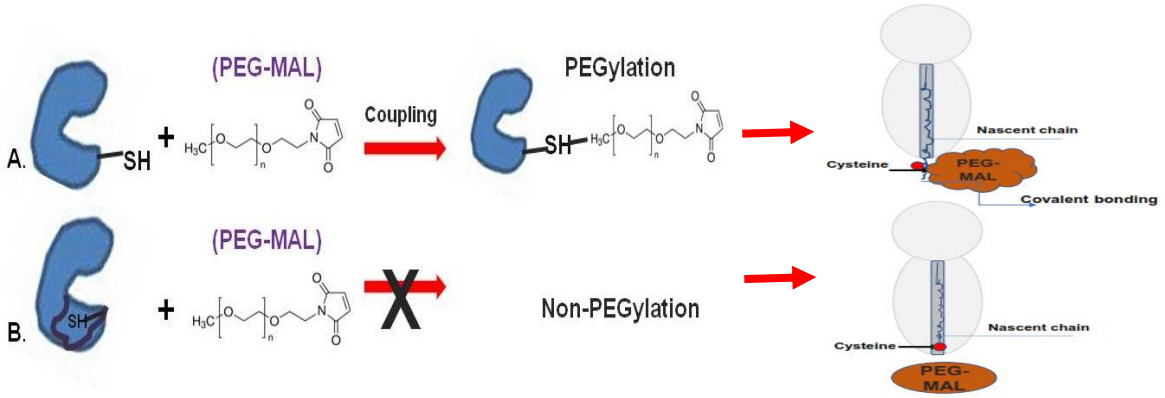

Figure 12: The PEGylation assay reactions; (A) represents PEG-MAL conjugate C-S bonding with a marker cysteine when a nascent chain is released from the ribosome and is successfully PEGylated, and (B) In comparison, the marker cysteine buried inside the ribosome tunnel without the PEGylation due to inaccessibility of PEG-MAL (Modified from Zhang et al., 2016).

Cross-linking Assay

Cross-linking assay is a chemical process that combines two or more molecules by a covalent coupling. Modification of cross-linking technique is thought to arise from the chemical reaction with the specific functional groups within the proteins (Hemaprabha, 2012). Recently, this technique is more preferable and more likely to be used, including identifying protein-protein interaction and detecting interaction of proteins within the ribosome subunit. Currently, this approach is being used for determining the region of ribosomal RNA. Ideally, the posttranslational proteins are treated with the cross-linker reagents conjugated with the specific amino acids which are bound with either the same or different proteins, such as bis-methyl suberimidate (BS^3) which combines lysine-lysine and results in amine-amine linkage. Another example of a cross-linker is bismaleimidohexane (BMH) that can form a covalent bond between cysteine residues and target sulfhydryl-to-sulfhydryl formation. In most cross-linking techniques, the specific molecules are led to form the covalent bonds between proteins (Wittmann.1976). Therefore, the cross-linking reaction is a more likely interaction in both neighbour surface hydrophilisation and enhancing surface hydrophobicity of proteins. Using experimental strategies, the cross-linking method will be achieved according to various important factors, such as; natural stabilisation, spanning, and targeting position of the crosslinks (Tyagi & Gupta, 1998). Regarding the folding and assessment of proteins, technology has been extensively developed and used for many decades in various chemical modifications (Wittmann, 1976). Hence, this project, cross-linking is one of the selective approaches to be used for detecting the protein from the secondary to tertiary structure.

Project Objectives:

1) To analyse the earliest *in vitro* folding event of Kcv within the ribosome exit tunnel from the secondary to tertiary structure especially in the first transmembrane domain.
2) To scrutinise the influence of some amino residues, such as cysteine, lysine, and methionine mutagenesis of Kcv on the initial folding.
3) To distinguish the Kcv topological structure formation from different chemical modifications and the radio-labelling technique.
4) To investigate the interaction of the nascent chain, ribosome, and protein targeting pathway (SRP54 and L23).

MATERIALS AND METHODS

Escherichia coli Strains

The *E.coli* strains used in this project are as follows:

1. C41 competent cell: F-*ompT hsdSB* (rB-mB-) *gal dcm* (DE3)
2. DH5α™ Competent cells:

F–Φ80*lac*ZΔM15Δ (*lac*ZYA-*arg*F) U169 *rec* 1 *end*A1 *hsd*R17-
(rK–, mK+) *pho*A *sup*E44 λ– *thi*-1 *gyr*A96 *rel*A1

Plasmid Vector

pTrc99A is a bacterial expression vector with a lacI promoter which was induced by isopropyl-β-Dthiogalactopyranoside (IPTG). This plasmid contains ampicillin resistant genes which act as a selectable marker as well as containing a multiple cloning site which is useful for restricting enzyme cutting and cloning as shown in (Fig. 13).

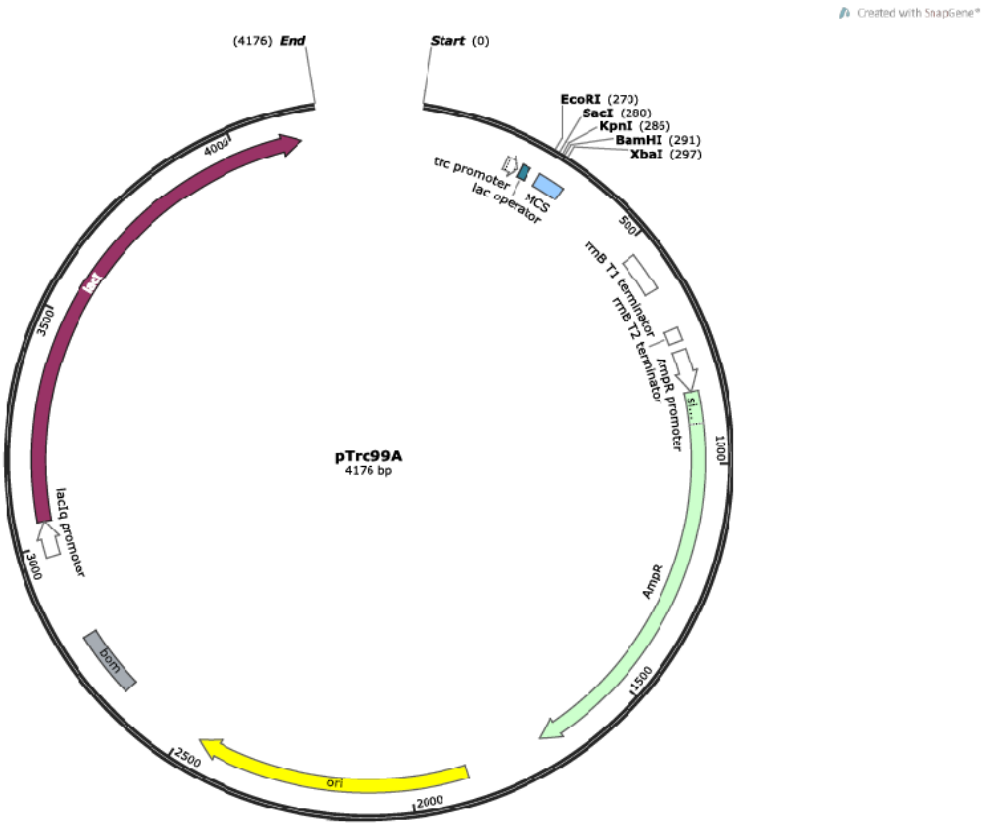

Figure 13: Plasmid mapping of pTrc99A, restricting enzymes and ampicillin resistant gene.

Transformation

The Kcv gene; cysteine engineered (L8C) and wild type gene sequence were constructed into the pTrc99A as a vector. 1 µL of each plasmid DNA was added with 100 µL of the competent cells DH5α *E.coli* into a sterile eppendorf and then incubated on ice for 15 minutes. The cells were heat shocked for 2 minutes at 42^0C and placed on ice again for 5 minutes. After that, 1mL of autoclaved media; Lysogeny broth (LB) was then added to the components and mixed in a shaking incubator at 37ºC for an hour, followed by spinning the cells at 7,000 rpm in the microcentrifuge for 5 minutes, then 800 µL of the supernatant was removed. The remaining cells were streaked onto the sterilized LB/Ampicillin plates and the plates were then left on the bench for 10 minutes. Finally, the transformed plates were placed upside down for incubation overnight at 37ºC.

Preparation of Ribosome Nascent Chains for L8C

Transcription templates were generated from linear DNA and amplified from a PCR kit (Takara). The 5' primer of this reaction was located at the *trc* promoter (5' CTGAAAT GACGTGTTGACA ATTAACATCCGG-3') in the pTrc 99A, while the reverse primers were designed in different lengths of amino acids of Kcv containing 30aa, 40aa, 50aa, 60aa, and 70aa, respectively without a stop codon in the sequence. S-30 extract was provided from C41 (Woolhead et al., 2006). The PCR products were purified by a Quick PCR purification Kit (invitrogen). These PCR products were used in *in vitro* transcription/ translation reactions. The reaction is composed of total volume at 25 µL; 10 µL translation premix, 2.5 µL Amino acids (exclude methionine), 7.5 µL S-30 extract (MW 35,000), 1 µL Antisense oligonucleotide or ssrA 200 ng/ml, 2.5 µL Linear DNA, and radiolabelled [^{35}S] ^{Met}. These components were incubated at 37ºC for 30 minutes and left on ice for 5 minutes. The reactions of 30aa, 40aa, 50aa, 60aa, and 70aa were overlaid on 100 µL 0.5 M sucrose cushion and centrifuged at 100,000 rpm in the TLA-100 rotor for 6 minutes at 4ºC. Supernatants of all reactions were carefully aspirated and then the pellets resuspended with 8 µL RNC buffer, 1 µL RNaseA, and 1 µL EDTA (5 mM final volume). Later, the reactions were transferred to a fresh eppendorf, followed by incubation at 26ºC for 10 minutes and 10 µL protein gel sample buffer was added. Thereafter, the samples were boiled at 65ºC for 10 minutes and 10 µL of the sample was run on SDS-PAGE gel, the gel washed with destaining solution for an hour, gel dried with the dryer machine at 65ºC for 1.5 hours before being placed over the cassette in the dark room and developed into a film overnight (as desirable resolution) with the Kodak X-Omat.

Polymerase Chain Reaction (Regular Amplified PCR)

dsDNA sequence of interest was amplified by desirably designed forward and reverse oligonucleotide primers (Appendix). The proper restriction sites are required for digestion in forward and reverse primers. All primers in this project were purchased from Integrated DNA technologies, Inc. The plasmid of interest as the template and components were prepared on ice in thin-walled PCR tubes. The regular PCR program is shown below:

10x DNA polymerase buffer	10 µL
dNTP mix (2.5 mM each: dATP,dCTP,dGTP,dTTP)	8 µL
Forward primer (100 pMol)	1 µL
Reverse primer (100 pMol)	1 µL
dsDNA **(**Template**)** ~ 100ng**/** µL	1 µL
Ex Taq DNA polymerase	0.5 µL
Nucleus free water	**bring up to 100 µL**

PCR reactions were undergone using the Applied Bioscience 2720 thermal cycler in stand program as following:

Temp	Step	Time	Cycle
94°C	Initial	1 minute	1 Cycle
94°C	Denaturing	30 seconds	30 cycles
56°C	Annealing	30-60 seconds	
72°C	Elongation	1 minute	
72°C	Final Elongation	8 minutes	1 cycle
4°C		Hold	Hold

The standard conditions for PCR can be appropriately set with the melting temperature of the interest primers. Generally, the optimal annealing temperature is approximately 5°C lower than the lowest melting temperature of the designed primers. When the PCR condition was completed, the products were purified by a PCR clean-up Kit (Invitrogen, PureLink™) and were run on a 1% agarose gel to confirm whether the obtained products were the correct molecular weight.

SOC Media for *E.coli* S-30 Extract Preparation

0.05% (w/v) NaCl, 0.5% Yeast Extract, 2% (w/v)Tryptone, 10 mM $MgCl_2$, 10 mM $MgSO_4$, 20 mM Glucose. The components were mixed together and put through a sterilised filter. The SOC media stocks were kept in the freezer until further use.

Preparation of *E.coli* S-30 Extract

C41(DE3) cells from a frozen glycerol stock were streaked on an LB-agar plate and grown overnight at 37^{O}C. From the plate, two single colonies were picked to be inoculated separately in the 5 mL LB-broth and grown overnight at 37^{O}C with the shaker at 300 rpm. The following day, both two 5 mL were merged to inoculate the 500 mL SOC media. The culture was grown at 37^{O}C with the shaker at 300 rpm until it reaches A_{600}-0.8. At this step, 1 litre of ice was slowly added to the culture and centrifuged at 10,000 rpm for 10 minutes at 4^{O}C. The supernatant was removed and the pellets were resuspended in 100 mL of Buffer 1 and centrifuged again at 10,000 rpm for 10 minutes at 4^{O}C. The supernatant was then discarded and the pellet resuspended in 100 mL of the Buffer 1 and recentrifuged for 10 minutes at 4^{O}C. The pellet was collected by removing the supernatant and the cell was weighed and resuspended in Buffer 2 to a final concentration 0.5 g/mL. After that, lysozyme (100mg/mL stock) was then added to a final concentration of 1mg/mL. Following 15 minutes incubation on ice, the suspension cell was disrupted through a French press at 8,000 psi. Disrupted cells were centrifuged at 17,000 rpm for 30 minutes at 4^{O}C. The supernatant was maintained and treated with 0.15 volumes of Run-out premix at 26^{O}C for 70 minutes. Following the treatment, the extract eliminated the contaminant by dialysing 3 times using a Slide-A-Lyzer Dialysis Cassette 3500 MWCO in Buffer 3 for approximately 1 hour each. For the final step, the extract was centrifuged at 10,000 rpm at 4^{O}C for 10 minutes and aliquoted to 1 mL and immediately snap frozen in the liquid Nitrogen and to be stored at -80^{O}C.

***In vitro* Transcription/Translation in *E.coli* S-30 Extract translation**

The translation components were mixed in the *E.coli* transcription/translation system in the standard protocol of Dr. Cheryl Woolhead (approximately 25 µL). Each translation reaction was added as outlined in the information below.

Component	Volume
Translation premix	10 µL
1 mM each L-amino acid (without methionine)	2.5 µL
Linear DNA (~100 ng/ µL)	2.5 µL
E.coli S-30 extract	7.5 µL
[^{35} S] methionine	10 µCi
5 µg/µl of anti-ssrA oligonucleotide (5'- TTAAGCTGCTAAAGCGTAGTTTTCGTCGTCGTTTGCGACTA-3')	1 µL

Total volume 2.5 µL

Following the incubating reaction at 37^{O}C for 30 minutes, the reaction was quenched by chilling on ice for 5 minutes. The sample was run on a SDS-PAGE gel, followed by the autoradiography analysis.

Translation Premix Stock

137.5 mM HEPES (pH7.5), 520 mM K Glu, 68.75 mM NH_4OAc, 48.25 mM MgOAc, 4.25 mM DTT, 3 mM ATP, 2 mM each rNTPs, 6.25 ug/mL creatine Kinase, 200 mM creatine phosphate, 444 ug/mL *E.coli* tRNA, 2 mM IPTG, 60 mg/mL PEG 8000, 170 µM folinic acid, 1.6 mM cAMP

PEGylation Assay

PEGylation assay was initially started with S-30 *in vitro* transcription/translation reaction in total volume at 25 µL individually with truncation linear DNA, such as 30aa, 40aa, 50aa, 60aa, and 70aa, respectively. The reactions were centrifuged by being placed over 100 µL of 0.5 M sucrose cushion for 6 minutes at 100,000 rpm at 4^{o}C in TLA-100 rotor (Beckman). In this step, the pellets contained the ribosome bound nascent chains. The pellets were gently pipetted up and down for resuspending in 60 µL PEG buffer (20mM HEPES (pH 7.2), 100 mM NaCl. 5 mM $MgCl_2$ and 50 µM DTT). Next, the samples were divided into equal volume at 30 µL of each reaction into two fresh eppendorf tubes, including tube number 1 for an additional 30 µL PEG-MAL (1mg/100 µL; PEG-MAL/ PEG buffer) and tube number 2 as a control containing 30 µL of PEG buffer only. The samples were then chilled on ice for two hours. Consequently, 5 µL of 100 mM DTT was added to quench the reaction and left at room temperature for 10 minutes. With each reaction, 600 µL of NaOAc (pH 4.7) was added and 600 µL of 2% CTAB and incubated on ice for 15 minutes to precipitate the ribosome nascent chains. Then all samples were centrifuged at 14,000 rpm for 15 minutes at room temperature. Each supernatant was removed and the pellet remained and 1mL of acetone was added and chilled on dry ice for 10 minutes, then the samples were centrifuged at 14,000 rpm at 4^{o}C for 10 minutes. The pellets were heated to remove acetone at 50^{o}C for 10 minutes. Thereafter, 15 µL of 1 mg/ml RNAseA in distilled H_20 were added to the tube then incubated at room temperature for 10 minutes. Following this, 15 µL of sample buffer was added into each sample and boiled with the heat block at 65^{o}C for 10 minutes. Finally, all samples both of PEGylation and Non-PEGylation were run on the SDS-PAGE gels, the gels washed with the proper destaining solution (400 mL Methanol, 70 mL Acetic acid, and 530 mL distilled water), then dried for 1.5 hours and the process developed into a film overnight with the Kodak X-Omat.

Investigation of ribosome nascent chain protein interaction in the 1st TM domain by chemical cross-Linking assay using 1,6-Bismaleimidoheane (BMH) and immuno-precipitation

To start the experiment, the ribosome nascent chains were generated by increasing four times the components of S-30 *in vitro* transcription/translation in the final volume at 100 µL. The intermediate lengths were prepared individually from linear DNA containing 30aa, 40aa, 50aa, 60aa, and 70aa. Next, the individual reaction was divided into two portions in ultracentrifugation tubes; 7 µL (A) and 93 µL (B) in the total 10 reactions. All reaction tubes were placed over 100 µL of 0.5 M sucrose cushion. Following this, the reactions were

centrifuged in a TLA-100 rotor (Beckman) at 100,000 rpm for 6 minutes. In this step, before cross-linking with 1,6-Bismaleimi-doheane (BMH) investigation, the ribosome nascent chains were generated. A portion of the pellets (A) were mixed with 8 µL of RNC buffer, 1 µL RNase A (1 mg/mL ddH_20) and 1 µL of 5 mM EDTA and incubated at 26^oC for 10 minutes. The samples (A) were heated in 2X Tricine sample buffer at 65^oC for 5 minutes. After cross-linking with BMH investigation, the pellets (B) were resuspended in 88 µL of 1 mM BMH in 1 mM DMSO and incubated at 30^oC for 15 minutes. Cross-linking reactions were terminated by the addition of 10 µL of 1 M DTT and then incubated at room temperature for 15 minutes. At the end of cross-linking reaction, the fresh tubes (B-new; 30aa,40aa.50aa.60aa, and 70aa) 7 µL of cross-linked products were added then mixed well with 8 µL of RNC buffer, 1 µL RNase A (1 mg/mL ddH_20) and 1 µL of 5 mM EDTA and incubated at 26^oC for 10 minutes. All samples (B-new) were heated in 2X Tricine sample buffer at 65^oC for 5 minutes, whereas the remaining samples then had the 9 µL of cold 100% TCA added to precipitate the pellets which were then incubated on ice for 20 minutes and centrifuged at 14,000 rpm at 4^oC. The upper parts of the samples were aspirated to get pellets for use in Immunoprecipitation assay. The TCA pellets were kept in the -20 freezer until further use. The 65^oC heated (A-B new) samples (before/after cross-linking) were run on a SDS-PAGE gel, the gel was then washed with the proper destaining solution (400 mL Methanol, 70 mL Acetic acid, and 530 mL distilled water) then the gel was dried for 1.5 hours and the process developed into a film overnight with the Kodak X-Omat.

Investigation of ribosome nascent chain protein interaction in the 1st TM domain by chemical cross-linking assay using Bis (sulfosuccinimidyl) suberate: BS^3 and immunoprecipitation

Like the previous cross-linking assay using BMH, cross-linking using BS^3 was performed. The ribosome nascent chains were generated by increasing four times the components of S-30 *in vitro* transcription/translation in total volume at 100 µL. The intermediate lengths were made from each linear DNA, including 30aa, 40aa, 50aa, 60aa, and 70aa. Then, each reaction was divided into two portions in ultracentrifugation tubes; 7 µL (called A) and 93 µL (called B) in total 10 tubes of both. All reaction tubes were placed over 100 µL of 0.5 M sucrose cushion. The reactions were centrifuged in a TLA-100 rotor (Beckman) at 100,000 rpm for 6 minutes. This step was before cross-linking with lysine cross-linker (BS^3) investigating in the ribosome nascent chains. The aliquot of the pellets (called A) was mixed with 8 µL of RNC buffer, 1 µL RNase A (1mg/mL ddH_20) and 1 µL of 5 mM EDTA and incubated at 26^oC for 10 minutes. The samples (A) were heated in 2X Tricine

sample buffer at 65°C for 5 minutes. After cross-linking with BS^3, the pellets (called B) were resuspended in 88 µL of 1 mM BS^3 in RNC buffer and incubated on ice for 2 hours. Cross-linking reactions were terminated by adding 5 mL of 1M Tris (pH8.0) and then incubated at room temperature for 15 minutes. At the end of the cross-linking reaction, the fresh tubes of 7 µL of cross-linked products (called B-new; 30aa,40aa.50aa.60aa, and 70aa) were added then mixed well with 8 µL of RNC buffer, 1 µL RNase A (1 mg/mL ddH_20) and 1 µL of 5 mM EDTA and incubated at 26°C for 10 minutes. All samples (B-new) were heated in 2X Tricine sample buffer at 65°C for 5 minutes, whereas cold 9 µL of 100% TCA was then added to the remaining samples to precipitate the pellets and incubated on ice for 20 minutes and centrifuged at 14,000 rpm at 4°C. The upper parts of samples were aspirated to get the pellets to be used in Immunoprecipitation assay. The TCA pellets were kept in the -20°C freezer until further use. The 65°C heated (A-B new) samples (before/after cross-linking) were run on a SDS-PAGE gel, the gel washed with the proper destaining solution (400 mL Methanol, 70 mL Acetic acid, and 530 mL distilled water) dried for 1.5 hours over the dryer machine and the process developed into a film overnight with the Kodak X-Omat.

Investigation of ribosome nascent chain protein interaction in the 1st TM immunoprecipitation (IP) Assay of Cross-linked products

The cross-linked pellets were resuspended in 50 µL of solubilisation buffer (235 µL Trix buffer (23% Glycerol, 333 mM Tris base, 26 mM EDTA pH8), 157 µL of 10% SDS, and 8 µL of 100 mM Phenylmethane Sulfonyl Fluoride (PMSF), mixed well by vortex and heated to dissolve the remaining at 95°C for 5 minutes. Afterward, 1 mL of cold low-salt RIPA buffer was added (150 mM NaCl, 50 mMTris pH 8, 1% IGEPAL CA-63, 0.5% Deoxycholic acid and 0.1% SDS), respectively. Then, the samples were isolated by centrifugation at 14,000 rpm for 10 minutes at 4°C. 1 mL of supernatants were collected from the samples and then divided into 2 fresh tubes for the addition of antibodies; either anti-L23 or another one for anti-SRP54 (SRP protein, homologous to the prokaryotic Ffh) and followed by incubation on ice for 2 hours. For the preparation of hydrate protein-A sepharose, 0.1 g of beads were added into a facol tube and washed in 10 mL of water and continued washing in 10 mL of cold low-salt RIPA buffer. After the washing step, 500 µL of low-salt RIPA buffer was added to resuspend the beads, 30 µL washed beads were added in each reaction and slowly rotated in the cold room (4°C) for 30 minutes. To harvest the incorporated pellets by spinning the beads at 5,000 rpm for 1 minute at 4°C, the supernatant was then removed, and the bead pellets washed 3 times; twice with 1 mL of high-salt RIPA and once in 1 mL low-salt RIPA buffer. Finally, 15 µL of 1X Tricine sample buffer was added to the bead pellets, mixed by vortex for 10 seconds and boiled at 95°C for 5 minutes, and the whole samples run, except the residue, to the Tricine

SDS-PAGE gel and the same previous steps of the electrophoresis analysis performed.

Mutagenesis

The experiment was the first mutagenesis of the Kcv wild type by replacing cysteine to leucine at position 8 (L8C) and a reverse primer to construct a cysteine was made. The replacement of a cysteine was to be performed in the correct sequence. The reverse primers were designed to replace three site lysine residues in the 'L8C', mainly K29 to Isoleucine, K46/47 to methionine. An individual single methionine constructed M15L and M15/23/26L was made by the same standard protocol (Appendix). The mutagenesis was carried out by following the instructions of the QuickChange Lightning Site-Directed Mutagenesis Kit (Statagene, California, USA). Typically, in each reaction containing 5 µL of 10X reaction buffer, 1 µL of dsDNA template (Kcv WT, L8C or replacement other interest residues), 1.25 µL 125 ng) of forward and reverse primer (diluted from the stock 10x to be ~100 pmol), 1 µL of dNTP mix, 1.5 µL of QuickSolution reagent, ddH_2O added to bring up the total volume to 50 µL, and then 1 µL of QuickChange Lightning Enzyme. The replacement mutagenesis was used as the regular PCR recycling program. However, the annealing temperature for proper mutagenesis was at 60^{o}C. Next, PCR products were transformed to DH5α purified plasmid DNA by QIAprep Spin Miniprep Kit (Qiagen, Germany). The construct in the Kcv sequence was confirmed by DNA sequencing and Services, Medical Science Institute, School of Life Science, University of Dundee, Scotland, UK.

Polymerase Chain Reaction (Regular amplified PCR) for Site-Directed mutagenesis

PCR reactions were undergone using the Applied Bioscience 2720 thermal cycler in stand program as follows:

Temp	Step	Time	Cycle
94^{o}C	Initial	1 minute	1 Cycle
94^{o}C	Denaturing	30 seconds	30 cycles
58^{o}C	Annealing	30-60 seconds	
72^{o}C	Elongation	1 minute	
72^{o}C	Final Elongation	8 minutes	1 cycle
4^{o}C		Hold	Hold

PCR products of single mutagenesis were added with 1 µL of the restriction enzyme DNP1 for 1 hour at 37ºC. The Dpn enzyme will digest methyl groups on the backbone of the parental DNA molecules. 1 µL of the final reaction is introduced to transform with 50 µL of DH5α. A single colony is picked for inoculation with LB media at 37ºC. overnight and plasmid DNA is prepared using a Miniprep Kit as described previously and run on a 1% agarose gel to check whether it is the correct molecular weight. The plasmid DNA sequence was confirmed by DNA sequencing and Services, Medical Science Institute, School of Life Science, University of Dundee, Scotland, UK.

Polyacylamide Gel Electrophoresis and Radio-autography

The proteins of interest were radio-labelled [^{35}S] ^{Met} as described previously in the translation/transcription method. After running the samples, the slab SDS-PAGE gels were flushed with destaining solution, dried with the Gel dryer for 70-80 minutes at 57-60ºC, the dried gel fixed in the cassette, followed by the x-ray film put over the dried gel (only the red light in the dark room). Developing times for the films varied from 16-72 hours.

RESULTS

In order to experimentally assess the early stage of the folding event of the potassium channel Kcv during synthesis, previous research has suggested that the topological assessment is one of the most efficient techniques to distinguish effectively the protein folding in some types of the membrane proteins, including these potassium channels. Based on the theoretical hallmark region of this fast biogenesis, observation of the mechanism should begin first with the transmembrane domains which manifest a helical structure inside the ribosome which has been newly synthesised. Essentially, most proteins kinetically fold naturally from N-terminus to C-terminus. Hence, we initially carried out the single cysteine mutagenesis near the border of the first transmembrane domain, (the N-terminus of Kcv at position 8) making a replacement from a leucine to a cysteine called '(L8C),'

In the basic principle, cysteine is the key residue for mass-tagging (site specific) to determine the topological protein structure by band-shift. With the L8C translation system, the mRNA truncators which lack stop codons were translated and radio-labelled [^{35}S] ^{Met} in the cell-free system, or the prokaryotic S-30 *in-vitro* expression system. In the intermediate translation products, post-translational modification techniques were then employed to determine the secondary & tertiary structures of the nascent chain by PEGylation which can give an indication of whether the polypeptide chain is in folded, compact form or in an unfolded, conformation and followed by the final investigation was further ensured again by cross-linking assay, respectively. The truncated peptides were generated from the ribosome nascent chain complex (RNCs) by changing the selective amino acid sequence of the L8C. Throughout the *in vitro* system, we were able to investigate the L8C. This is the shortest potassium channel consisting of 94 amino acids (aa) with two transmembrane domains, typical C-terminus region nearly embedded into the membrane, and a central glycosylation site (Fig.14A-B). A cysteine mutagenesis relies on its remarkable property and also incorporates the specific sites in the Kcv (WT) sequence for the post-translational modification (Fig. 14C).

(14A)

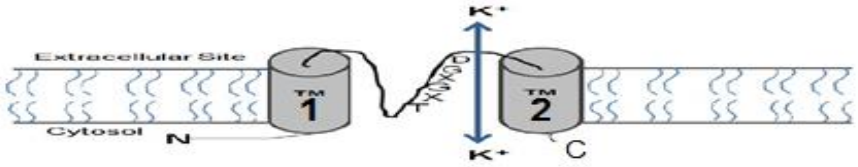

(14B)

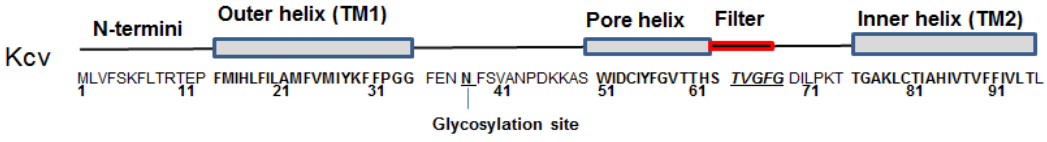

(14C)

Kcv gene (WT)

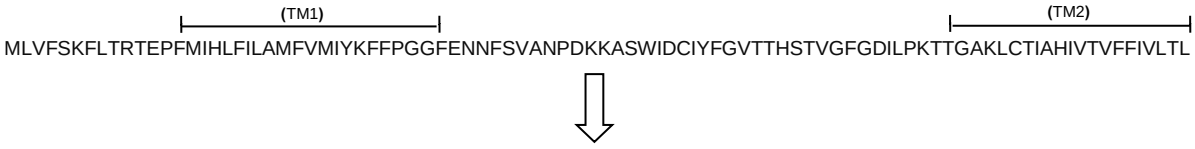

Engineered Cysteine (Constructed Cysteine at position 8, Kcv L8C)

Cysteine null mutant

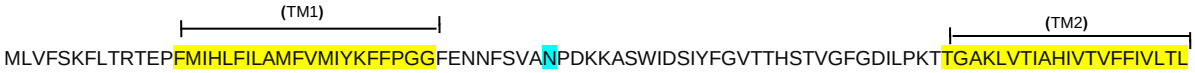

X – Transmembrane domain, X– Glycosylation site

Figure 14: The schematic diagrams of PBCV-1, Kcv protein in the lipid membrane. Transmembrane domains 1 and 2 (TM1/2) are formed by a regulatory central domain containing a conserve (TXGXGD) sequence (14A). The full amino acids sequence of Kcv the TM1 & TM2 (14B), (pore region, selectivity filter sequence); and the sequences of wild type/engineered Cysteine (L8C) of the Kcv genes (14C), are highlighted respectively.

PEGylation assay to investigate the L8C nascent chain in the ribosome exit tunnel

The PEGylation technology is widely used as a chemical modification technique to specifically site PEGylate target via a cysteine free residue (Lu & Deutsch, 2001) that also can be applied to examine the interface structure of the nascent peptide chain within the ribosome tunnel by accessibility of the large molecule thiol reagent. In this technique, a single replacement cysteine (L8C) was introduced in the protein as a cysteine marker that can be modified by labelling with the methoxypolyethylene glycol maleimide (PEG-MAL).

The PEG-MAL is a large thiol molecule ~5 kDa inaccessible through the ribosome tunnel which has an average diameter of 15 Å. Therefore, the PEGylation will not occur if the cysteine is inside the ribosome tunnel (Fig.15A). By comparison, for the PEGylation with a sulfhydryl group on cysteine side chain to be successful, the PEG-MAL thiolate must be outside the ribosome tunnel (Fig.15B).

In addition, the reaction causes the PEG-MAL to actively form irreversible thioester bonds with the sulfhydryl groups on a single cysteine residue, or C-S linkage between cysteine and PEG-MAL will be formed. Hence, the PEGylation of L8C will add 5 kDa to the molecular weight of the nascent chains of translation products. The distance connected by the nascent chain from the PTC to the exit of the tunnel not only depends on the number of amino acid residues, but also on the structures of the peptide chain.

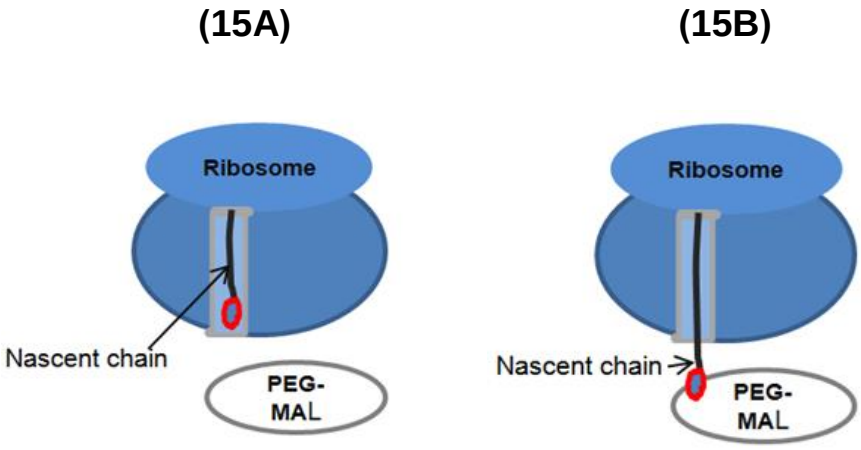

Figure 15: Schematic diagram of the PEGylation reaction with methoxypolyethylene glycol maleimide (PEG-MAL), the nascent chain buried cysteine marker inside the ribosome that is not PEGylated (15A). In contrast (15B), illustrates when the nascent chain gets longer, the marker is released from outside the ribosome tunnel and can be thiolated by PEG-MAL referring to a PEGylated formation.

After confirmation of the cysteine engineered sequence, the dsDNA was amplified to linear DNA using a PCR reaction. By changing the reverse primers to give an intermediate length requirement to 30aa, 40aa, 50aa, 60aa and 70aa respectively, eventually five interest truncators (30-70aa) were created (Fig. 16A). The linear DNA without a stop codon was then introduced to a coupled transcription/translation system using a prokaryotic 30-S lysate *in vitro* expression system. The translation was radio-labelled by [^{35}S] ^{Met} to generate the ribosome nascent chain complex (RNCs) intermediates. All translation products were then split into two portions, the first half was treated in 1mM PEG buffer; as a control (non-PEG-MAL); and 1mM PEG-MAL (with PEG-MAL) was added to the other half, then chilled on ice for two hours. The nascent chains were then analysed by SDS-PAGE in the post-translational modification using PEGylation technique.

The PCR reaction showed that the five bands of the truncated linear DNA of each length that had a cysteine substituted at position 8 (L8C), gradually increased in molecular weight to the correct size as expected on a 1% agarose gel (Fig. 16B). Following this, the truncators of linear DNA *in vitro* which were transcribed, translated and incorporated with tRNA in the ribosome. These truncated DNA then generated the ribosome nascent chain complexes (RNCs) accurately, both in their size & different lengths, which were experimentally bound to the ribosome as various translation intermediates.

Consequently, the obtained transcription/ translation products are used further for PEGylation analysis (Fig. 16C). As the control, the non-treatment PEG-MAL bands present only the translation nascent chains slightly increased in their various sizes and lengths (Fig. 16D1). The PEGylation images of L8C show that the cysteine marker would be effectively PEGylated at the lengths of the nascent chain. Although the size of the bands on the SDS-PAGE gel increased as expected, multiple unexpected bounds are apparently seen in each lane potentially due to mis-starting translation at alternative methionine residues in the N-terminus region. PEGylation analysis, in the shortest lengths 30-40aa, however, do not show the PEGylation. In regard to efficiency of the adduct bands a negligible PEGylation can be seen appearing within 50aa in an original x-ray film of the process, but it might fade out after scanning. As a result, it still has not presented a clear shift band from this intermediate length (Fig.16D2). However, we suspected that the PEGylation would occur around 50aa from a tiny adduct band where a possible cysteine marker (L8C) becomes exposed from the ribosome tunnel. If the PEGylated band reaches the ribosome at 50aa, the L8C nascent chain would be approximately a 42aa bridge from the distal tunnel up to the peptide transference centre (PTC). In theory, throughout the ribosome exit tunnel to the PTC can host a full helical nascent chain roughly 60aa. From these initial L8C PEGylated results, we were inspired to further probe the findings with the other experimental strategies involved.

(16A)

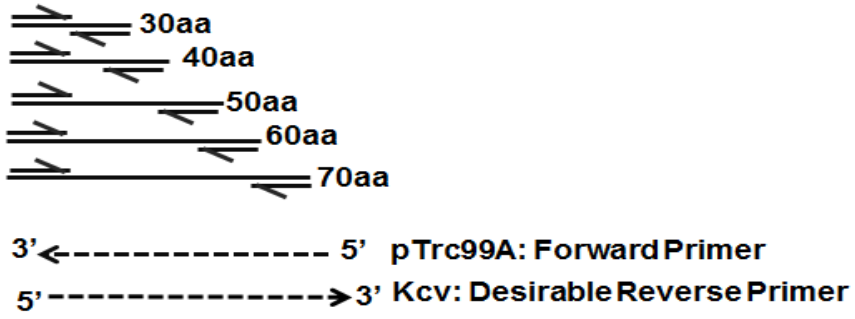
30aa
40aa
50aa
60aa
70aa
3'<---------- 5' pTrc99A: Forward Primer
5'---------->3' Kcv: Desirable Reverse Primer

(16B)

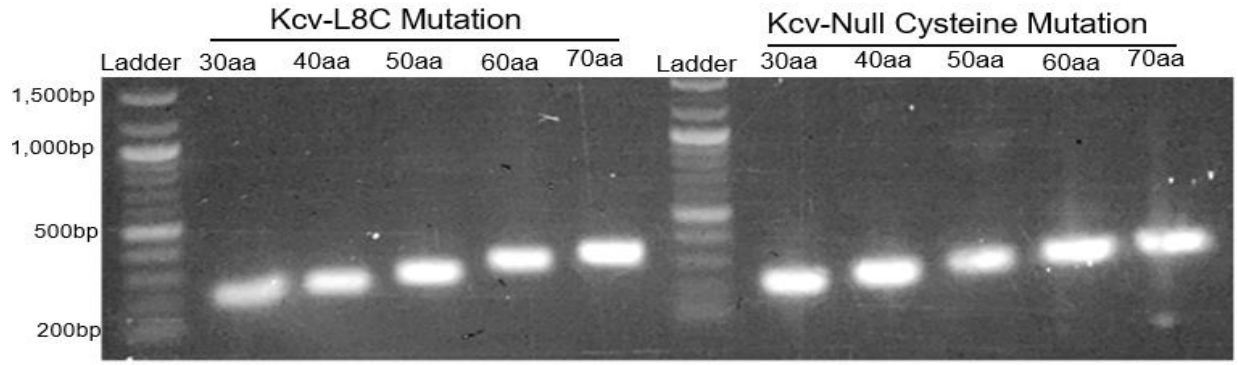
Kcv-L8C Mutation
Kcv-Null Cysteine Mutation
Ladder
30aa
40aa
50aa
60aa
70aa
Ladder
30aa
40aa
50aa
60aa
70aa
1,500bp
1,000bp
500bp
200bp

(16C)

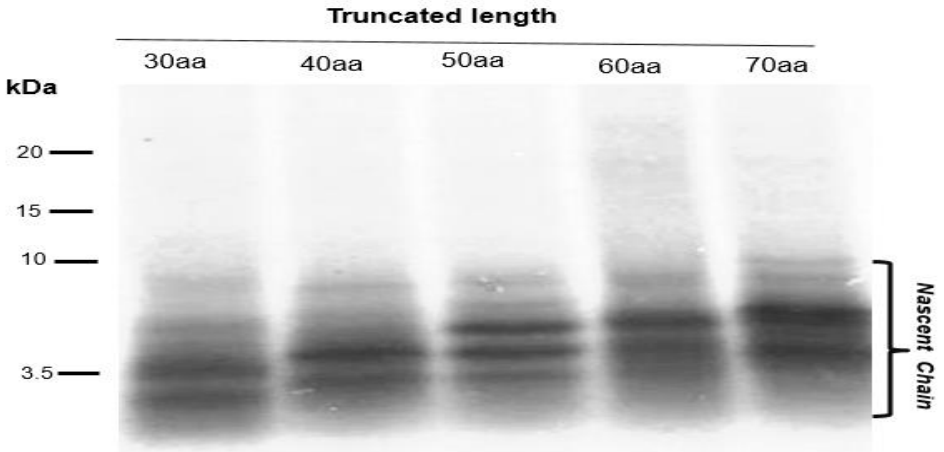
Truncated length
30aa
40aa
50aa
60aa
70aa
kDa
20
15
10
3.5
Nascent Chain

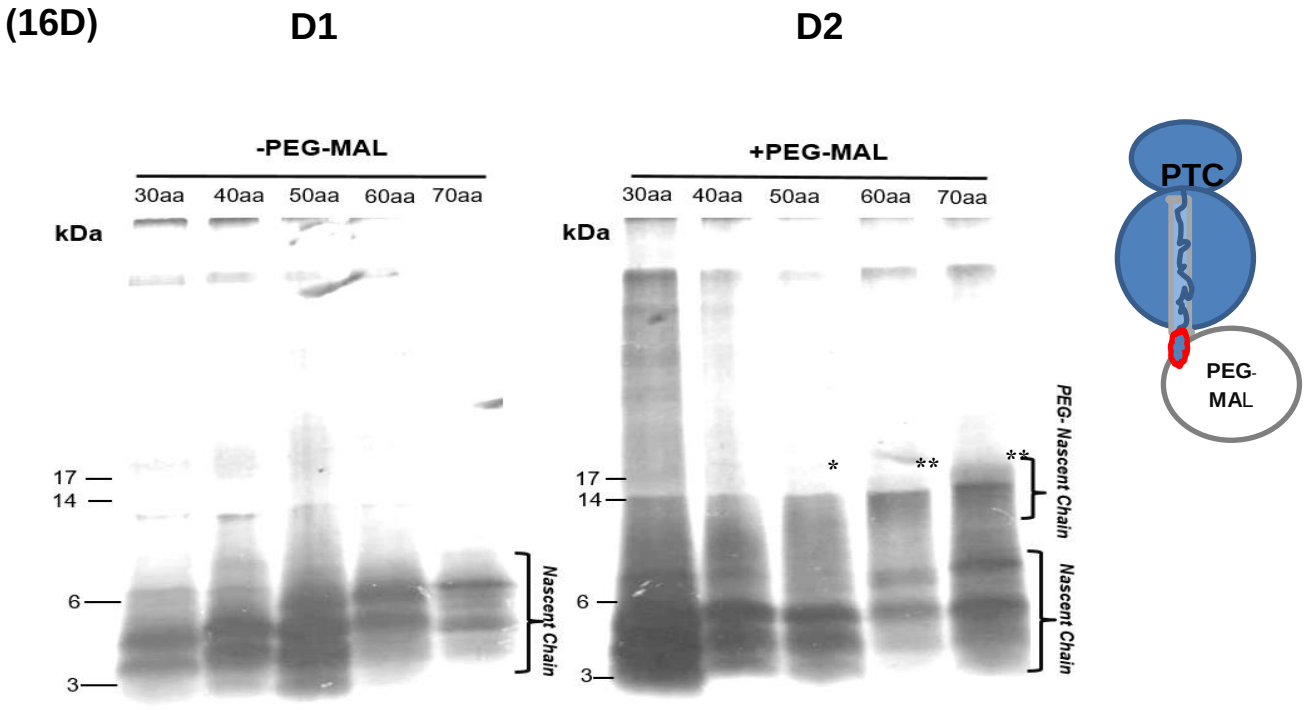

Figure. 16: The schematic diagrams show that the truncators of linear DNA were generated from a single forward primer and by changing the reverse primers, the interest truncator lengths were achieved by the PCR program. The linear DNA lacks a stop codon to maintain the nascent peptide inside the ribosome. To ensure PCR products quality control, the obtained linear DNA truncators were run on a 1% agarose gel (16A). The transcription of linear DNA to mRNA was synthesised corresponding to the production of peptide intermediates of 30-70aa to be installed with RNCs in the prokaryotic S-30 *in vitro* transcription/translation system (16B). All RNCs were generated, radio-labelled [^{35}S] ^{Met} and separated on a 4-12% SDS-PAGE gel (16C).

For the PEGylation analysis, the intermediate lengths translation products were allocated into two portions; the first half was treated in 1mM PEG Buffer, as a control (without PEG-MAL), and the second half was incubated in 1mM PEG-MAL (with PEG-MAL). The PEGylation assay was resolved on a 10-12% SDS-PAGE gel. Eventually, the PEGylation images were presented without PEG-MAL treatment (Fig. 16D1), and also with PEG-MAL treatment, where the PEGylated formation of the nascent chains increased in size ~5kDa (Fig. 16D2).

L8C chemical cross-linking assay using BMH and incorporating cross-linked product for IP assay upon ribosome bound nascent chains

In this strategy, to monitor the secondary/tertiary structure, the cross-linking approach is introduced to specifically conjugate between two cysteines. These are L8C and 1,6-bismalei-midohexane (BMH) (homo cysteine cross-linker). The reaction will occur between sulfhydryl groups of the nascent chain and BMH that will form the covalent bonds. Following the cross-linking experiment, the immunoprecipitation (IP) technique is to be subsequently employed to identify the associated protein.

Radio-labelled [^{35}S] ^{Met} translation reaction of 100 µL was applied as described previously (material and method section) and was used to generate the nascent chain with intermediate lengths of 30aa,40aa,50aa,60aa, and 70aa, respectively. The total translation products were treated in parallel both with and without BMH, then incubated on ice for 30 minutes. A sample of the cross-linking experiment was allocated before treatment (-) without BMH as a control; and after treatment (+) with BMH followed by separation on a 4-12% bis-tris gel, washed, dried, and X-rayed onto film in a dark room. In the associated experiment, the remaining cross-linked products were then precipitated with 100% TCA (denaturing condition) and used for immunoprecipitation experiments (IP). Each sample was split for two antibodies referring to ribosomal proteins; (L23) and (SRP54 homologue of Ffh), the first half had only anti-L23 added; and the other half with anti-SRP54 added then incubated on ice for 2 hours, followed by the pull-down technique with the hydrate protein A-Sepharose. The IP samples were run on the 4-12% bis-tris gels, washed, dried, and X-rayed onto film in a dark room. Finally, both of the cross-linked and IP films were developed with the X-Omat machine after a week, however the IP films require at least two weeks. The individual sizes of the associated proteins were approximately 14.89 kDa (L23), and 48.5 kDa (SRP54), but coupled with a nascent chain, this will add approximately 3-7 kDa.

The cross-linking results show that the translated nascent chain peptides bands gradually increase in size from the lowest amino acid length (30aa) to the highest amino acid length (70aa) for both without (-) and with (+) BMH. The intermediates lengths of with +BMH show the weak bands corresponding to the size of the signal recognition particle protein (SRP54) from 60aa to 70aa. (Fig. 17A). In comparison, these interaction bands can be clearly identified by immunoprecipitation assay (IP). In regard to the L8C/L23 cross-linked bands, they can be precipitated with anti-L23 to approximately 22 kDa which is the size of ribosomal L23 when the nascent chains are 50-70aa (Fig. 17B). However, the presence of L8C/SRP54 cross-linked bands are precipitated with anti-SRP54 indicating the SPR54 size to be about 48-49 kDa with the strongest bands ranging from 50-70aa (Fig. 17C).

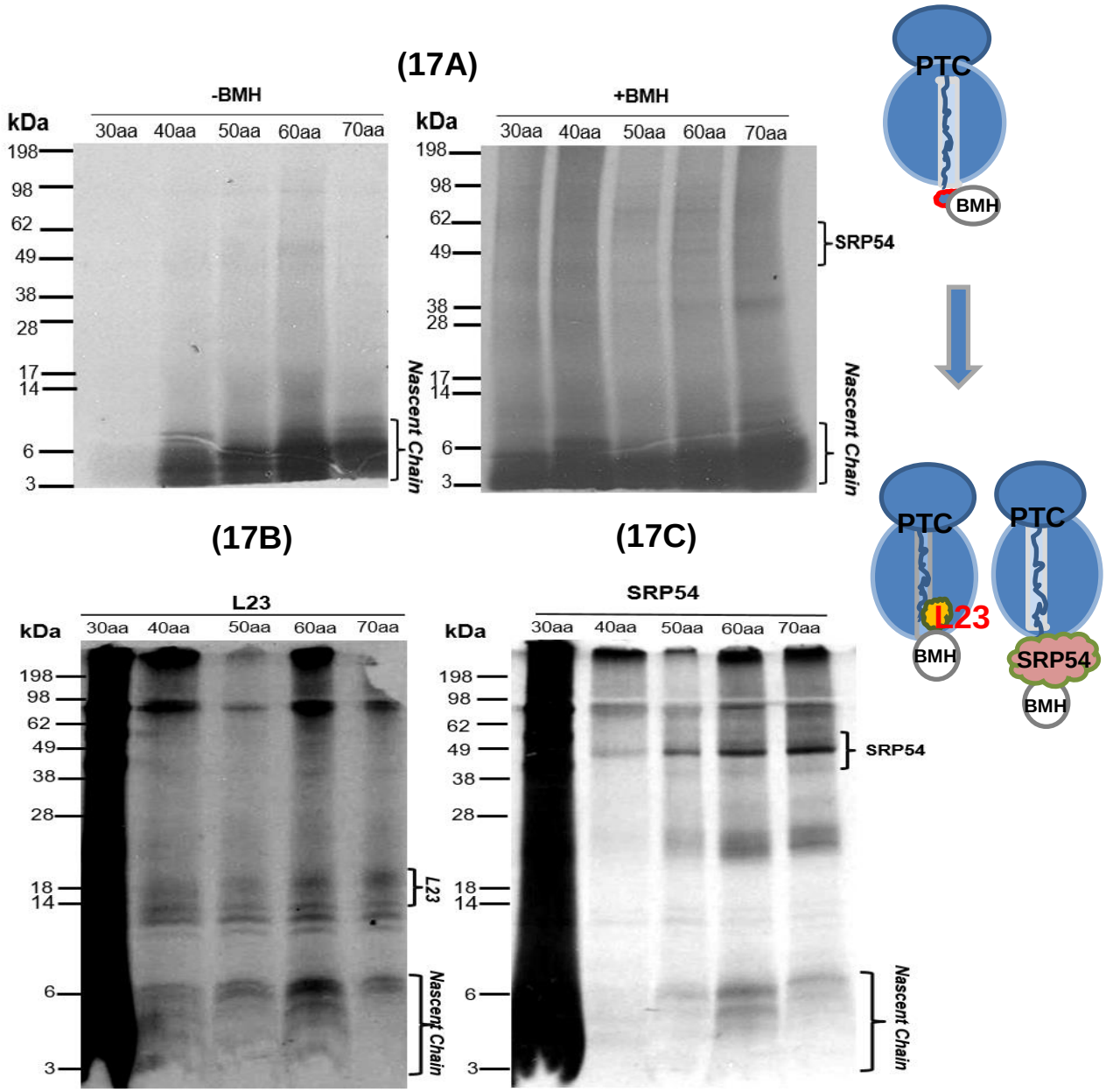

Figure 17: Cross-linking assay of L8C was initially carried out in the prokaryotic S-30 *in vitro* transcription/translation system. The RNCs were synthesised and radio-labelled [^{35}S] ^{Met}, the N-terminus intermediates ranging from 30-70aa. The translation samples were split into two portions, to treat before (-) treatment with BMH as a control; and after treatment with (+BMH). Cross-linked samples were resolved on a 4-12% bis-tris gel (17A). Followed by the encompassed experiment, all sample cross-linked products were precipitated with 100% TCA and immunoprecipitated (IP) under denaturing conditions before being equally divided and treated with two antibodies; the first half incubated with anti-L23. The anti-L23 precipitated the right size of ribosomal protein L23 at approximately 16 kDa and raised the molecular weight of other ribosomal proteins (17B). The other half was treated with the anti-SRP54, which indicated the adduct size of SRP54 to be above 49 kDa (17C). The immunoprecipitated samples were analysed on a 4-12% bis-tris gel.

Lysine mutagenesis (K29I/K46/47M) for investigating Kcv structure at the 1st transmembrane domain

Previous cross-linking experiments using the cysteine-cysteine cross linker, BMH, have been established to determine the potassium channel Kcv, during *in vitro* synthesis system. The BMH cross-linking determined only a single mutant cysteine (L8C) when probing the secondary and tertiary structure. However, we would like to determine what the exact interacting protein in the exit ribosome tunnel specifically is. Therefore, we incorporated the analysis with another residue in the protein, called lysine-lysine cross-linker, BS^3. In order to achieve this experiment, we required only a single lysine in the first transmembrane segment. Then, we deliberately replaced the three lysine (K) residues which are located near the N-terminus region with two selective amino acids; at position K29 with isoleucine 'K29I' and at the other two positions; K46 and K47 with methionines 'K46/47M' combined into the primary mutagenesis L8C. In this "three lysine mutagenesis", we aimed to keep only a specific lysine for cross-linking at position 6 to monitor topological structure and the folding feature in the first transmembrane at the N-terminus. Based on increasing the protein properties, the mutation at K29 with isoleucine was thought to increase hydrophobic ability in the first transmembrane domain as well as to enable determination of the SRP targeting interaction. Additionally, the two substitution sites of K46/47M were preferable in promoting the ability of radio-labelled [^{35}S] ^{Met} in the protein which could be seen clearly on the SDS-PAGE gel. The dsDNA was confirmed as being the right sequence after the substitution process (Fig. 18A). To generate linear DNA, the dsDNA was amplified using PCR reaction to a different truncator by changing reverse primers to form the five intermediate lengths; 30aa, 40aa, 50aa, 60aa, and 70aa, respectively (Fig.18B). All intermediate lengths of ribosome nascent chains were synthesised in prokaryotic *S*-30 *in vitro* expression system (Fig. 18C), which is used to further scrutinise post-translational modifications such as cross-linking assay and immunoprecipitation as follows:

(18A)

(18B)

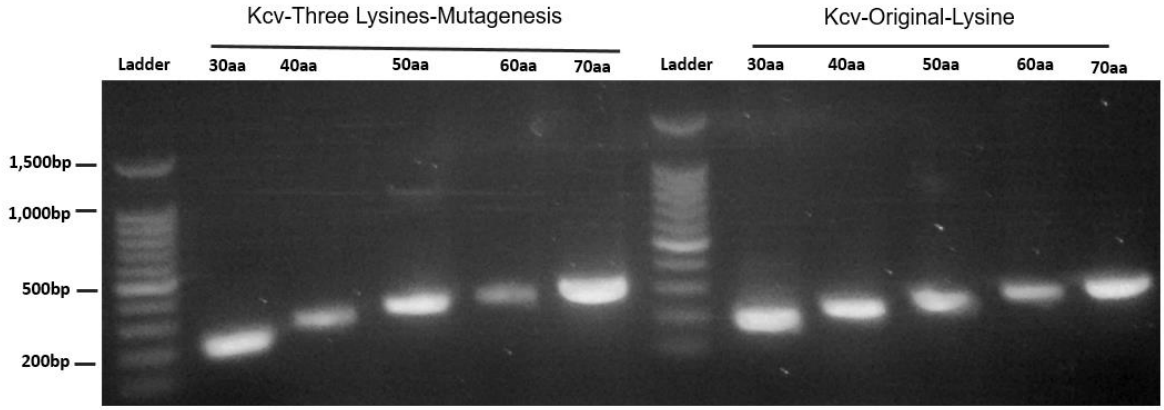

Figure 18: The replacement of three lysines in the L8C sequence K29I/K46/K47M (18A), The truncated linear DNA of various lengths was generated from the PCR reaction by changing reverse primers that lack the stop codons in a plasmid DNA template. All intermediates lengths 30-70aa were separated on a 1% agarose gel for the quality control (18B).

(18C)

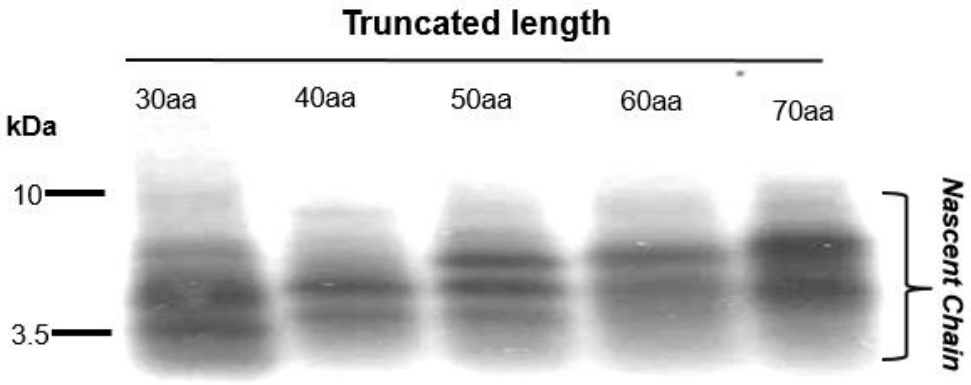

Figure 18C: The RNCs of three lysines substitution K29I/ K46/47M were generated and radio-labelled [^{35}S] ^{Met}, the various N-terminus intermediate lengths in prokaryotic S-30 *in vitro* expression system ranging from 30-70aa. All intermediates lengths were resolved on a 10-12% SDS-PAGE gel. Each intermediate length shows gradual increase in size containing extra bands. These translation products will be employed for the cross-linking assay and immunoprecipitation analysis.

Chemical cross-linking assay of lysine mutagenesis in Kcv (K29I/K46/47M) using BS^3 and incorporating cross-linked products for IP assay to investigate ribosome bound nascent chains

The cross-linking using BMH was used in the previous experiment for investigating and analysing the protein interaction with the ribosomal proteins (L23 and SRP54) at the exit of the ribosome tunnel. Hence, in this experiment strategy we used another option. The lysine-lysine cross-linker bis(sulfosuccinimidyl)suberate (BS^3) to examine the interaction among nascent chains, and ribosomal proteins when lysine in the L8C sequence has been replaced at three sites; K29IK46/47M. Therefore, the lysine marker is only available in the N-terminus region at site K6. We examined the five truncated intermediate lengths varying from 30-70aa (at intervals of 10aa). However, there are another two lysines available within the C-terminus region K72 and K77 in the full length, located in the region downstream and far from the first transmembrane domain which is not necessary to detect.

In the concept of the experiment, the 6K (Lys) is a measured position for detecting the protein structure by forming free single lysine with BS^3 and the two molecules are cross-linked. This experiment was initially carried out through the regular cross-linking protocol and their cross-linked products were introduced for precipitating with 100% TCA (denaturing condition) and followed by IP assay with two selective antibodies, including anti-L23 and anti-SRP54. Eventually, the samples were resolved on a 10-12% SDS-PAGE gel. The gels were well dried, put into a cassette and films developed. A cross-linking film was the first developed over-night, whereas the IP of cross-linked film was later developed for approximately a month.

The cross-linking results reveal that the nascent chain intermediate bands gradually increased from the lowest amino acid (30aa) to the highest amino acid (70aa) of both non-treated and treated with BS^3, while the samples were treated with BS^3 providing intensive back ground for all translation peptides over all intermediates. The interaction of the nascent chain and the ribosomal proteins cannot be seen while analysing with the cross-linking processes (Fig. 19A). On the other hand, the immunoprecipitation (IP) anti-L23 bands reached the clearest from 50-70aa of about 22 kDa which indicate the size of ribosomal protein L23 (Fig. 19B). Meanwhile the anti-SRP54 bands were present around the upper nascent chain peptides ranging from 50-70aa at about 50 kDa indicating the molecular weight of ribosomal protein SRP54 and showing the strongest signal from 60-70aa (Fig. 19C).

(19A)

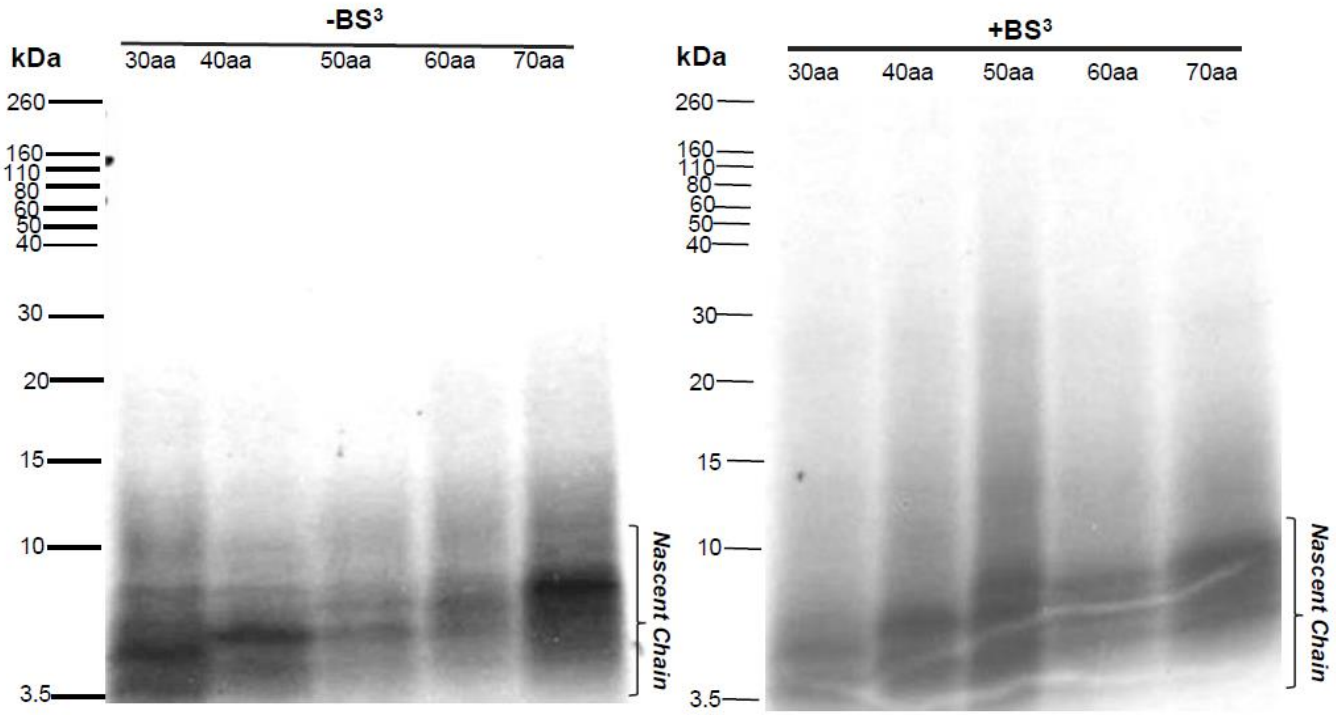

Nascent chains were cross-linked using BS^3

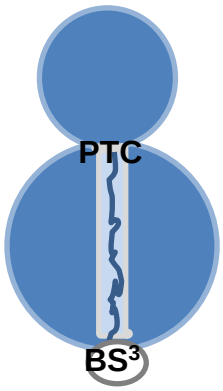

Cross-linked products incorporation with Immunoprecipitation assay

(using two antibodies; L23 and SRP54)

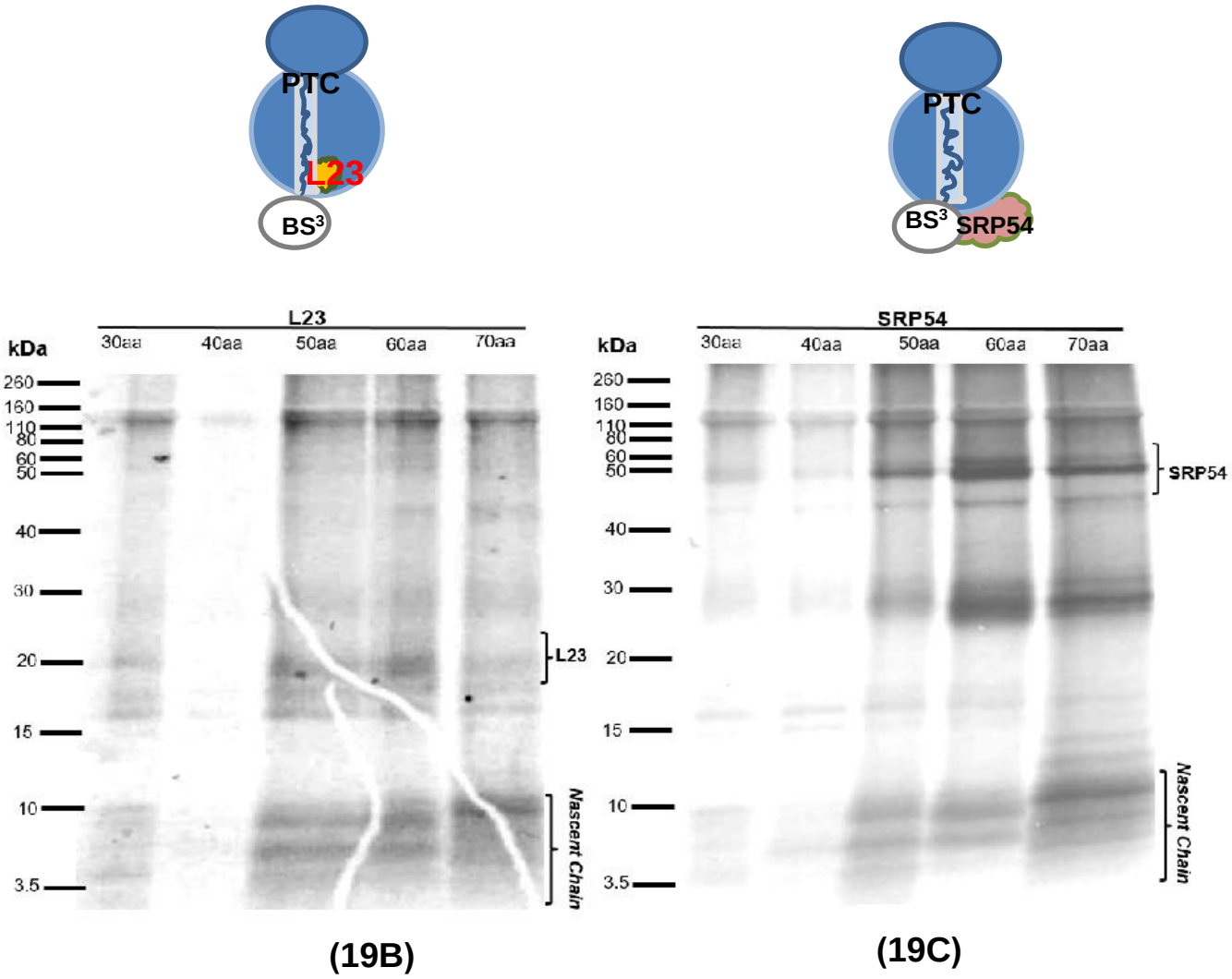

Figure 19: Cross-linking assay of the L8C constructed of three lysines K29I/ K46/47M. The experiment was carried out in the prokaryotic S-30 *in vitro* transcription/translation system. Firstly, the protein was radio-labelled [^{35}S] ^{Met} the N-terminus intermediates lengths ranging from 30-70aa (at intervals of 10aa). Following this, the cross-linking was carried out before treatment (-) without BS^3, (as a control) and after treatment (+) with BS^3. The cross-linked samples were resolved on a 10-12% SDS-PAGE gel and developed onto the film over-night. The images of both treatments with BS^3 (+) & without (-), indicate apparent translation products (Fig. 19A).

In a further associated experiment, the cross-linked products were precipitated with 100% TCA (denaturing condition) and introduced for immunoprecipitation with two antibodies (IP), Each sample was split into two portions, the first half treated with anti-L23 and the other half treated with anti-SRP54, then both incubated on ice for two hours. Afterwards, in order to obtain the RNCs, the reactions were pulled down with hydrate protein A-Sepharose. The protein pellets can participate with anti-L23 to increase to the size of ribosomal protein L23 approximately 16 kDa (Fig. 19B). Whereas the protein treated with anti-SRP54 raised the adduct bands to ribosomal protein SRP54 (Fig. 19C), The samples were resolved on a 10-12% SDS-PAGE gel and developed onto film for about a month.

A single methionine mutagenesis to investigate the improvement results of the nascent chain in the ribosome exit tunnel

While doing several progressive post-translational modifications, we found that there were some extra bands existing in the translation products. Therefore, the bands of the nascent chain peptides in S-30 in *vitro* translation system are clearly required for various further analysis. As we well know, methionine is the first initial transcription amino acid, therefore it was absolutely essential to clarify what the main methionine is to transcribe mRNA. We first replaced only a single methionine at the site 15 with leucine (M15L), of both L8C and three lysines substituted (K29I/K46/47M) to their sequences in order to compare which is the proper mutagenesis to present a clear band on a SDS-PAGE gel. At primary mutagenesis, the L8C contains four methionines in sequence at the positions; 1, 15, 23 and 26 (Fig. 20A), respectively, while three lysine substitutions (K29/I/K46/47M) contain six methionines at the positions; 1, 15, 23, 26, 46 and 47, respectively (Fig. 20B).

The findings of the linear DNA truncation (Fig. 20C), and the translation products in each intermediate length of these mutations unfortunately show the weaker translation in general. However, the specific nascent chain bands of the translation product are a little bit clearer (Fig. 20D).

(20A)

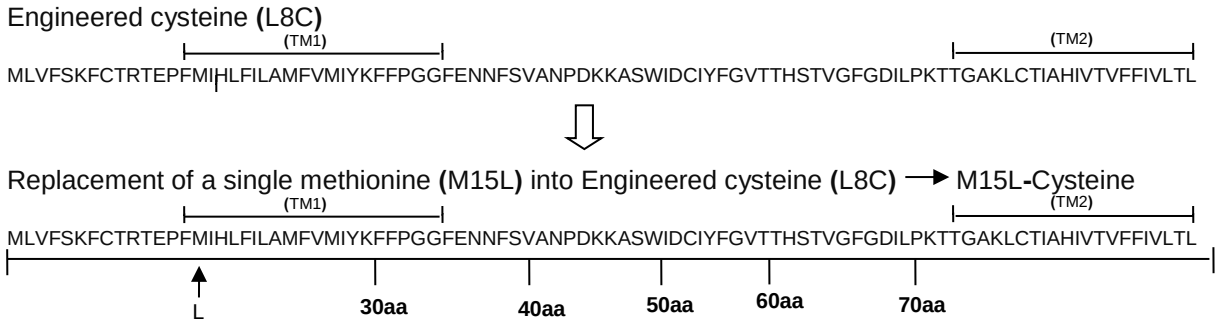

(20B)

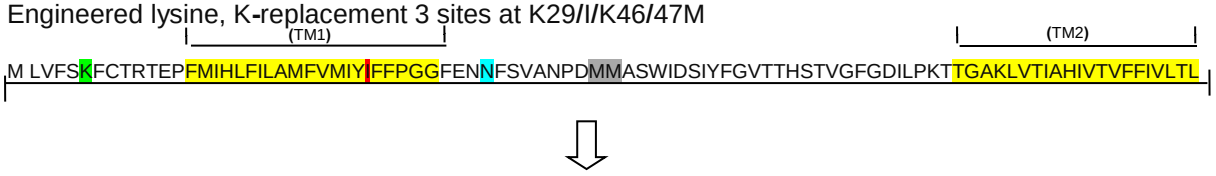

Replacement of a single methionine **(**M15L**)** into Lysine mutagenesis,

K**-**replacement 3 sites at K29**/**I**/**K46**/**47M ⟶ M15L**-**Lysine

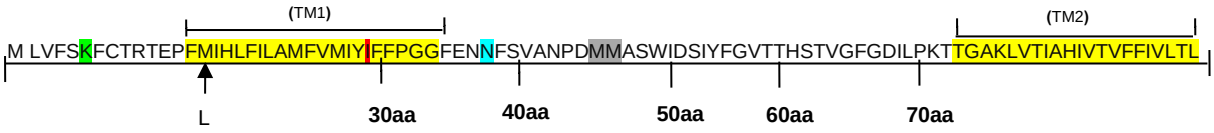

Figure 20: Diagram of two mutagenesis of replacement of a single methionine engineered to a single leucine at site 15; (i) L8C to M15L-Cysteine (20A), and (ii) replacement in single three lysines engineered (K29I /K46/47M) to M15L-Lysine (20B).

(20C)

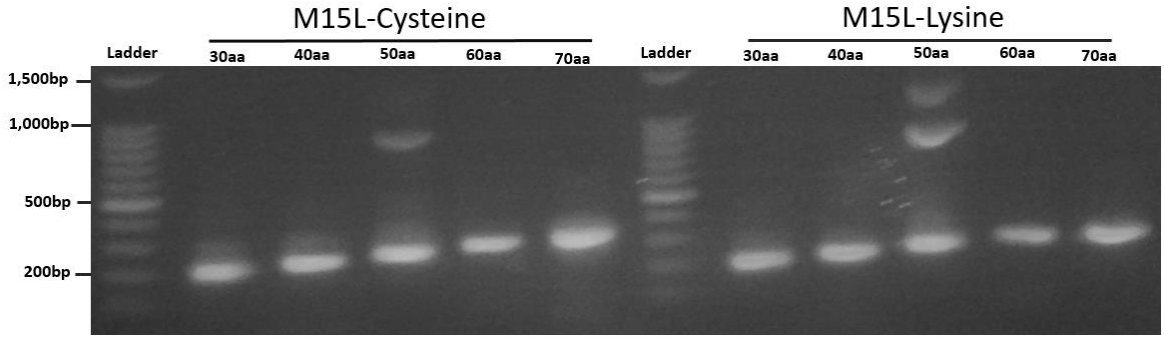

Figure 20C: The truncation of linear DNA, in which a single methionine was substituted instead of leucine at site 15 (M15L) of both M15L-cysteine (L8C) and M15L- three lysine substitutions (K29I /K46/47M) were made. The linear DNA of intermediate lengths is generated from the PCR reaction by changing reverse primers that lack stop codons in a plasmid DNA template and all intermediate lengths will be used for translation reactions.

(20D)

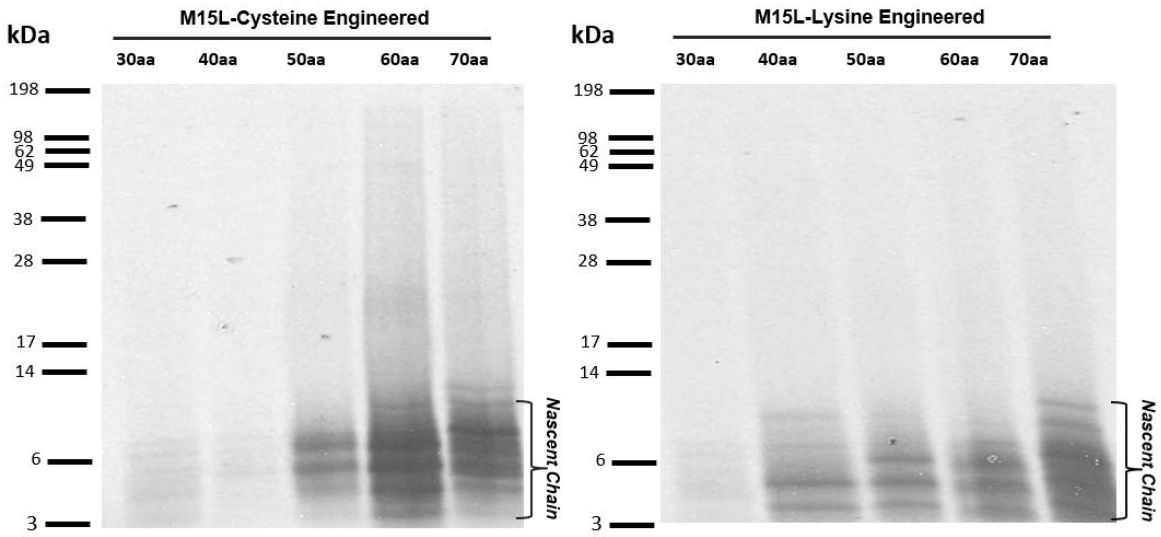

Figure 20D: Comparison between RNCs of a single methionine mutagenesis at site 15 instead of leucine in both of the M15L-Cysteine (L8C) and M15L- three lysine substitutions K29I/K46/47M.The RNCs were generated and radio-labelled [^{35}S] ^{Met}, the N-terminus intermediates lengths ranging from 30-70aa (at intervals of 10 aa) in prokaryotic S-30 *in vitro* transcription/translation system. All translation samples were resolved on a 10-12% SDS-PAGE gel. Only translation products of M15L-Cysteine were selected to be used for PEGylation.

PEGylation assay (M15L-Cysteine) to investigate the Kcv nascent chain in the ribosome exit tunnel

In order to get the improvement in the topological structure of the protein by a cysteine mass-tagging in position 8 of M15L-Cysteine (Fig. 20A), the PEGylation technique was carried out once again to observe the early protein folding in the first transmembrane domain through the shift bands on electrophoresis gels, which indicate the peptides have been mass tagged. Like the previous PEGylation assay, the standard translation reactions were prepared at 25µL. These reactions were split into two portions, the first half was incubated using 1mM PEG buffer as a control (without -PEG-MAL, see appendix); the second half incubated with 1mM PEG-MAL (with +PEG-MAL) and incubated on ice for two hours. PEGylation samples were analysed on a 10-12% SDS-PAGE gel.

The PEGylation analysis shows that the nascent chain peptides from 30-70aa have increased explicitly in size both as a control without treatment (-PEG-MAL, see in Fig. 21A) and containing (+PEG-MAL, see in Fig. 21B). In comparison, the shift-bands of the nascent

chains which are treated with the thiol reagent (+PEG-MAL), show a stronger signal from 50-70aa if the nascent chain becomes longer which indicated that the PEGylation between the intra-molecular sulfhydryl-sulfhydryl linkage and possibly at the 50aa reached from the ribosome tunnel are conjugated. It implies that a cysteine marker (L8C) is released from the ribosome tunnel when measuring approximately 42aa from the exit tunnel to the peptide transfer centre (PTC). The PEGylation bands from 50-70aa display apparent detailed topology of the secondary protein in M15L-Cysteine mutagenesis (Fig. 21B).

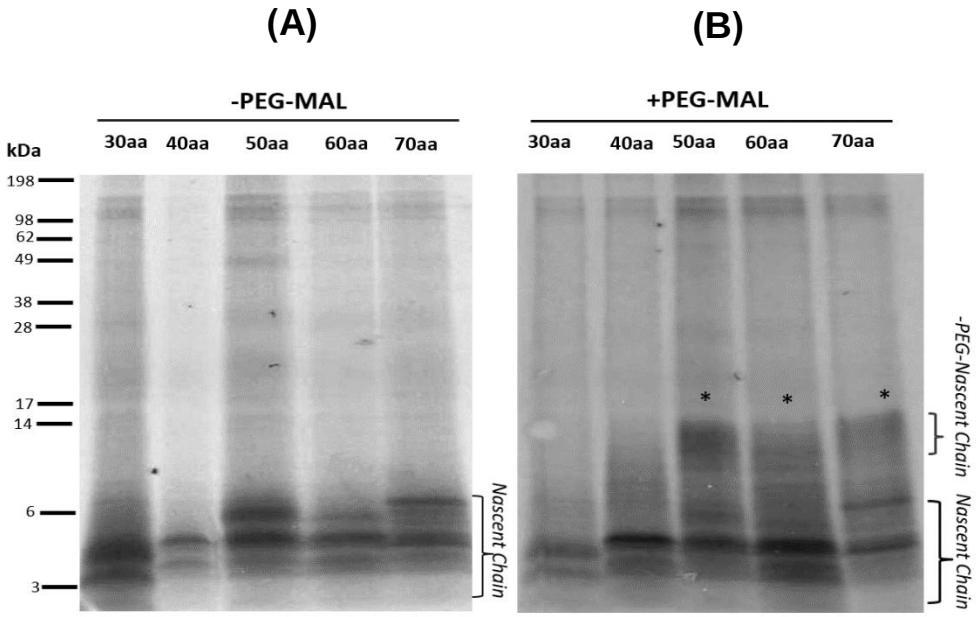

Figure 21: PEGylation event of the replacement of a single methionine mutagenesis at site 15 to leucine; M15L-Cysteine (L8C). The RNCs were generated and radio-labelled [^{35}S]^{Met}, in the prokaryotic S-30 in *vitro* transcription/translation system with the N-terminus intermediate lengths ranging from 30-70aa (at intervals of 10aa). The translation products were split into two portions, the first half incubated in 1mM PEG Buffer (without-PEG-MAL) as a control (21A), while the other half incubated in 1mM PEG-MAL(+PEG-MAL). The PEGylated shift-bands clearly appear over the nascent chains varying from 50-70aa (21B). The samples were resolved on a 10-12% SDS-PAGE gel.

Three single methionine mutagenesis to investigate the improvement in results of the nascent chain in the ribosome exit tunnel

In regard to the previous results of a single methionine mutagenesis M15L-Cysteine (L8C), some improvement was evident. In order to see if this could be improved more, further mutations were made. Therefore, an additional replacement of two single methionines to two leucines, which are located close to the first transmembrane domain, at the sites M23/26L were subsequently designed. After confirmation, the mutagenesis sequences are shown in (Fig. 22). The substitution of M15/23/26-Cysteine and M15/23/26-Lysine were incorporated into linear DNA through a PCR amplification reaction without the stop codons. Associated experiments, *in vitro* translation, cross-linking and immunoprecipitation assay were then carried out, respectively.

(22A)

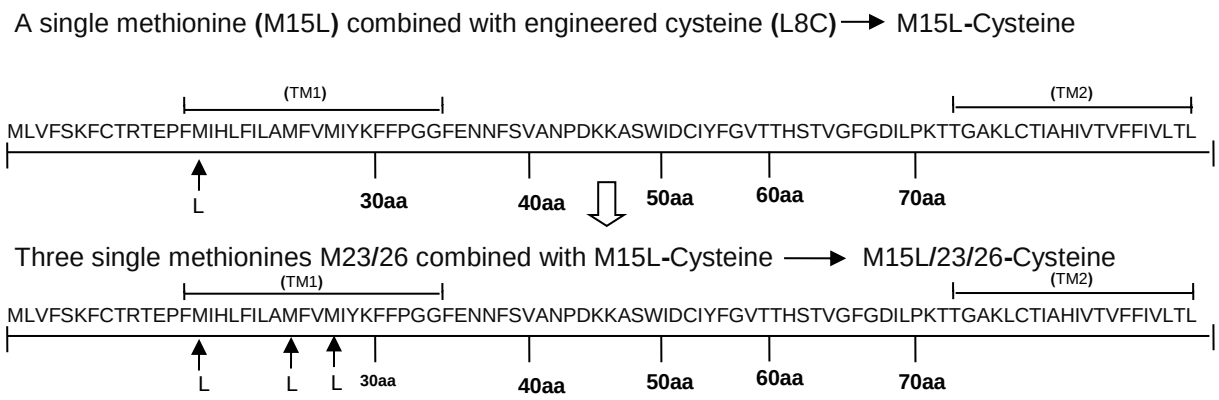

(22B)

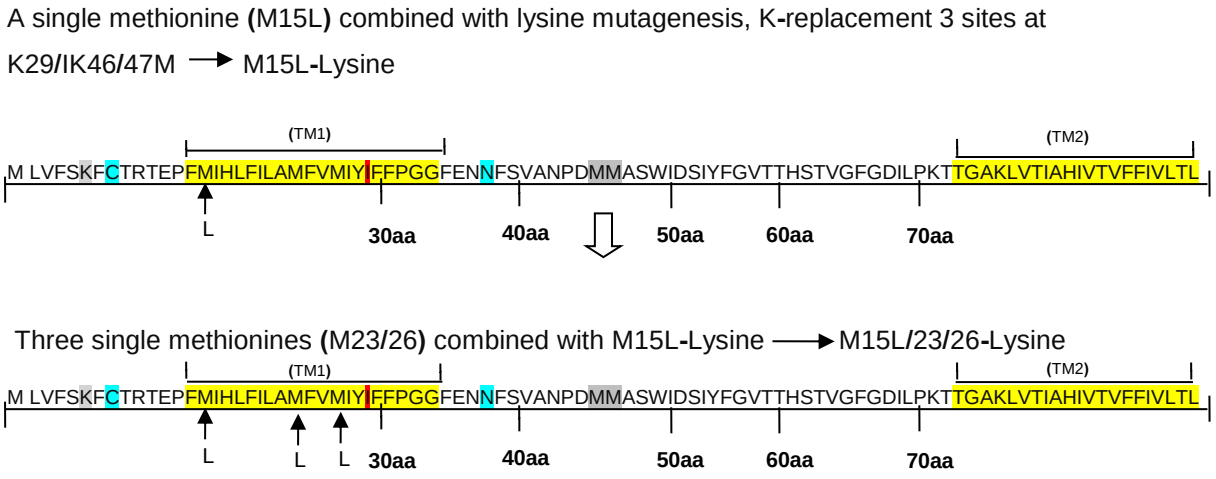

Figure 22: Diagram of replacement of three single methionines engineered to three leucines at three sites 15/23/26 in two Kcv mutagenesis; (i) L8C to M15/23/26L-Cysteine (22A), and (ii) eventually the presence sequence of three lysines engineered (K29I/ K46/47M) to M15/23/26L-Lysine (22B).

(22C)

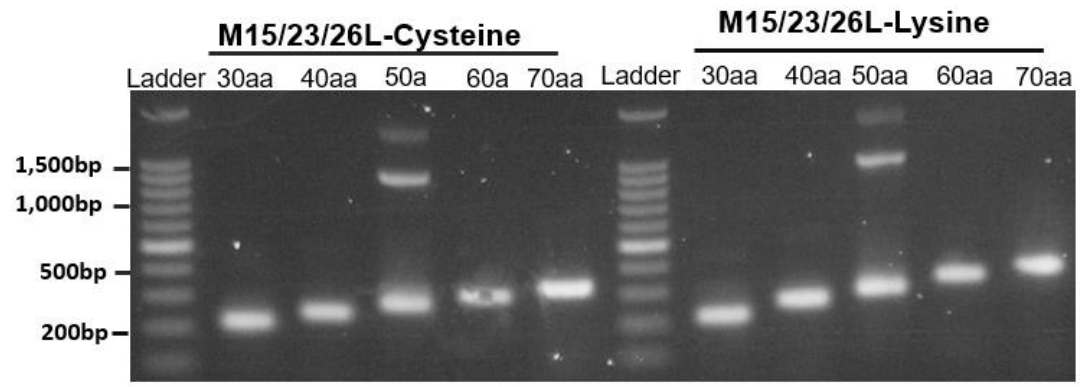

Figure 22C: The truncation of linear DNA with the replacement of three single methionine to three leucines of two mutagenesis (i) L8C to M15/23/26L-Cysteine and (ii) K29I/K46/47M to M15/23/26L-Lysine. The linear DNA was synthesised from the PCR reaction by changing reverse primers that lack stop codons in a plasmid DNA template. These truncated linear DNA will be introduced for further prokaryotic S-30 *in vitro* transcription/translation reaction.

(22D)

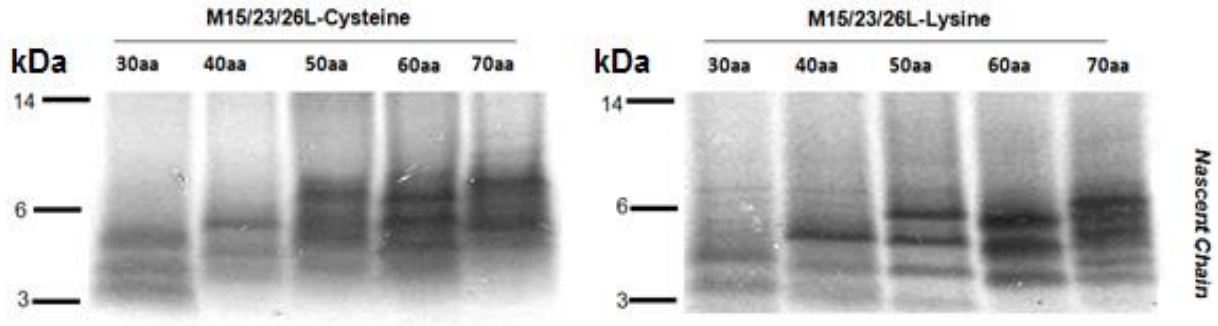

Figure 22D: The RNCs of replacement of single three methionines mutagenesis to three leucines in both two mutagenesis; (i) L8C to M15/23/26L-Cysteine and (ii) K29I/K46/47M to M15/23/26L-Lysine. The RNCs were generated and radio-labelled [^{35}S] ^{Met}, the N-terminus in various intermediate lengths ranging from 30-70aa (at intervals of 10 aa) in the prokaryotic S-30 *in vitro* translation system. All translation truncations were resolved on a 10-12% SDS-PAGE gel. Consequently, selection of only the translation products of M15/23/26L-Lysine substitutions (K29I/K46/47M) will be used for another cross-linking and IP assay.

Chemical cross-linking assay with BS^3 and IP assay of Kcv mutagenesis M15/23/26L-Lysine upon ribosome bound nascent chains

In this experiment, we used a lysine-lysine cross linker, BS^3 whose reaction occurs between the end of the reactive group of BS^3 and the functional group of the engineered Kcv. To provide the protein for this experiment, L8C was substituted for three single lysines (K29I/K46/47M) and then, three single methionines replaced leucines at three sites 15, 23, and 26, respectively. The combination mutagenesis is called 'M15**/**23**/**26**-**Lysine' **(**Fig**.** 22B**).** Three residues of lysine in the full sequence are available at three sites K6, K72 and K7, however the last two residues are most likely to be located close to the second transmembrane & C-terminus domain which was not necessary to determine. Hence, K6 (Lys) is a single lysine marker in the first transmembrane domain that is used to conjugate an amide-amide reaction.

The replacement strategy of three methionines is designed to maintain only a single methionine at the first position of the sequence (Fig. 22B). Ideally, maintenance of only one methionine in the protein sequence is to elucidate if we can get the improvement of intermediate lengths on the SDS-PAGE gel. Furthermore, if we obtained this manifestation, the cross-linking experiment was started with 100 µL translation reactions, including five intermediate lengths; 30aa, 40aa, 50aa, 60aa, and 70aa, respectively.

All five reactions were carried out in two steps; before and after treatment with BS^3. Each translation reaction was split into two portions, first 7 µL of reaction was overlaid on a sucrose cushion and centrifuged, with the supernatant removed before treatment (-) without BS^3, and the remaining was overlaid on a sucrose cushion, centrifuged, the supernatant aspirated and 1mM BS^3 added before incubation on ice for 2 hours after treatment (+) with BS^3.

Hereafter, each reaction was taken for after treatment with -BS^3. Both treatments were purified on a 10-12% SDS-PAGE gel, while the remaining cross-linked products were precipitated with 100% TCA (denaturing condition). The pellets were then used for immunoprecipitation (IP). Each intermediate length reaction was divided into two equal portions for two antibodies. Either anti-L23 or anti-SRP54 were then incubated on ice for 2 hours pulled down with hydrate protein A-Sepharose. The samples were resolved on a 10-12% SDS-PAGE gel and developed onto film for about a month. IP bands were presented above the translation product; L23 molecule size at 14.89 kDa and SRP at 48.5 kDa. The samples were resolved on a 10-12% SDS-PAGE gel.

The cross-linking showed that each intermediate band (RNCs) slightly increased in size from the lowest amino acid length (30aa) to the highest amino acid length (70aa), The

nascent chains of non-treated (-BS^3) and treated with (+BS^3) were presented by size from the bottom of the gels.

However, the samples which were treated with (+BS^3) present the interacting peptide bands over two nascent chains from 60-70aa, which indicated SRP bands at about 62 kDa and other indigenous background bands (Fig. 23A). While these cross-linked products were detected using immunoprecipitation (IP) with 2 antibodies, the RNCs/L23 cross-linked bands were precipitated with anti-L23 obviously displaying from 50-70aa of about 20 kDa, which is the size of ribosomal protein L23 (Fig. 23B).

Whereas the RNCs/ SRP54 cross-linked were precipitated with anti-SRP54 indicating the bands over nascent chain peptides ranging from 50-70aa at about 49 kDa which is the size of ribosomal protein SRP54 (Fig. 23C). However, there are two remarkably strong bands from 60-70aa as well as other unexpected lower and upper background bands in existence.

(23A)

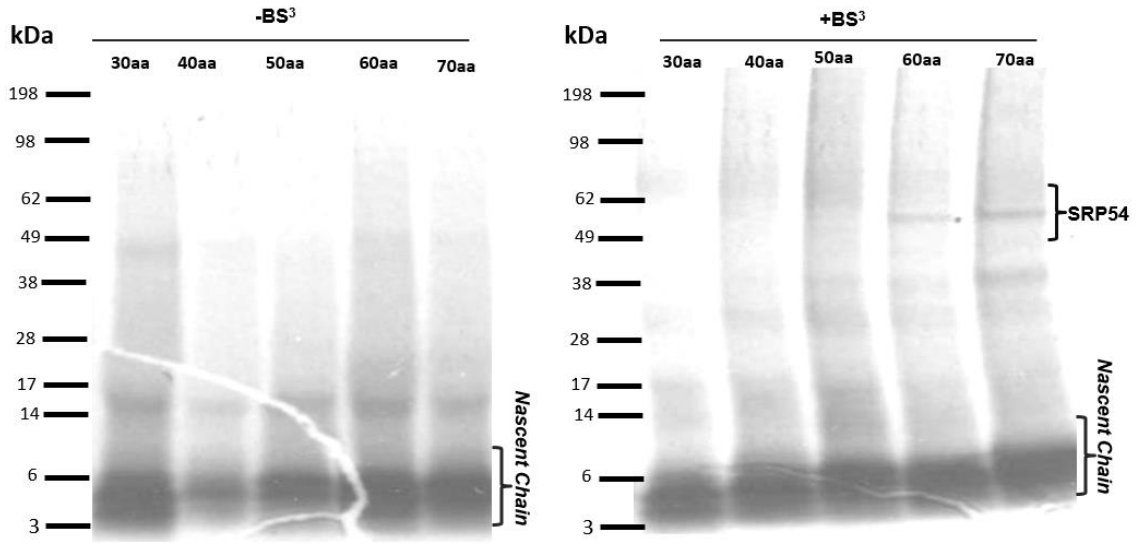

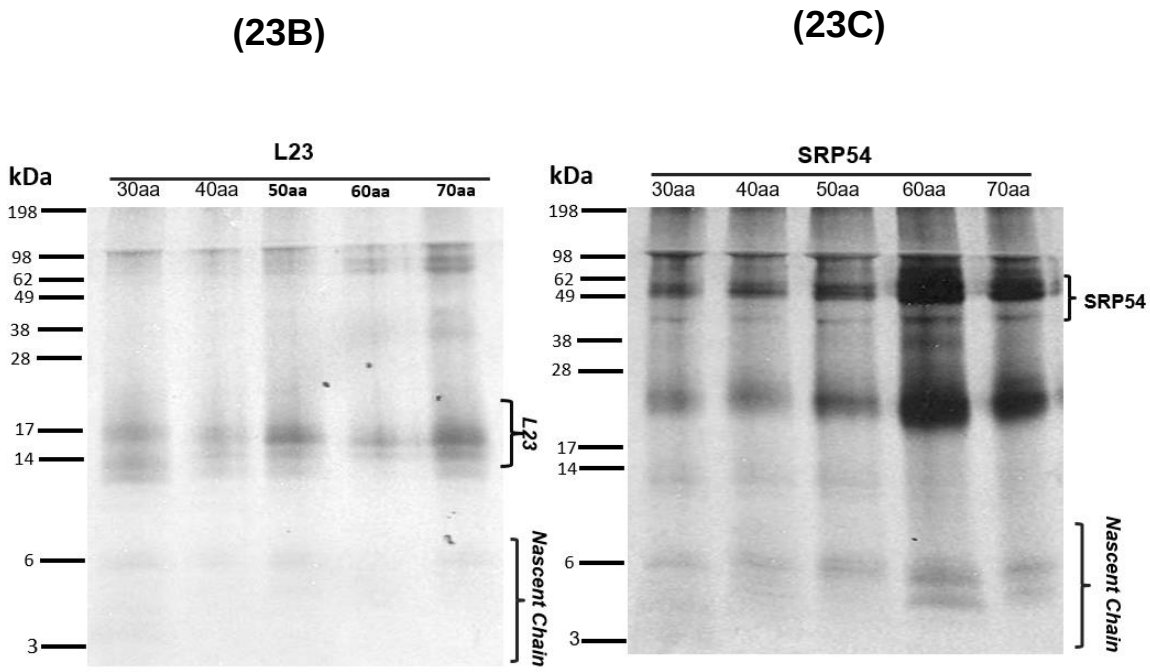

Figure 23: Cross-linking analysis of the M15**/**23**/**26L**-**Lysine was carried out in the prokaryotic S-30 *in vitro* transcription/translation system. The RNCs were generated and radio-labelled [^{35}S] ^{Met}, the N-terminus intermediate lengths varying from 30-70aa (at interval 10aa). Cross-linking assay, each intermediate length was incubated before (-) treatment with BS^3 as a control and after (+) treatment with BS^3. The cross-linked samples were resolved on a 10-12% SDS-PAGE gel (23A). In an associated experiment, cross-linked products of all intermediate lengths were used for immunoprecipitation (IP). Each sample was split to be treated with two antibodies; the first half incubated with anti-L23 and the other half incubated with anti-SRP54, then chilled on ice for two hours. After that, the incubated antibody reactions were pulled down with hydrate protein A-Sepharose. The samples were resolved on a 10-12% SDS-PAGE gel. The immunoprecipitation images show that the RNCs/anti-L23 were precipitated and raised to the ribosomal L23 at about 16 kDa, including other higher molecular weight of ribosomal proteins (23B), whereas RNCs/anti-SRP54 cross-linked can raise the strong intensity band of ribosomal protein SRP54 to be above 49 kDa, containing other unexpected lower/higher molecular weight of SRP proteins (23C).

DISCUSSION

Previous studies have been carried out in the 'Woolhead' lab to investigate the formation of secondary structure within the ribosome tunnel using the F_0c protein from *E. coli.* The F_0c is present in the bacterial inner membrane and is a short protein containing only 79 amino acids with two transmembrane domains, separated by a loop, with the short terminal. FRET analysis has revealed that the first transmembrane domain of F_0c begins to fold inside the ribosome tunnel and forms a compacted nascent chain within the exit tunnel of the ribosome before leaving and subsequently binding to SRP for membrane targeting (Robinson et al., 2012)

Further study from our group has shown this is not a regular event which occurs with every protein. The GPCR family is the largest group of transmembrane proteins comprising many diverse types of proteins, with the common theme being that each has seven transmembrane domains. Therefore, one of the GPCR members is preferable as a large membrane protein model for selection to ascertain the early protein folding. The human ortholog GPCR GPR35 is a plasma membrane receptor expressed in a wide variety of tissue and cell types. Recent work on the GPCR GPR35 has shown that the first transmembrane domain does not fold until it has reached the membrane translocation site at Sec61 in endoplasmic reticulum (ER) (Cherry, 2016 Unpublished).

However, my work which is presented here, is on the viral potassium channel, Kcv, which is a miniature protein (10.6 kDa) consisting of two transmembrane domains and resembling the common features of F_0c as shown in the previous study by Robinson et al. (2012). Furthermore, recently published work found that during both studies of *in vitro* and in *vivo* (in live bacteria) that the small protein domains which range in size 4-10 kDa have the early folding during translation while still inside the ribosome. The folding proteins possess three formational classes of secondary structures; α-helical, β-sheet, and mixed α+ β (Marino et al., 2016). Recent evidence on the co-translational folding event or folding during translation is still limited. However, from my experimental investigation using the post-translational modification, several example parts of the small model protein, Kcv, were obtained. The results of this project therefore reveal that the folding of Kcv should begin during translation within the ribosome due to the communication mechanism of the ribosome and the targeting transportation.

In the Kcv typical structural arrangement, a total of 94 assigned amino acid residues modulate as an ion channel in different structural functions; S-helix (1-13aa), TM1 (14-32aa), Loop1 (33-49aa), P-helix (50-62aa), Filter 63-68aa), Loop2 (69-75aa) and TM2 (46-94aa), respectively. The main structure has helical transmembrane domains of approximately 18 amino acids each that play vital roles in the interaction against the hydrophobic region in the lipid bilayer to span the pore and function as an ion channel (Tayefeh et al., 2009). The experimental detail in each critical step of early folding investigation is shown below;

Determining the secondary structure of the 1st transmembrane domain in ribosome bound nascent chain complexes using PEGylation assay

For the reference, contribution of amino acid inside the ribosome tunnel, Lu and Deutsch (2005) suggests that the nascent chain could be accommodated inside the ribosome tunnel depending on the structures; an α-helix ~1.5 Å per residue while an extended conformation (stretched chain) ~ 3.4 Å per residue. Based on the evidence from PEGylation, findings indicate that the first transmembrane domain of Kcv appears to be completely compacted in secondary structure in the ribosome tunnel, most likely in an alpha helical conformation. The PEGylation analysis of engineered cysteine (L8C) indicates the primary clue of a tiny shift-band when the nascent chain reaches a length of around 50aa (Fig.16D). To confirm the PEGylation results (Fig.21), the experiment was presented with the explicit adduct bands from 50aa using the PEGylation method to probe combination mutagenesis of M15L-Cysteine (additional substitution M15L to L8C).

An explanation of mass-tagging within the large ribosome is as follows: the cysteine residue in Kcv (L8C) is gradually monitored from the PTC in each defined truncated length. If the nascent chain conformation of the Kcv (L8C) is approximately at 30aa length, the cysteine marker is at a position 22 residues from the PTC (where the centre of the top of the large ribosome is). This is located too deep within the ribosome tunnel and the thiol PEG-MAL molecule is too large to access through the narrow tunnel for mass-tagging. However, when the nascent chains are at least 50aa, with the cysteine 42 residues from the PTC, the cysteine is released from the exit site and can actively conjugate with the PEG-MAL molecule as shown on an electrophoresis gel from truncated lengths 50-70aa. Therefore, structure inside the tunnel can be monitored by the timing of the PEGylation. And the PEGylation results can detect the primary transmembrane domain would begin to fold on the ribosome. On the other hand, it should be noted that we would expect the initial extra 13aa which is exposed from the ribosome nascent chain to be unfolded due to its N-terminus region.

Investigation of ribosome nascent chain protein interaction in the 1st TM domain using cross-linking assay and immunoprecipitation

Upon exiting the ribosome tunnel Kcv is likely to interact with chaperones to guide it to the membrane. To determine this process two homobifunctional cross-linkers were used; cysteine-cysteine (BMH) and lysine-lysine cross-linker (BS^3). Both cross-linkers demonstrated results that correspond to the PEGylation assays. In detail, the cross-linking results showed that the high truncated lengths have the adduct bands of cross-linked with the SRP54 homologue Ffh (two truncated lengths 60-70aa). Indicating that the first transmembrane domain binds to SRP upon exiting the ribosome.

A cross-linked band of ~50 kDa is just visible when it starts being released from the tunnel at approximately 60aa, providing further evidence of a compacted structure in the ribosome tunnel. To confirm the identity of this band an immunoprecipitation assay was used. The immunoprecipitation has introduced separately, two antibodies to distinguish the protein interaction, these were anti-L23 and anti-Ffh (SRP homologue of prokaryotes). The immunoprecipitation results found and confirmed the protein interaction between the nascent chain and ribosomal protein L23 and the targeting protein Ffh (SRP) varying from 50-70aa (Fig.10). The interaction between the nascent chain peptide and ribosomal protein (L23) and the signal recognition particle (SRP54 conserved part of SRP) is the universal principle of the beginning of protein targeting (Houben et al., 2005).

BS^3 used a different method by crosslinking lysine residues, to create a single targeted lysine, three endogenous lysines were replaced as follows (K29I/ K46/47M), leaving just K6 which is the only lysine marker present in the N-terminus sequence to be monitored with the lysine of BS^3. Unfortunately, the cross-linking assay using BS^3 cross-linker indicates only the bands of nascent chain lengths, but neither inefficient bands of ribosomal protein L23 nor the signal recognition particle SRP54 (Ffh) are visibly clear. However, initial folding in the first transmembrane can be predicted, accounting for the BMH induced adduct band on SDS-PAGE gels starting around 50-60aa.

To improve the reporter signal, three additional methionines were mutated into the Kcv sequence (M15/23/26L) combined with three single lysines mutagenesis (K29I/K46/47M +L8C) which resulted in an improvement of results both of cross-linking and immuno-precipitation (IP) images in the same manner as shown in previous results. Interestingly, immunoprecipitation analysis of cross-linked products shows more explicit intensity of interaction in the height bands (50-70aa) both of anti-L23 and anti-Ffh (Fig.23). Therefore, it can be suggested that the three methionine mutagenesis incorporated into a previous

construction with only a single methionine available in the first transmembrane domain would enable the best observations and give insight into protein folding and eliminate the extra bands in the translation products. Altogether, this phenomenon can explain that a single methionine codon in a mRNA of defined truncated lengths would be insured for initial starting of the translation process and result in clearer bands in each sequential step of the experiment, including translation products, cross-linked products, and immunoprecipitation images. However, although we can gain clearer bands, we still cannot get a single band in the translation products as expected from the consecutive mutagenesis.

The mutagenesis of Kcv for experimental purposes

The mutagenesis relies on the amino acid position and properties for our experimental purposes. In this project, we carried out the construction of the three critical processes step by step. We can replace the amino acid residues of the subject matter interest based on its native properties. First, a cysteine engineered (L8C) is used for the cysteine marker in the first transmembrane region for the PEGylation assay which is the proper site for conjugation with PEG-MAL and the results for further experiments. Second, three lysines engineered K29I/K46/47M for the cross-linking method show improvement only in the cross-linked immunoprecipitation assay. Because of the amino acid residue properties, an isoleucine at position 29 is a non-polar side chain with hydrophobicity while two replacement methionines K46/47M which are for the increasing radio-labelling activity with a radioactive reagent, [^{35}S] ^{Met} result in the increased capture of intensity bands in the X-ray film. Furthermore, these two methionine substitutions increase the hydrophobicity in the Kcv domain. Hence, in this lysine mutagenesis, improvements in the results of cross-linked immunoprecipitation are manifested. Third, three methionines mutagenesis M15**/**23**/**26L**-**Lysine are obtained from the combination with three single replacements and a single methionine remains from this mutagenesis for starting codon**.** Eventually, the improvement of the Kcv insertion studies was detailed using SDS**-**PAGE gels and autoradiography for analysis, this being the best approach to separate the small size protein**.** For better understanding of function, this mutagenesis could be used to monitor the role of Kcv function**.**

T**he Kcv folding in prokaryotic (S30) *in vitro* transcription/translation system**

Much previous published work has supported this Kcv folding profile, that the sequential processes of the Kcv folding pathway initially is based on the prokaryotic (S30) *in vitro* transcription/translation expression system. For the coupling transcription/translation process to be sufficient and efficient, the supplements involve, for example, amino acids,

energy sources, nucleotides and salts (Nirenberg & Mattaei, 1961). *In vitro* transcribed mRNA is employed for the reactions to be adequately radioactively labelled with Sulfur-35 radioactive reagent [methionine amino acid labelled] ^{35}S-Met which can be detected by X-ray film, using an X-Omat developer, as an autoradiography trough when dried on a SDS-PAGE gel. The ribosome nascent chains (RNCs) were installed from the truncated mRNA without the stop codons to prevent the nascent chain being released from the ribosome (Huter et al., 2017).

The translation is variable depending on environments and organisms, for example, the translation rates *in vivo* are faster than *in vitro* systems (Fedyukina & Carvagnero, 2011). However, the translation in the *in vitro* system can also be described in four main steps; initiation, elongation, termination, and recycling. In regard to the synthesis rate of prokaryotic *in vitro* system, the ribosome translates mRNA into the amino acid sequence that is needed for the Kcv nascent chain to be synthesised at approximately 10-20 amino acid/second (Cabrita et al., 2016), whereby the different codons and structural elements in mRNA attributes determine the elongation rate and further proper folding. (Goldman et al., 2015).

Generally, the classical hypothesis of protein folding process is that folding starts early from the secondary elements and is then followed by the tertiary structure which is formed by the compaction of the secondary structure (Kim & Baldwin, 1982). Regarding this principle of folding formation, we would expect that Kcv would have the early process of folding on the ribosome. During the translation of Kcv, the evidence provided here suggests that the alpha helical transmembrane of Kcv initiates folding in the ribosome emerging from the ribosome tunnel. The communication of the nascent chain and ribosomal protein L23 and targeting protein (SRP54) correspond to the delivery pathway. Generally, if we give an outline of the Kcv transportation, we see that L23 is first seen by the nascent chain at 50aa in length, this is much later than with and extended peptide (~30aa). L23 contains an external affinity site for bacterial SRP, so the nascent chain is transferred between L23 and Ffh at ~60aa from the PTC (Kramer et al., 2002; Luirink & Sinning, 2004; Akopian et al., 2013).

Recruitment by SRP occurs as the transmembrane domain emerges from the ribosome tunnel. The C-terminal M domain of Ffh contains a hydrophobic cleft that has numerous methionine residues that can be associated to the central part of the nascent chain signal. Also, the NG domain (GTPase domain) of Ffh can make a reciprocal contribution for binding to the signal of the exported nascent chain (Cross et al., 2009).

The RNC/SRP complex then targets the Kcv towards the membrane. It is unknown if other membrane machinery is required for membrane integration or if this occurs spontaneously.

Conclusion

In summary, this study has investigated if the first transmembrane domain of Kcv would fold in the ribosome tunnel during translation. Apparently, PBCV-1 Kcv is the shortest potassium channel protein composed of just 94 amino acids with two transmembrane domains. It is possible that the initial folding process and conformation of small protein domains occurs in the ribosome rather than in the plasma membrane. According to the evidence from previous research, this may be a cellular mechanism to prevent protein mis-folding in the hydrophilic cell cytosol. Regarding my results using PEGylation and chemical cross-linking, both approaches show the same event of the first TM domain compacting early in the ribosome exit tunnel. Therefore, based on our previous studies, it is possible to support the hypothesis that the small membrane proteins such as Kcv and F_0c appeared to follow this folding pathway of initial transmembrane domain compaction inside the ribosome tunnel before insertion into the membrane. This does not appear to be consistent with larger proteins such as the seven transmembrane domains GPCRs. This mechanism could be indicative of an easier insertion route for small hydrophobic proteins such as Kcv and F_0c, which do not require the many protein component and membrane co-factors for targeting and insertion that larger proteins such as GPCRs do.

Future Direction

In order to carry out on an extensive investigation of the viral potassium channel Kcv, high potential techniques to elucidate other questions of the proteins underlying structures and functions should be examined further. NMR spectroscopy is the effective machine to investigate the folding of three-dimension structure such as the N-terminus region from which we can select the most interesting model to incorporate with interest sources. X- ray crystallography can be used to solve both structure and function. Kcv structure will be determined in terms of its various parts in more detail, such as cations crossing the channel between the outside- inside of the cell, the conduction pathway, the backbone structure, Oxygen atom or Hydrogen atom. Furthermore, mutagenesis for changing the properties of amino acids in the Kcv should be focused on, for instance the hydrophobicity of the transmembrane domains and the effect of protein targeting by replacing some amino residues.

BIBBILOGRAPHY

1. Ackerman, M.J., Clapham, D.E. 'Ion channels-Basic science and clinical disease,' The New England Journal of Medicine. 1997. 336 (22):1575-586.
2. Akopian, A., Shen, K., Zhang, X., Shan, S.O. 'Signal recognition particle: An essential protein targeting machine', Annual Review of Biochemistry. 2013. 82: 693-721.
3. Alberts, B., Johson, A., Lweis, J., Raff, M., Roberts, K., Walter, P. 'Membrane protein.' In Molecular Biology of the Cell. 2002. 4th (Edit.). Garland Science: New York, USA.
4. Allnér, O., Nilsson, L. 'Nucleotide modifications and tRNA anticodon-mRNA codon interaction on the ribosome', RNA, Cold Spring Harbor Laboratory Press. 2011. 17 (12): 2177-188.
5. Ban, N., Nissen, P., Hansen, J., Moore, P. B., Steitz, T. A. 'The complete atomic structure of the large ribosomal subunit at 2 .4 Å resolution', Science. 2000. 289 (5481): 905-920.
6. Beckert, B., Kedrov, A., Sohmen, D., Kempt, G., Wild, K., Sinning, I., Stahlberg, H., Wilson, D., Beckmann, R. 'Translation arrest by a prokaryotic signal recognition particle is mediated by RNA interaction', Nature structural & Molecular Biology Article. 2015. 22: 767-773.
7. Beckmann, R., Spahn, C.M., Eswar, N., Helmers, J., Penczek, P.A., Sali, A., Frank, J., Blobel, G. 'Architecture of the protein-conducting channel associated with the translating 80S ribosome', Cell. 2001. 107: 361-372.
8. Beckstein, O. 'Principles of gating mechanisms of ion channels', 2004. A thesis of Doctor of Philosophy, Molecular Biophysics and Merton College, Oxford University.
9. Berg, J.M., Tymoczko, J.L., Stryer, L. 'Eukaryotic protein synthesis differs from prokaryotic protein synthesis primary in translation initiation', In Biochemistry. 5th(Edit). 2002. New York: W.H. Freeman.

10. Bernstein, H.D., Zopf, D., Freymann, D.M., Walter, P. Functional substitution of the signal recognition particle 54-kDa Subunit by its *Escherichia coli* homolog. Proc Natl Acad Sci USA. 1993. 90(11): 5229-233.

11. Bhushan, S., Gartmann, M., Halic, M., Armache, J.P., Jarasch, A., Mielke, T., et al. 'α-helical nascent polypeptide chains visualized within distinct regions of the ribosome exit tunnel', Nature Structural and Molecular Biology. 2010. 17: 313-317.

12. Booth, P. J. 'The trials and tribulations of membrane protein folding *in vitro*', Biochimica et Biophysica Acta (BBA)-Biomembrane. 2003:1610 (1): 51-56.

13. Bordo, O., Argos, P. 'The role of side-chain hydrogen bonds in the formation and stabilization of secondary structure in soluble proteins', Journal of Molecular Biology. 1994. 243(3): 504-19.

14. Borrell, J.H., Domènech, O., Keough, K. 'Membrane protein-lipid interactions: Physics and chemistry in the bilayer', Springer International Publishing. 2016. 1st (Edit). Switzerland.

15. Bradding, P., Wulff, H. 'Ion channels. Chest Clinic', Thorax. 2013. 68: 974-977.

16. Branden C., Tooze, J. 'Introduction to protein structure', 1999. 2nd (Edit). Garland Publishing, Inc. United States of America.

17. Braun, C.J., Lachnit, C., Becker, P., Henkes, L.M., Arrigoni, C., Kast, S.M., Moroni, A, Thiel,G., Schroeder, I. 'Viral potassium channels as a robust model system for studies of membrane-protein interaction', Biochimica et Biophysica Acta (BBA)-Bomembranes. 2014; 1838 (4): 1096-103.

18. Buckingham, S.D., Kidd, J.F., Law, R.J., Franks, C.J., Sattelle, D.B. 'Structure and function of two-pore-domain K+ channels: contributions from genetic model organisms', Trends in Pharmacological Science. 2005. 26(7): 361–367.

19. Cabrita, L.D., Dobson, C.M., Christodoulou, J. ‘Protein folding on the ribosome’, Current Opinion in Structural Biology. 2010, 20: 33-45.

20. Cabrita, L.D., Casaignau, A.M.E., Launay, H.M.M., Woudby, C.A., Wlodarski, T., Camilloni, C., Karyadi, M.E., Robertson, A.L., Wang, X., Wentink, A., Goodsell, L.S., Woolhead, C, A., Vendruscolo, M., Dobson, C.M., Christoduolou,J. ‘A structural ensemble of a ribosome-nascent chain complex during cotranslation protein folding’, Natural Structure & Molecular Biology. 2016. 23 (4): 278-285.

21. Carlson, E.D., Gan, R., Hodgman, C.E., Jewett, M.C. ‘Cell-free protein synthesis: Applications come of age’, Biotechnology Advances, 2012. 30(5): 1185-1194.

22. Carter, A P., Clemons, W. M., Brodersen, D. E., Morgan-Warren, R. J., Wimberly, B. T., Ramakrishnan, V. ‘Functional insights from the structure of the 30S ribosomal subunit and its interactions with antibiotics’, Nature. 2002. 407(6802): 340–8.

23. Carter, A.P., Clemen, W.M.Jr., Brodersen, D.E., Morgan-Warren, R.J. Hartch, T., Wimberly, B.T., Ramakrishnan, V. ‘Crystal structure of an initiation factor bound to 30S ribosome subunit’, Science. 2001. 291 (5503): 498-501.

24. Chavatte, L., Kervestin, S., Favre, A., Jean-Jean, O. ‘Stop codon selection in eukaryotic translation termination: comparison of the discriminating potential between human and ciliate eRF1s’, The EMBO Journal. 2003. 22 (7): 1644-653.

25. Cherry, J. ‘A biochemical analysis into the co-translational folding of a G-protein-coupled receptor: GPR35’, 2016. PhD thesis. Molecular, Cell and Systems Biology, College of Medical, Veterinary and Life Science, University of Glasgow, United Kingdom.

26. Christodoulou group (Protein folding on the ribosome). Co-Translation protein folding. University College London. Available from https://www.ucl.ac.uk/smb/christodoulou/research/cotranslational-folding.[Access 14th February, 2016].

27. Cooper, G.M., Hausman, R.E. 'The cell: A molecular approach', 2009. 5th (Edit.). Sinauer Associates, Inc. USA.

28. Cross, B.C.S., Sinning, I., Luirink, J., High,S. 'Delivering proteins for export from the cytosol,' Nature Reviews/Molecular Cell Biology. 2009. 10:255-264.

29. Cross, M.O. 'Examining the effect of pH on the structure and stability of CLIC1 with E228L and E85L CLIC1 variants', 2013. The thesis for the degree of Master of Science. University of Witwatersrand, Johannesburg, South Africa.

30. Dallas, A., Noller, H.F. 'Interaction of translation initiation factors with the 30S ribosomal subunit', Molecular cell. 2001. 8 (4): 855-864.

31. Deisenhofer, J., Epp, O., Miki, K., Huber, R., Michel, H. 'Structure of the protein subunit in the photosynthetic reaction centre at Phodoseudomonas viridis at 3 Å resolution', Nature. 1985. 1,318 (6047): 618-624.

32. Dill, K.A. 'Dominant force in protein folding,' Biochemistry. 1990. 29: 7133-155.

33. Doherty, D.H., Rosendahn, M.S., Smith, D.J., Hughes J.M., Chlipala, E.A., Cox, G.N. 'Site-specific PEGylation of engineered cysteine analogues of recombinant human granulocyte-macrophage colony-stimulating factor', Bioconjugate Chemistry. 2005. 16(5): 1291-1298.

34. Dombkowski, A.A., Sulta, K.Z., Craig, D.B. 'Protein disulfide engineering. FEBS Letters', 2014. 588(2): 206-212.

35. Doyle, D.A., Morais Cabral, J., Pfuetzner, R.A., Kuo, A., Gulbis, J.M., Cohen,S.L.,Chait, B.T., MacKinnon, R. 'The structure of the potassium channel: molecular basis of K^+ conduction and selectivity', Science. 1998. 3;280(5360):69-77.

36. Duadna, J.A., Batey, R.T. 2004. 'Structural insight into the signal recognition particle', Annual Review of Biochemistry. 2004. 73: 539-57.

37. Fedyukina, D.V, Cavagnero, S. 'Protein folding at the exit tunnel', Annual Review of

Biophysics. 2011. 40:337-359.

38. Ferreira-cerca, S., Pöll,G., Gleizes, P-E., Tschochner,H., Milkereit, P. 'Roles of eukaryotic ribosomal proteins in maturation and transport of pre-18S rRNA and ribosome function,' Molecular Cell. 2005. 20:263-275.

39. Frohns, F., Käsmann, A., Kramer, D., Schäfer, B., Mehmel, M., Kang, M., Van Etten, J. L., Gazzarrini,S., Moroni, A. Thiel, G. 'Potassium ion channels of Chlorella viruses cause rapid depolarization of host cells during infection', Journal of Virology. 2006. 80: 2437–244.

40. Gabashivili, I.S., Sokolowski, B.H., Morton, C.C., Gierch, A.B. 'Ion channel gene expression in the inner ear,' Journal of the Association for Research Otolaryngology. 2007. 8: 305-328.

41. Gaulerzi, C.O., Pon, C.L. 'Initiation of mRNA translation in prokaryotes', Biochemistry. 1990. 29: 5881-589.

42. Gazzarrini, S., Van Etten., DiFrancesco, D., Thiel, G., Moroni, A. 'Voltage-dependence of virus-encode miniature K+ channel Kcv', The Journal of Membrane Biology. 2002. 187: 15-25.

43. Gazzarrini, S., Severino, M., Lombardi, M., Morandi, M., DiFrancesco, D., Van Etten, J.L., Thiel, G., Moroni, A. The viral potassium channel Kcv: structural and functional features. FEBS Letters. 2003. 552: 12-16.

44. Gazzarrini,S.,.Kang, M., Abenavoli, A., Romani, G., Olivari, C., Gaslini, D., Ferrara, G., Van Etten, J.L., Kreim, M., Kast, S.M., Thiel, G., Moroni, A. 'Chlorella virus ATCV-1 encodes a functional potassium channel of 82 amino acids'', Biochemical Journal. 2009. 420(2): 295-303.

45. Gebhardt, M., Hoffgaard, F., Hamacher,K., Kast, S.M., Moroni, A., Thiel,G. 'Membrane anchoring and interaction between transmembrane domains are crucial

for K^+ channel function', Journal of Biological Chemistry. 2011. 286 (13): 11299-306.

46. Goldman, D.H., Kaiser, C.M., Milin, A., Righini, M., Tinoco, I.Jr., Bustamante, C. 'Ribosome. Mechanical force releases nascent chain-mediated ribosome arrest *in vitro* and *in vivo*', Science. 2015. 348(6233):457-460.

47. Grant, A.O. 'Cardiac ion channels,' Basic science for the clinical electrophysiologist. 2009. 2: 185-194.

48. Green, R., Noller, H. F. 'Ribosomes and translation', Annual review of biochemistry. 1997. 66: 679–716.

49. Greiner, T., Fronhs, F., Kang, M., Van Etten, J.L. Käsmann, A., Moroni, A., Hertel, B., Thiel, G. 'Chlorella viruses prevent multiple infections by depolarizing the host membrane', Journal of General Virology. 2009. 90: 2033-2039.

50. Gualerzi, C.O., Brandi, L., Caserta, E., Garofalo, C., Lammi, M., La Teana, A., Petrelli, D., Spurio,R., Tomsic, J., Pon, C.L. 'Initiation factors in the early event of mRNA translation in bacteria', Cold Spring Harbor Symposia on Quantitative Biology. 2001. (66): 363-76.

51. Gutman, G.A., Chandy, K.G., Grissmer, S., Lazdunski, M., McKinnon, D., Pardo, L.A., et al. 'International union of pharmacology. LIII. Nomenclature and molecular relationships of voltage-gated potassium channels', Pharmacological Reviews. 2005. 57 (4): 473–508.

52. Hartz, D., McPheeters, D.S., Gold, L. 'Selection of the initiation tRNA by *Escherichia coli*. Initiation factors', Genes & Development. 1989. 3:1899-912.

53. Hegde, R.S., Keenan, R.J. 'Tail-anchored membrane protein insertion into the endoplasmic reticulum', Nature Reviews; Molecular Cell Biology. 2011. 12:787-798.

54. Heginbotham, L.,Lu, Z.,Abramson,T., Mackinnon, R. 'Mutations in the K+ channel signature sequence', Biophysical Journal. 1994. 66(4):1061-067.

55. Hemaprabha, E. ‘Chemical crosslinking of proteins: A review’, Journal of Pharmaceutical and Scientific. 2012. 1 (1): 22-26.

56. Hershey, J.W.B., Sonenberg, N., Mathews, M.B. ‘Principle of the translational control: An overview’, Cold Spring Harbor Perspective in Biology. 2012. 4:1-10.

57. Hertel, B., Tayefeh, S., Kloss, T., Hewing, J., Gebhardt, M., Baumeister, D., Moroni, A., Thiel, G., Kast, S.M. ‘Salt bridges in the miniature viral channel Kcv are important for function’, European Biophysics Journal. 2010. 39 (7): 1057-1068.

58. Hibino H., Inanobe, A., Furutani, K., Murakami, S., Findlay, I., Kurachi, Y. ‘Inwardly rectifying potassium channels: their structure, function, and physiological roles’, Physiological Reviews. 2010. 90: 291–366.

59. Hille, B. 1992. ‘Ion channels of excitable membranes’ 2nd (Edit.). Sunderland, MA: Sinauer Associates, Inc. U.S.A.

60. Hille, B. 2001. ‘Ion channels of excitable membranes’ 3rd (Edit). Sunderland, MA: Sinauer Associates, Inc. U.S.A.

61. Hodgman, C.E., Jewett, M.C, ‘Cell-free synthetic biology: Thinking outside the Cell’, Metabolic Engineering. 2012. 14(3): 261–269.

62. Houben, E.N.G., Zarivach, R., Oudega, B., Luirink, J. ‘Early encounters of nascent membrane protein’. Journal of Cell Biology. 2005. 170(1):27-35.

63. Huang, T., Wan,S., Xu,Z., Zheng, Y., Feng, K.Y., Li, H.P., et al. ‘ Analysis and prediction of translation rate based on sequence and functional features of mRNA', PloSONE. 2011. 6(1): e16036.

64. Hubbard, R.E., Haider, M.K. ‘Hydrogen bonds in proteins: Role and strength’, Encyclopedia of Life Sciences, John Wiley & Sons, Ltd. 2010. 1-7.

65. Hussain, T.,Llácer, J.L., Wimberly, B.T.. Kieft, J.S., Ramkrishanan, V. ‘Large-scale movement of IF3 and tRNA during bacterial translation initiation;’ Cell. 2016. 167 (1):

133-144.

66. Huter,P., Müller, C., Beckert, B., Arenz,S., Berninghausen,O., Beckmann, R., Wilson, D.N. 'Structural basis for ArfA-RF2-mediated translation termination on mRNA lacking stop codons', 2017. Nature. 541:546-549.

67. Jenni, S., Ban, N. 'The chemistry of protein synthesis and voyage through the ribosomal tunnel', Current Opinion in Structural Biology. 2003. 13: 212-219.

68. Kandel, E.R, Schwartz, J.H, Jessell, T. M. 'Principles of Neural Science' 2000. 4th (Edit). New York: McGraw-Hill. USA.

69. Kang, M., Graves, M., Mehmel, M., Moroni, A., Gazzrrini, S.,Thiel, G., Gurnon, J.R., Van Etten, J.L. 'Genetic diversity in Chlorella viruses flanking Kcv, a gene that encodes a potassium ion channel protein', Virology. 2004. 326 (1): 150-159.

70. Kang, M., Moroni, A., Gazzarrini, S., Van Etten, J.L. 'Are chlorella viruses a rich source of ion channel genes?', FEBS Letters. 2003. 552: 2-6.

71. Karp, G. 'Cell and molecular biology: Concepts and experiments', 2006. 6th (Edit.). John Willey & Sons, Inc. USA.

72. Karshikoff, A., Jelesarov, I. 'Salt bridges and conformational flexibility,' Biotechnology & Biotechnological Equipment. 2008. 606-611.

73. Kauzmann, W. 'Some factors in the interpretation of protein denaturation', Advance in Protein Chemistry. 1959. 14: 1-63.

74. Keenan, R.J. Freymann, D.M. Stroud, R.M., Walter, P. 'The signal recognition particle', Annual Reviews of Biochemistry. 2001. 70:755-75.

75. Killian, J.A. 'Synthetic peptides as models for intrinsic membranes', FEBS Letters. 2003. 555: 134-138.

76. Kim, P.S., Beldwin, R.L. 'Specific intermediates in the folding reactions of small proteins and the mechanism of protein folding', Annual Review of Biochemistry, 1982.

51:459-489.

77. Kim, D. ‘Review: Physiology and pharmacology of two-pore domain potassium channels’, Current Pharmaceutical Design. 2005. 11(21): 2717-736.

78. Kim, D.M., Swartz, J.R. ‘Efficient production of a bioactive, multiple disulfide-bonded protein using modified extracts of *Escherichia coli’*, Biotechnology and Bioengineering. 2004. 85 (2) 122–129.

79. Korobeinnikova, A.V., Garber, M.B., Gongadze, G.M. ‘Ribsomal protein: structure, function, and evolution’, Biochemistry (Moscow). 2012. 77(6): 562-574.

80. Kozak, M. ‘ Initiation of translation in prokaryotes and eukaryotes,’ 1999. 234: 187-208.

81. Kramer, G., Rauch, T., Rist, W., Sonja, V., Palzelt, H., Schulze-Specking, A., Ban, N., Deuerling, E., Bukau, B. ‘L23 protein function as a chaperone docking site on the ribosome’, Nature. 2002: 419: 171-174.

82. Kramer, G., Boehring, D., Ban, N., Bukau, B. ‘The ribosome as a platform for co-translational processing, folding and targeting for newly a synthesized proteins’, Nature Structural & Molecular Biology. 2009. 16 (6): 589-597.

83. Kubo, Y., Adelman, J.P., Clapham, D.E., Jan, J.Y., Karschin, A., Kurachi, Y., Lazdunski, M., Nichols, C.G., Seino, S., Vandenberg, C.A. ‘International Union of Pharmacology. LIV. Nomenclature and molecular relationship inwardly rectifying potassium channels’, Pharmacological. Review. 2005. 57 (4): 509-526.

84. Kuo, A., Gulbis, J.M., Antcliff J.F., Rahman, T., Lowe, E.D., Zimmer, J., Cuthberson, J., Ashcroft, F.M., Ezaki, T., Doyle, D.A. ‘Crystal structure of the potassium channel KirBac1.1 in the closed state’, Science. 2003. 300 (5627): 1922–926.

85. Kuo, M.M., Haynes, W.J., Loukin, S.H., Kung, C., Saimi, Y. ‘Prokaryotic K (+) channels: from crystal structures to diversity’, FEMS Microbiology Reviews. 2005. 29(5): 961–985.

86. Kwon, Y.C., Jewett, M.C. 'High-throughput preparation methods of crude extract for robust cell-free protein synthesis', Scientific Reports. 2015. 5 (8663): 1-8.

87. Laursen, B.S., Sørensen, H.P., Mortensen, K.K., Sperling-Peterson, H.U. 'Imitation of protein synthesis in bacteria', Microbiology and Molecular Biology Review. 2005. 69 (1): 101-123.

88. Lesser, G.J., Rose, G.D. 'Hydrophobicity of amino acid subgroup in proteins'. Proteins. 1990. 8 (1): 6-13.

89. Lin, K.F., Sun, C.S., Huang, Y.C., Chan, S.I., Koubek,J.R., Wu, T.H., Huang, J.J.T. 'Cotranslational protein folding within the ribosome tunnel influence trigger-factor recruitment', Biophysical Journal. 2012, 102 (12): 2818-827.

90. Lins, L., Brasseur, R. 'The hydrophobic effect in protein folding', The FASEB Journal. 1995. 9:535-540.

91. Lockwood, A.H. Chakraborty, P.R., Maitra, U. 'A complex between initiation factor IF2, guanosine triphosphate, ad fMet-tRNA: an intermediate in initiation complex formation', In Proceeding of the National Academy of Science of the United States of America. 1971. 68(12): 3122-126.

92. Lu, J., Deutsch, C. 'Pegylation: A method for assessing topological accessibilities in Kv1.3.', Biochemistry. 2001. 40 (44): 13288-301.

93. Lu, J., Deutsch, C. 'Secondary structure formation of transmembrane segment in Kv channel', Biochemistry. 2005. 44(23): 8230-243.

94. Luirink, J., ten Hagen-Jongman, C.M., van der Weijden, C.C., Oudega, B., High, S., Dobberstein, B., Kusters, R. 'An alternative protein targeting pathway in *Escherichia coli*: studies on the role of FtsY', The EMBO Journal. 1994. 13 (10): 2289-296.

95. Luirink, J., Sinning, I. 'SRP-mediated protein targeting: structural and function revisited', Biochimica et Biophysica Acta (BBA)-Molecular Cell Research. 2004. 1694 (1-3): 17-35.

96. Lütcke, H. ‘Signal recognition particle (SRP), a ubiquitous initiator of protein translocation’, European Journal of Biochemistry. 1995. 228(3): 531-550.

97. Marino, J., von Heijne. G., Beckmann, R. ‘Small protein domains fold inside the ribosome exit tunnel’, FEBS Letters. 2016. 590 (5): 655-650.

98. Mathie, A., Clarke,C.E., Ranatunga, K.M., Veale, E.L. ‘What are the roles of the many different types of potassium channel expressed in cerebellar granule cells?’, Cerebellum. 2003. 2(1): 11-25.

99. Mayeur, G.L., Fraser, C.S., Peiretti, F., Block, K.L., Hershey, J.W. ‘Characterization of eIF3k, a newly discovered subunit of mammalian translation initiation factors eIF3’, European of Journal Biochemistry. 2003. 270 (20): 4133-139.

100. Mehmel, M., Rothermel, M., Meckela, T.,Van Etten, J.L., Moroni, A., Thiel., G. ‘Mini review: Possible function for virus encoded K+ channel Kcv in the replication of chlorella virus PBCV-1’,. FEBS Letters. 2003. 552 (1): 7-11.

101. Merrick, W.C. ‘Mechanism and regulation of eukaryotic protein synthesis’, Microbiology Reviews. 1992. 56 (2) 291-315.

102. Meuzelaar,H., Tros,M., Huerta-Viga, A., van Dijk, C.N., Vreede, J., Woutersen, S. ‘Solvent-exposed salt-bridges influence the kinetics of α-helix folding and unfolding,’ The Journal of Physical Chemistry Letters. 2014. 5:900-904.

103. Milon, P., Carotti, M., Konevega, A.L., Wintermeyer, W., Radnina, M.V., Gualerzi, C.O. ‘The ribosome-bound initiation factor 2 recruits initiator tRNA to the 30S initiation complex’, EMBO Reports. 2010. 11(4): 312-316.

104. Minor Jr., D.L ‘Potassium channels: life in the post-structural world’, Current Opinion in Structural Biology. 2001, 11: 408-414.

105. Minor Jr., D.L. ‘Searching for interesting channels: pairing selection and molecular evolution methods to study ion channel structure and function,’ Molecular BioSystems. 2009. 5(8): 802-810.

106. Nagai, K., Oubridge, C., Kuglstatter, A., Menichelli, E., Isel, C., Jovine, L. 'Structure, function, and evolution of the signal recognition particle', The EMBO Journal. 2003. 22 (14): 3479-485.

107. Nugent, T. 'Transmembrane protein structure prediction using machine learning', 2010. Thesis of Doctor of Philosophy, Department of Computer Science, University College London.

108. Nirenberg, M.W., Matthaei, J.H. 'The dependence of cell-free protein synthesis in *E. coli* upon naturally occurring or synthetic polyribonucleotides', Proceedings of the National Academy of Science. 1961. 47(10): 1588-602.

109. Pace. C.N., Scholtz, J.M., Grimsley, G.R. 'Forces stabilizing proteins', FEBS Letter. 2014. 588: (14):2177-184.

100. Pace, C.N., Fu, H., Fryar, K.L., Landua, J., Trevino, S.R. Shirley, B.A. Hendricks, M.M., Iimura, S., Gajiwala, K., Scholtz, J.M., Grimsley, G.R. 'Contribution of hydrophobic interaction to protein stability', Journal of Molecular Biology. 2011: 408 (3): 514-528.

101. Pagliuca, C., Goetze, T. A., Wagner, R., Thiel, G., Moroni, A., Parcej, D. 'Molecular properties of Kcv, a virus encoded K+ channel', Biochemistry. 2007, 46 (4): 1079–090.

102. Parsegian, A. 'Energy of an ion crossing a low dielectric membrane: solutions to four relevant electrostatic problems', Nature. 1969. 221:844–846.

103. Petrelli, D., La Teana, A., Garofalo, C., Spurio, R., Pon, C.L., Gualerzi, C.O. 'Translation Initiation factor IF3: Two domains, five functions, one mechanism?', The EMBO Journal. 2001. 20 (16): 4560-569.

104. Petsko, G.A., Ringe, D. 'Protein structure and function', New Science Press. Ltd. London. UK. 2004, pp.10-13.

105. Plugge, B., Gazzarrini, S., Nelson, M., Cerana, R., Van Etten, J.L, Derst, C., DiFrancesco, C., Moroni, A., Thiel, G. 'A potassium channel protein encoded by Chlorella virus PBCV-1', Science. 2000. 287 (5458): 1641-644.

106. Pongs, O., Kecskemethy, N., Muller, R., Krah-Jentgens, I., Baumann, A., Kiltz, H.H., Canal, I., Llamazares, S., Ferrus, A. 'Shaker encodes a family of putative potassium channel proteins in the nervous system of Drosophila', The EMBO Journal. 1988. 7 (4): 1087–096.

107. Ramakrishnan, V. 'Ribosome structure and the mechanism of translation', Cell, 2002. 8 (4):557-572.

108. Rastogi. S.C. 'Protein synthesis in eukaryotes', In Cell Biology, 2nd (Edit). 2002. New Age International (P) Limited, Publishers.

109. Robinson, J.M., Kosolapov, A., Deutsch, C. 'Tertiary quaternary structure formation of voltage-gate potassium channel; Method for studying channel structure function', In Ion channels methods and protocols. 2006. Humana Press, Totowa: New Jersy, USA.

110. Robinson, P.J., Findlay, J.E., Woolhead, C.A. 'Compaction of a prokaryotic signal-anchor transmembrane domain begins with the ribosome tunnel and is stabilized by SRP during targeting', Journal of Molecular Biology. 2012. 423:600-612.

111. Roux, B., Berneche, S., Egwolf, B., Lev, B., Noskov,S.Y., Rowley,C.N., Yu, H. 'Ion selectivity in channels and transporter,' The Journal of General Physiology. 2011. 137(5):415-426.

112. Salkoff, L., Wei, A.D., Baban, B. et al. 'Potassium channel in *C. elegans'*, 2005. WormBook Research. WormBook, Pasadena (CA).

113. Schluenzen, F., Tocilj, A., Zarivach, R., Harms, J., Gluehmann, M., Janell, D., Bashan, A., Bartels, H., Franceschi, F., Yonath, A. 'Structure of functionally activated small ribosomal subunit resolution at 3.3 angstrom resolution', Cell. 2000. 102 (5): 615–623.

114. Seidelt, B., Innis, C. A., Wilson, D. N., Gartmann, M., Armache, J.P., Villa, E., Trabuco, L. G., et al. 'Structural insight into nascent polypeptide chain-mediated translational stalling', Science. 2009. 326 (5958): 1412-415.

115. Schrempf, H., Schmidt, O., Kümmerlen, R., Hinnah, S., Müller, D., Betzler, M., Steinkamp, T., Wagner, R. ' A prokaryotic potassium ion channel with two predicted transmembrane segments from *Streptomyces lividans'* , The EMBO Journal. 1995. 14(21):5170-178.

116. Shim, J.W, Yang, M., Gu, L.Q. '*In vitro* synthesis, tetramerization and single channel characterization of virus-encoded potassium channel Kcv', FEBS Letters. 2007. 581 (5): 1027–1034.

117. Shine, J., Dalgarno, L. 'The 3'-terminal sequence of *Escherichia coli* 16S ribosomal RNA: complementary to nonsense triplets and ribosome binding sites', In Proceedings of the National Academy of Science of United States of America. 1974. 71(4): 1342-346.

118. Siotto, F., Martin, C., Rauh, O., Van Etten, J.L., Schroeder, I., Moroni, A., Thiel, G. 'Viruses infecting marine picoplancton encode functional potassium ion channels', Virology. 2014. 466-467: 103-111.

119. Svitkin, Y.V, Pause, A., Haghighat, A., Pyronnet, S., Witherell, G., Belsham, G.J., Sonenberg, N. 'The requirement for eukaryotic initiation factor 4A (elF4A) in translation is the direct proportion to the degree of mRNA 5' secondary structure', RNA. 2001. 7 (3): 382-394.

120. Swartz, J.R. 'Transforming biochemical engineering with cell-free biology', AIChE Journal. 2012. 58 (1): 5–13.

121. Tabassum, N, Feroz, A. 'Ion channels and their modulation', Journal of Applied Pharmaceutical Science. 2011. 1(1): 20-25.

122. Tayefeh, S., Kloss, T., Kreim M., Gebhardt, M., Baumeister, D., Hertel, B., Richter, C., Schwalbe, H., Moroni, A., Thiel, G., Kast, S.M. 'Model development for the viral Kcv potassium Channel', Biophysical Journal. 2009. 96(2):485-498.

123. Tayefeh, S(a). 'Computational study of the Kcv potassium channel', PhD. Thesis for Diploma degree in Biology. 2007. Universität Darmstadt, Germany.

124. Tayefeh, S(b). Kloss, T., Thiel, G., Hertel, B., Moroni, A., Kast, S.M. 'Molecular

dynamics simulation of the cytosolic mouth in Kcv-type potassium channels', Biochemistry. 2007. 46 (16): 4826-839.

125. Thangudu, R.R., Monoharan, M., Srinivasan, N., Cadet, F., Sowdhamini, R., Offmann, B. 'Analysis on conservation of disulphide bonds and their structural features in homologous protein domain families', BioMed Central Structural Biology. 2008. 8(55): 1-22.

126. Thiel, G., Moroni, A. Dunigan, D., Van Etten, J.L. ' Initial events associated with virus PBCV-1 infection of *Chlorella* NC64A', Progress in Botany Fortschritte der Botanik. 2010. 71(3): 169-183.

127. Thiel, G., Baumeister, D., Schroeder, I., Kast, S.M., Van Etten, J.L., Moroni, A. 'Minimal art: or why small viral K^+ channels are good tools for understanding basic structure and function relations', Biochimica et Biophysica Acta (BBA)-Biomembranes. 2011. 1808(2): 580-588.

128. Tyagi, R., Gupta, M.N. 'Chemical modification and chemical cross-linking for protein/enzyme stabilization', Biochemistry (Moscow). 1998. 63(3): 334-344.

129. Vagin, O., Kraut, J.A., Sachs, G. 'Role of N-glycosylation in trafficking of apical membrane protein in epithelia,' American Journal of Physiology Renal Physiology. 2009. 296(3): 459-469.

130. Vester, B., Garrett, R.A. 'Structure of protein L23-RNA complex located at the A-site domain of the ribosomal peptidyl transferase centre', Journal of Molecular Biology. 1984. 179 (3): 431-452.

131. Vinothkumar, K.R., Henderson, R. 'Structure of membrane proteins,' Quarterly Reviews of Biophysics. 2010. 43(1): 65-158.

132. Voss, N.R., Gerstein, M., Steitz, T.A., Moore, P.B. 'The geometry of the ribosomal polypeptide exit tunnel', Journal of Molecular Biology. 2006. 360 (4): 893-906.

133. Walter, P., Blobel, G. 'Translocation of proteins across the endoplasmic reticulum. II. Signal recognition protein (SRP) mediates the selective binding to microsomal membranes of in-vitro-assembled polysomes synthesizing secretory protein', Journal

of Cell Biology. 1981. 91 (2):551–556.

134. Wang, K., Xie,S., Sun, B. `Viral protein function as ion channels,' Biochimica et Biophysica Acta (BBA)-Biomembranes. 2011. 1808:510-515.

135. Watson, H. 'Biological membranes', Essay in Biochemistry. 2015. 59: 43-70.

136. Watson, H.R., Wunderley, L., Andreou, T., Warwicker, J., High, S. 'Reorientation of the first signal-anchor sequence during potassium channel biogenesis at the Sec61 complex', Biochemical Journal. 2013. 456 (2):297-309.

137. White, P.J. 'The molecular mechanism of sodium influx to root cells', Trends in Plant Science. 1999. 4 (7): 245-246.

138. Whitford, D. 2005. 'Proteins Structure and Function', John Wiley Sons, Ltd. England.

139. Wilkins, R., Cross, S., Megson, I., Mereditch, D. 'The organization of cell membranes: the plasma membrane', in Oxford handbook of medical sciences. 2011. 2nd (Edit.). Oxford University Press; New York, USA.

140. Williamson, M. 'How proteins work' 2012. Garland Science, Taylor & Francis Group, LLC. USA.

141. Wimberly, B.T., Brodersen, D. E., Clemons, W. M., Morgan-Warren, Jr. R.J., Carter A. P., Vonrhein C., Hartsch, T., Ramakrishna, V. 'Structure of the 30S ribosomal subunit', Nature, 2000. 407: 327-339.

142. Wilson, D.N., Daudna Cate, J.H. 'The structure and function the eukaryotic ribosome,' Cold Spring Harbor Perspective in Biology. 2012. 1-17.

143. Wittmann, H.G. 'The seventh sir Hans Krebs lecture; Structure, function and evolution of ribosome', European Journal of Biochemistry. 1976, 61:1-13.

144. Woudby, C.A., Launay, H., Cabrita, L.D., Christodoulou, J. 'Protein folding on the ribosome studied using NMR spectroscopy', Progress in Nuclear Magnetic Resonance Spectroscopy. 2013, 74: 57-75.

145. Woolhead, C.A., Johnson,A.E., Bernstein,H.D. 'Translation arrest requires two-way communication between a nascent polypeptide and the ribosome', Molecular Cell.

2006. 22(5): 587-598.

146. Yutani, K., Ogasahara, K., Tsujita, T., Sugino, Y. 'Dependence of conformational stability on hydrophobic of the amino acid residues in a series of variant proteins and substituted at a unique position of the tryptophan synthase α subunit', Proc. Natl. Acad. Sci. USA. 1987. 84 (13): 4441-444.

147. Zhang, Q., Zhao, Y.,Yang, B., Fu, C., Zhao, L., Wang, X., Wei, Y., Tao, L. 'Lighting up the PEGylation via the hantzsch reaction', Polymer Chemistry. 2016. 7:523-528.

148. Zhang, K., Kaufman, R.J. 'Protein folding in the endoplasmic reticulum and unfolded protein response,' Molecular chaperones in health and disease. 2006. Springer-Verlag Berlin Heidelberg.

149. Zhou, H.X. 'Influences of crowded cellular environments on protein folding binding, and oligomerizaton: Biological consequences and potentials of atomistic modeling', FEBS Letters. 2013. 587 (8): 1053-061.

APPENDIX

Information of Kcv gene

Nucleotide Sequence

UniProtKB - Q84568 (KCV_PBCV1)

Protein

ATGTTAGTGT TTAGTAAATT TCTAACGCGA ACTGAACCAT TCATGATACA TCTCTTTATT 20aa
CTCGCAATGT TCGTGATGAT CTATAAATTC TTCCCGGGAG GGTTCGAAAA TAACTTCTCT 40aa
GTTGCAAACC CGGACAAAAA GGCATCATGG ATAGATTGTA TATACTTCGG AGTAACGACA 60aa
CACTCTACTG TCGGATTCGG AGATATACTG CCAAAGACGA CCGGCGCAAA GCTTTGTACG 80aa
ATAGCACATA TAGTAACAGT GTTCTTCATC GTTCTAACTT TATGA 94aa

Kcv Amino Acid Sequence (original sequence)

M L V F S K F L T R T E P F M I H L F I L A M F V M I Y K F F P G G F E N N F S V A N P D K K A S
W I D S I Y F G V T T H S T V G F G D I L P K T T G A K L V T I A H I V T V F F I V L T L

X – Transmembrane Domain, X – Glycosylation site

Primers used to synthesise the linear DNA Fragments

Forward primer for PCR reaction to synthesise linear DNA for S-30 extract *in vitro* transcription/translation system using the pTrc99A primer 5' ⟶ 3'; 5'-CTG AAA TGA GCT GTT GAC AAT TAA TCA TCC GC-'3

Table 2: Reverse primers list and their sequences for PCR reaction to generate truncation linear DNA (Kcv engineered Cysteine)

Experiment	Primer Name	Primer Sequence 5' ⟶ 3'
Translation/PEGylation/ Cross- linking Assay/IP Assay	Kcv 30aa rev.	'GAA TTT ATA GAT CAT CAC GAA CAT TGC GAG'
	Kcv 40aa rev.	'AGA GAA GTT ATT TTC GAA CCC TCC CGG GAA'
	Kcv 50aa rev.	'CCA TGA TGC CTT TTT GTC CGG GTT TGC AAC'
	Kcv 60aa rev.	'TGT CGT TAC TCC GAA GTA TAT ACA ACT TAT'
	Kcv 70aa rev.	'CAG TAT ACT TCC GAA TCC GAC AGT AGA GTG'

Table 3: Cysteine mutagenesis (L8C) and primers

Experiment	Gene Replacement	Primer Name	Primer Sequence 5' ⟶ 3'
Translation/ PEGylation/ Cross-linking Assay/ IP Assay	Leu ⟶ Cys (CTA) (TGC)	L8C Fwd.	`GTT TAG TAA ATTTTG CAC GCG AAC TGA ACC'
		L8C Rev.	'GGT TCA GTT CGC GTG CAA AAT TTA CTA AAC'

Engineered Cysteine (L8C)

M L V F S K F C T R T E P F M I H L F I L A M F V M I Y K F F P G G F E N N F S V A N P D K K A
S W I D S I Y F G V T T H S T V G F G D I L P K T T G A K L V T I A H I V T V F F I V L T L

Cysteine null mutant

M L V F S K F L T R T E P F M I H L F I L A M F V M I Y K F F P G G F E N N F S V A N P D K K A S
W I D S I Y F G V T T H S T V G F G D I L P K T T G A K L V T I A H I V T V F F I V L T L

Table 4: Single three lysines mutagenesis **(**three sites; K29I**/**K46**/**47M**)** and primers

Experiment	Gene Replacement	Primer Name	Primer Sequence **5'** ⟶ **3'**
Translation/ Cross Linking Assay	Lys ⟶ Ile (AAA) (ATA)	K29I Fwd.	'GCA ATG TTC GTG ATG ATC TAT ATA TTC TTC CCG G'
		K29I Rev.	'CCG GGA AGA ATA TAT AGA TCA TCA CGA ACA TTG'
	Lys ⟶ Met (AAA) (ATG)	K46/47M Fwd.	'GTT GCA AAC CCG GAC ATG ATG GCA TCA TGG ATA G'
		K46/47M Rev.	'CTA TCC ATG ATG CCA TCA TGT CCG GGT TTG CAA C'

Replacement of three residues into three sites of lysine in (L8C)

I M M

M L V F S K F C T R T E P F M I H L F I L A M F V M I Y K F F P G G F E N N F S V A N P D K K A
S W I D S I Y F G V T T H S T V G F G D I L P K T T G A K L V T I A H I V T V F F I V L T L

Table 5: Primers of a single methionine mutagenesis (Position M15L) Kcv gene from the 1st engineered Cysteine (L8C)

Experiment	Gene Replacement	Primer Name	Primer Sequence **5'** ⟶ **3'**
Translation/PEGylation	Met ⟶ Leu (ATG) (TTG)	M15L Fwd.	**'**CGC GAA CTG AAC CAT TCT TGA TAC ATC TCT TTA TTC TCG'
		M15L Rev.	'CGA GAA TAA AGA GAT GTA TCA AGA ATG GTT CAG TTC GCG'

Replacement in only one sight of methionine instead of leucine in three lysines substitution (K29I/K46/47M**)**

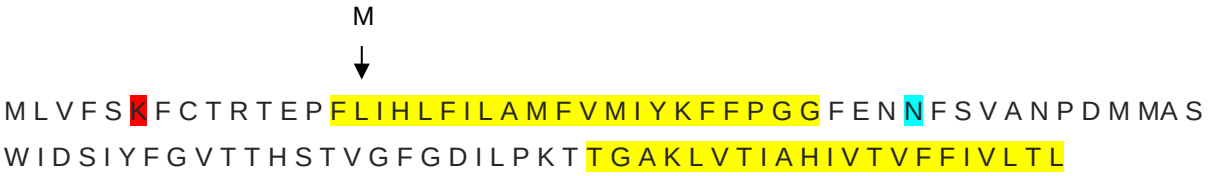

Table 6: Primers of single methionines mutagenesis (M23/26L) Kcv gene combination between the 1st engineered lysine (K29I/K46/47M) and the engineered methionine (M15L)

Experiment	Gene Replacement	Primer Name	Primer Sequence **5'** ⟶ **3'**
Translation/Cross - linking Assay/IP Assay	Met ⟶ Leu (ATG) (TTG)	M23/26L Fwd.	'CTT TAT TCT CGC ATT GTT CGT GTT GAT CTA TAA ATT CTT CC'
		M23/26L Rev.	'GGA AGA ATT TAT AGA TCA ACA CGA ACA ATG CGA GAA TAA AG'

Combination between single three methionines with three sights of leucine in three lysines substitution (K29I/K46/47M)

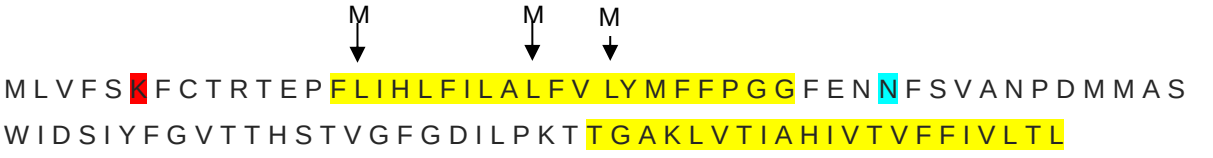

Agarose gel electrophoresis

Agarose gel electrophoresis was regularly used as part of the project, such as for DNA purification, quality control of PCR products as well as for the analysis of control digestion of the cloning products. Tris-acetate/EDTA. (TAE) was applied to dissolve the agarose powder. The concentration of agarose is defined depending on the fragment lengths. Hence, the Kcv intermediate lengths that are lower than 500bp are preferably used for the agarose concentration between 1-2% (w/v). For the preparation of agarose gel, agarose powder was dissolved in 1xTAE buffer and heated in the microwave at medium power for about 1 minute. The melted gel was left to cool down a little and 0.5 µg/mL of ethidium bromide was added. This was followed by the heated gel being poured into a combined casting and electrophoresis system. A comb was immediately placed into the gel during heating to allow all wells to set. After the gel is perfectly set, the chamber was filled with the TAE buffer and the comb was removed gently. The DNA samples were mixed by adding Loading Dye (6X) and loaded into an individual well on the gel. Then, the DNA markers either a 100bp or 1 kb (Promega) were mixed with ddH_20 before loading into the gel. The fragment samples were resolved at 80 volts for approximately 40 minutes and following this, visualised under UV light (the Bio-Rad, Molecular Imager ® Chemidoc XRS System).

Tricine-SDS-PAGE Gel

Acrylamide/bis-acrylamide (AB) 30%

Buffer Gel: 3M Tris-Hcl pH 8.45

APS: 10% Solution (Ammonium Persulfate)

Table 7: Components for preparing a 3 layered Tricine SDS-PAGE gel (10-12%) (2 gels)

Component	1st Layer-Separating	2nd Layer-Spacer	3rd Layer-Stacking
AB (30%)	8.4 mL	0.66 mL	0.534 mL
Buffer Gel pH 8.45	4.95 mL	0.67 mL	1 mL
Glycerol	1.95 mL	-	-
Water	-	0.68 mL	2.46 mL
APS10%	100 µL	10µL	40 µL
TEMED	10 µL	1µ L	4 µL
Time to leave gels set up	15 min	20 min	60 -90 min

- To make up two gels, the 1st layer should be poured into clean glass plates until the gels well is set enough and then followed by each other step.

Buffers used in the experiments

TAE Buffer (pH 8.0)

40 mM Tris
20 mM Acetic acid
1 mM EDTA
(stored at room temperature)

PEG Buffer

20 Mm HEPES pH 7.2,
100 mM NaCl,
mM $MgCl_2$

5

Solubilisation buffer stock (Kept in room temperature)

235 µL Trix buffer; 23% Glycerol, 333mM Tris base, 26 mM EDTA pH 8.0
157 µL of 10% SDS
8 µL of 100 mM Phenylmethane Sulfonyl Fluoride (PMSF)

RIPA Buffer (Low Salt)

150 mM NaCl

50 mM Tris pH 8.0

1% IGEPAL CA-630

0.5% Deoxycholic acid

0.1% SDS

HS-RIPA Buffer (High Salt)

500 mM NaCl

50 mM Tris pH 8.0

1% IGEPAL CA-630

0.5% Deoxycholic acid

0.1% SDS